

The role of Rho5 in *Kluyveromyces lactis*

A thesis submitted for the degree of
Doctor rerum naturalium
(Dr. rer. nat)

By
Marius Musielak
Osnabrück, August 2022

Department of Biology/Chemistry

Evaluated by:
Prof. Dr. rer. nat. Jürgen J. Heinisch
Prof. Dr. rer. nat. Achim Paululat

Table of contents

Table of Figures	iv
Table of Tables	iv
1. Introduction	1
1.1 The yeast <i>Kluyveromyces lactis</i>	1
1.2 Small GTPases.....	3
1.2.1 General features of small GTPases.....	3
1.2.2 The subfamily of Rho-GTPases	6
1.2.2.1 Functions of Rac homologues in different organisms.....	6
1.2.2.2 Cdc42 homologues and their function	9
1.3 The different functions of Rho5 in <i>Saccharomyces cerevisiae</i>	10
1.3.1 Structure and distribution of Rho5 and its GEF.....	10
1.3.2 Physiological functions of Rho5 in yeast	12
1.4 Aim of this thesis	17
2. Material and Methods	18
2.1 Materials.....	18
2.1.1 Media.....	18
2.1.2 Strains, plasmids and oligonucleotides	19
2.2 Methods	24
2.2.1 Methods for <i>E. coli</i>	24
2.2.1.1 Freeze transformation of <i>E. coli</i> (Hanahan, 1983)	24
2.2.1.2 Plasmid isolation from <i>E. coli</i> (with the GeneJET Plasmid Miniprep Kit from Thermo Scientific)	25
2.2.2 Methods for yeasts.....	25
2.2.2.1 Preparation of overnight cultures	25
2.2.2.2 Growth curves	25
2.2.2.3 Determination of chronological lifespan (CLS).....	26
2.2.2.4 Freeze-transformation of <i>K. lactis</i> (Klebe <i>et al.</i> , 1983)	26
2.2.2.5 Fast extraction of genomic DNA from yeast (Robzyk & Kassir, 1992).....	27
2.2.2.6 Medium-scale extraction of genomic DNA from yeast	27
2.2.2.7 Mating of yeast strains	28
2.2.2.8 Sporulation and tetrad dissection	28
2.2.2.9 Plasmid isolation from yeast	28

Table of contents

2.2.2.10 Fluorescence microscopy (Schmitz <i>et al.</i> , 2015)	29
2.2.2.11 Transmission electron microscopy (Backhaus <i>et al.</i> , 2010)	30
2.2.3 Methods for DNA analysis	31
2.2.3.1 Agarose gel electrophoresis	31
2.2.3.2 Polymerase chain reaction (PCR)	31
2.2.3.3 Use of restriction endonucleases	32
2.2.3.4 Ligation	33
2.2.3.5 Sequencing	33
2.2.3.6 DNA synthesis	33
3. Results	34
3.1 <i>In silico</i> analyses of the primary sequences of the DLR complex	34
3.2 Mutant and complementation analyses	36
3.2.1 <i>K/DLR</i> mutants do not display pronounced growth defects under standard growth conditions	36
3.2.2 Growth of <i>K/DLR</i> mutants upon application of different stresses	37
3.2.3 Effect of the <i>K/DLR</i> complex on the chronological lifespan	38
3.2.4 <i>K. lactis</i> strains lacking DLR components display morphological defects	39
3.2.4.1 TEM imaging of wild-type and <i>K/DLR</i> mutant cells	41
3.2.4.2 GFP- <i>K/Rho5</i> localizes to the bud neck during cytokinesis	44
3.2.5 Heterologous complementation of <i>rho5</i> -specific phenotypes in <i>S. cerevisiae</i> and <i>K. lactis</i>	46
3.3 Intracellular distribution of DLR components in <i>K. lactis</i>	48
3.3.1 <i>K/Rho5</i> , <i>K/Dck1</i> and <i>K/Lmo1</i> associate with mitochondria upon oxidative stress	48
3.3.2 <i>K/Rho5</i> , <i>K/Dck1</i> and <i>K/Lmo1</i> associate with mitochondria upon glucose starvation	52
3.4 <i>K/CDC42</i> localizations suggest shared functions with <i>K/Rho5</i>	53
3.4.1 <i>K/CDC42</i> is an essential gene	53
3.4.2 GFP- <i>K/Cdc42</i> translocates to mitochondria under oxidative stress	54
4. Discussion	57
4.1 Similarities between <i>ScRho5</i> and <i>K/Rho5</i>	57
4.1.1 Functionality of the <i>K/DLR</i> components fused to GFP and their localization under standard conditions	57
4.2 Several regions of <i>K/Rho5</i> , <i>ScRho5</i> and <i>HsRac1</i> may convey species-specific functions	59
4.3 <i>K/DLR</i> mutants display a variety of phenotypes that can be linked to stress signalling	62
4.3.1 <i>K/RHO5</i> shows no genetic interactions with different signalling pathways	62
4.3.2 <i>K/DLR</i> -deletion mutants do not affect the chronological lifespan	63

Table of contents

4.3.3 Possible functions of the <i>K/DLR</i> complex in mediating the response to different stressors in the medium.....	65
4.4 The <i>K/DLR</i> -complex regulates cytokinesis	67
4.6 <i>K/Cdc42</i> has overlapping functions with <i>K/Rho5</i>	70
5. Summary.....	73
6. References	74
7. Acknowledgments	88
8. Statutory declaration.....	89
9. Curriculum vitae	90

Table of Figures

Table of Figures

Figure 1: General features of small GTPases.....	3
Figure 2: Model of DOCK/ELMO autoregulation upon integrin stimulation in mammalian cells.....	8
Figure 3: Overview on the different functions of Rho5 in yeast.	10
Figure 4: Alignment of ScRho5 and HsRac1.	11
Figure 5: Comparison of the domain structures of DOCK to Dck1 and of ELMO to Lmo1.....	12
Figure 6: Rho5 as negative regulator of the CWI pathway.	12
Figure 7: Rho5 and its dimeric GEF in potential interactions with other small GTPases in <i>S. cerevisiae</i>	15
Figure 8: Pattern and concentration of the GeneRuler 1 kb DNA ladder.	31
Figure 9: Sequence alignments of Rho5, Dck1 and Lmo1 homologues.	35
Figure 10: Comparative growth assays of wild-type and <i>K/DLR</i> deletion strains.	38
Figure 11: Chronological lifespan in yeasts lacking <i>K/DLR</i> -components.	39
Figure 12: <i>K/DLR</i> deletion strains stained with Calcofluor white (CFW).	40
Figure 13: Frames from time-lapse imaging of wild-type and <i>K/DLR</i> deletion strains.	41
Figure 14: TEM images of wild-type and <i>K/DLR</i> deletion strains.....	42
Figure 15: Measurement of the cell wall thickness in deletion and wild-type strains.....	44
Figure 16: Microscopic images of the <i>Klrho5 Klmyo1</i> double deletion.....	44
Figure 17: Colocalization of <i>Klrho5</i> with <i>Klmyo1</i> and actin at the bud neck.	46
Figure 18: Complementation of the synthetic lethality of <i>Scrho5 Scsch9</i> double deletions.	47
Figure 19: Translocation of the <i>K/DLR</i> components under oxidative stress.	50
Figure 20: Life cell fluorescent imaging of <i>K/Dck1</i> -GFP and <i>K/Lmo1</i> -GFP together with a nuclear marker and vacuole staining.	51
Figure 21: Translocation of the <i>K/DLR</i> components under glucose starvation.	52
Figure 22: Complementation of the <i>Klcdc42</i> deletion by the wild-type gene.	54
Figure 23: Localization of GFP- <i>KlCdc42</i> at early budding sites.....	55
Figure 24: Translocation of GFP- <i>KlCdc42</i> to mitochondria upon oxidative stress.....	55
Figure 25: Amino acid sequence alignment of different fungal Rho5 homologues and <i>HsRac1</i>	59
Figure 26: Major pathways driving chronological lifespan.	64
Figure 27: Comparison of primary septae in <i>Klmyo1</i> deletions and in <i>Klrho5</i> , <i>Kldck1</i> and <i>Kllmo1</i> deletions.....	68

Table of Tables

Table 1: Yeast strains used in this thesis.....	19
Table 2: Plasmids used	22
Table 3: Oligonucleotides used in this study.....	23
Table 4: Standard PCR programs.....	32
Table 5: Complementation of the morphological defect of a <i>Klrho5</i> deletion with different homologues and alleles.....	47
Table 6: Important amino acids for specific <i>HsRac1</i> -DOCK interaction and their conservation between <i>K. lactis</i> , <i>S. cerevisiae</i> and human Rho5 homologues	61

1. Introduction

All living organisms are exposed to a multitude of environmental conditions and stimuli, such as mechanical forces, chemical agents, radiation, and changes in temperature and medium acidity. In order to properly react to these changing conditions, cells trigger distinctive and coordinated responses. In addition, the life cycle of an organism requires a tight regulation of cellular processes to avoid the generation of harmful metabolites and/or malignant cells, which frequently lead to cancer in higher eukaryotes. A proper regulation is not only essential for multicellular organisms, but also for single celled organisms. Small GTPases are often involved in the coordinated regulation of various pathways related to growth and stress response. They serve as molecular switches that transmit signals to downstream effectors. Because of their importance in humans and all eukaryotic cells, including the yeast *Saccharomyces cerevisiae*, small GTPases and their subfamily of Rho GTPases have been extensively studied. In this thesis the small GTPase Rho5 of *Kluyveromyces lactis* was examined for its functions in different signalling pathways.

1.1 The yeast *Kluyveromyces lactis*

The dairy yeast *Kluyveromyces lactis* is well known for its ability to ferment lactose, with the associated biotechnological applications (reviewed in Rodicio & Heinisch, 2013). It was first isolated from milk and participates in cheese production. *K. lactis* also occurs in other environments, for example in soil beneath Indian balsam (Naumov *et al.*, 2014).

Besides glucose as the preferred carbon source, the dairy yeast can also metabolize galactose, sucrose and maltose under aerobic conditions. Moreover, the disaccharide lactose can be fed into carbohydrate metabolism after its hydrolysis by β -galactosidase (Fukuhara, 2003). In contrast to the closely related baker's yeast *Saccharomyces cerevisiae*, glucose is not exclusively degraded through glycolysis in *K. lactis*, but approximately 40% is channelled through the pentose phosphate pathway (reviewed in Bertels *et al.*, 2021). Since *K. lactis* is a Crabtree-negative yeast, the energy generated from glucose is mainly produced by respiration, rather than alcoholic fermentation (Zeeman *et al.*, 1999). *K. lactis* is also petite-negative, meaning that mitochondrial

1. Introduction

respiration is an essential process, while *S. cerevisiae* can grow without respiration, relying solely on glycolysis in the cytosol (Chen & Clark-Walker, 1993).

With regard to its genetic constitution, *K. lactis* carries only six chromosomes with an estimated genome size of 10.6 Mb, as compared to the 16 chromosomes comprising 12 Mb of *S. cerevisiae*. However, in contrast to *S. cerevisiae*, *K. lactis* did not undergo a whole genome duplication during evolution (Sor & Fukuhara, 1989; Wolfe & Shields, 1997; Dujon *et al.*, 2004). In both yeasts homologous recombination plays an important role as part of genetic repair mechanisms and serves as a basis for genetic manipulations. While in *S. cerevisiae* homologous recombination is an efficient and predominant mechanism, *K. lactis* has a tendency for non-homologous recombination. One way to compensate for that is the deletion of the gene *KIKU80*. Its product forms part of a protein complex involved in non-homologous end-joining. The *Kiku80* deletion thus displays drastically reduced non-homologous end-joining, resulting in a significantly lowered background of unwanted transformants (Kooistra *et al.*, 2004).

S. cerevisiae has stable diploid and haploid phases, whereas the diploid phase of *K. lactis* is semi-stable. There, cells can be maintained in the diploid phase while growing logarithmically on rich medium, but tend to sporulate in stationary phase. Another difference, which complicates the handling of the dairy yeast in a laboratory, is that the mating efficiency in *K. lactis* is several magnitudes lower than in *S. cerevisiae*. Diploids thus need to be obtained by selecting for auxotrophic markers and/or antibiotic resistances (Zonneveld & Steensma, 2003). Otherwise, the life cycle of *K. lactis* is generally similar to *S. cerevisiae* with a doubling time of 80 min under optimal conditions, compared to 90 min for the baker's yeast (Zonneveld & Steensma, 2003; Salari & Salari, 2017). Both yeasts divide by budding and the underlying mechanisms seem to be similar, as well. Thus, five mitotic septins Cdc3, Cdc10, Cdc11, Cdc12 and Shs1 are involved in mediating cell division. Furthermore, core components of the cytokinesis machinery, like the contractile actomyosin ring (AMR), the chitin synthase Chs2, which forms the primary septum, and regulators like Iqg1, Hof1, Inn1, and Cyk3 seem to be at least partially conserved in sequence and function. However, certain phenotypic differences were observed in deletion mutants lacking these components. For example, a *Klmyo1* deletion is viable, while a *Scmyo1* deletion is lethal in most strain backgrounds (Rippert *et al.*,

2014; Rippert & Heinisch, 2016). Other signalling cascades related to cell growth and division, like the CWI pathway, appear to be conserved between the two yeast species, too (Backhaus *et al.*, 2010, 2011).

1.2 Small GTPases

Small GTPases are binary molecular switches that can be found in most living organisms and have a multitude of functions in cellular physiology and signalling pathways. For example, they can mediate actin polymerization, cell wall biosynthesis, gene expression, cell cycle progression, mitochondrial dynamics and many more (Olson *et al.*, 1995; Sulciner *et al.*, 1996; Hall, 1998; Cabib *et al.*, 1998; Fransson *et al.*, 2006). Small GTPases can be subdivided into seven families: Ras, Rab, Ran, Arf, Rho, Rag and Miro (Colicelli, 2004; Boureux *et al.*, 2007; Sekiguchi *et al.*, 2001).

1.2.1 General features of small GTPases

All proteins belonging to the seven subfamilies of small GTPases share common mechanisms of action and regulation. They cycle between an active GTP-bound state, in which they interact with their downstream effectors, and an inactive GDP-bound state. These states are interconverted by the help of ancillary proteins, the guanine nucleotide exchange factors (GEFs), the GTPase activating proteins (GAPs) and the guanine dissociation inhibitors (GDIs) (Figure 1A).

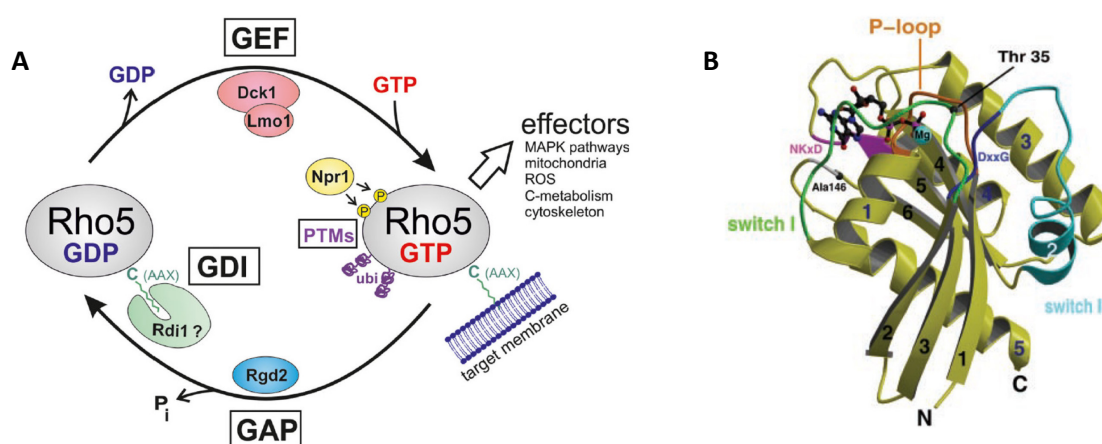


Figure 1: General features of small GTPases. A) Depiction of the GDP/GTP cycle of small GTPases with the example of *S. cerevisiae* Rho5. The picture includes regulatory proteins like GEFs, GAPs and GDIs and post-translational modifications, as well as some examples of effectors. See text for

1. Introduction

details on the depicted components (from Hühn *et al.*, 2020). B) Ribbon Plot of the threedimensional structure of a minimal G-domain. Conserved elements are highlighted by different colors and the nucleotide and Mg²⁺ are shown in ball-and-stick representation (from Vetter & Wittinghofer, 2001).

GEFs trigger the release of bound GDP, by lowering its affinity to the nucleotide binding side, which is brought about by inducing conformational changes in the P-loop and the switch I and II regions (Figure 1). *Vice versa*, this lowers the affinity for the GEF towards the GTPase, promoting its dissociation (Boriack-Sjodin *et al.*, 1998; Worthylake *et al.*, 2000; Goldberg, 1998; Renault *et al.*, 2001; Itzen *et al.*, 2006). The affinity for GDP and GTP is similar in all small GTPases, regardless of its association with a GEF. Therefore, it is the 10-fold higher intracellular concentration of GTP, which facilitates its binding and the concordant activation of the GTPase. Moreover, GEFs can also transiently stabilize the rather unstable nucleotide free state by extensive contact with the switch II region. Most GEFs display a high specificity towards their respective GTPases in engaging these contacts (Biou & Cherfils, 2004; Bourne *et al.*, 1990; Lai *et al.*, 1993; Mistou *et al.*, 1992; Snyder *et al.*, 2002; Vetter & Wittinghofer, 2001). Consequently the GEF activity is tightly regulated by autoinhibitory mechanisms, protein-lipid interactions, protein-protein interactions, intracellular localization, activation through second messengers like cAMP, post-translational modifications and positive feedback loops, by which the activated GEF/GTPase complex facilitates its further activation. Furthermore, some of those interactions can lead to allosteric conformational changes in the active centre and change the specificity of the GEF towards different GTPases (Aronheim *et al.*, 1994; Nimnual *et al.*, 1998; Innocenti *et al.*, 2002; Llorca *et al.*, 2005; Bos *et al.*, 2007; Gureasko *et al.*, 2008, 2010; Malaby *et al.*, 2013).

In contrast to GEFs, GAPs mediate the inactivation of small GTPases, by promoting their low intrinsic capacity to hydrolyse the gamma-phosphate from bound GTP (Scheffzek *et al.*, 1997; Vetter & Wittinghofer, 2001). Like GEFs GAPs are subject to complex regulations, which include protein-protein and protein-lipid interactions, second messengers, intracellular location, post-translational modification, and autoinhibitory functions (Miura *et al.*, 2002; Cullen & Lockyer, 2002; Inoki *et al.*, 2003; Canagarajah *et al.*, 2004; Yamada *et al.*, 2005).

1. Introduction

The third class of regulatory proteins for Rho and Rab GTPases are guanine dissociation inhibitors (GDI). They can extract GTPases from membranes and thus facilitate changes in their intracellular spatio-temporal distribution (Golding *et al.*, 2019). This facilitates the shuttling of GTPases between different cellular compartments (Lin *et al.*, 2003; Boulter *et al.*, 2010). Furthermore, binding of a GTPase to its GDI largely prevents its regulation by GAPs and GEFs. On the other hand, GEFs have been proposed to participate in the release of the GTPase from the GDI complex (Hancock & Hall, 1993; Worthylake *et al.*, 2000; Hoffman *et al.*, 2000; Ugolev *et al.*, 2008). GDIs also seem to act as chaperones, protecting GTPases from proteolytic degradation, retaining a pool of GTPases in the cytoplasm, and may also mediate the crosstalk between different GTPases (Boulter *et al.*, 2010). Like GEFs and GAPs, GDI activities can be regulated by lipid-protein and protein-protein interactions, as well as post translational modifications (Oishi *et al.*, 2012; Xiao *et al.*, 2014; Fauré *et al.*, 1999).

Small GTPases are not only regulated by these ancillary proteins, but also by interactions directly with each other or mediated by their effector proteins (Delprato, 2012). Moreover, their activities can be modulated by posttranslational modifications, such as phosphorylation, ubiquitination and prenylation (reviewed in Hodge & Ridley, 2016).

In addition to their common mechanisms of action, all small GTPases share a central domain of approximately 20 kDa. This so called G-domain mediates the interaction with the bound nucleotide and downstream effector proteins. As depicted in Figure 1B, it consists of five helices located on both sides of a mixed six stranded β sheet. Further, the G-domain includes five conserved regions, labelled G-1 to G-5, which are important for the specific binding of the nucleotide as well as the cofactor Mg^{2+} . The N/TKXD-Motive in the G4-region and the phosphate binding loop (P-loop) in the G1-region are essential to form these folds. Two other indispensable structures are the switch I and switch II regions, whose distinct conformations are determined by the bound nucleotide. The release of the γ -phosphate after the hydrolysis of GTP to GDP is responsible for conformational changes in these regions. This leads to the relaxation of the two switch regions into the GDP-bound state. Only then can the small GTPase interact with its GEFs (Saraste *et al.*, 1990; Bourne *et al.*, 1991; Sprang, 1997; Vetter & Wittinghofer, 2001).

1.2.2 The subfamily of Rho-GTPases

Ras-homologous (Rho) proteins are small GTPases that were first isolated from *Aplysia* abdominal ganglia (Madaule & Axel, 1985). They can be divided into seven subgroups: Cdc42, Rac, Rho, RhoD, Rnd, RhoH/TTF and RhoBTB (Aspenström *et al.*, 2004; Boureux *et al.*, 2007). Of those, Rac, Rho and Cdc42 have been most extensively studied, with the human Rac1 being of special interest, as multiple types of cancer have been associated with its malfunction (Kazanietz & Caloca, 2017).

In addition to the general features mentioned in chapter 1.2.1, Rho GTPases carry a specific insert of about 13 residues between the G4 and G5 motifs, and a poly basic region (PBR) preceding the CAAX-motif at the C-terminal end (reviewed in Schaefer *et al.*, 2014). This Rho-specific insert mediates its activation by GEFs and its interaction with downstream effectors. Its exact length and sequence varies between different Rho GTPases, determining the high specificity towards their effector proteins (McCallum *et al.*, 1996; Freeman *et al.*, 1996; Zong *et al.*, 1999, 2001; Thomas *et al.*, 2007). The CAAX box serves as a target for lipid modifications, like prenylation and palmitoylation, which facilitate membrane association as well as GDI binding, thus mediating the correct spatio-temporal distribution of Rho GTPases. The PBR typically comprises approximately ten amino acids with high sequence variations and further promotes association with membranes through its electrostatic interactions with the negatively charged phospholipids. Furthermore, it could bind to several proteins, among them GEFs and kinases and may contain sequences for intracellular localization. For example, the PBR of *HsRac1* contains a nuclear localization sequence (NLS) (Williams, 2003; Lanning *et al.*, 2004; ten Klooster & Hordijk, 2007; Lam & Hordijk, 2013). In the context of this thesis, Rac1- and Cdc42-homologues are of special interest.

1.2.2.1 Functions of Rac homologues in different organisms

Rac homologues are involved in many signalling pathways and regulate a multitude of cellular functions (for an overview see Hühn *et al.*, 2020). One of the most prominent functions is the regulation of actin polymerization. For instance, in human fibroblasts *HsRac1* mediates the formation of membrane ruffles and activates another small GTPase, RhoA, which in turn induces the formation of stress fibres (Ridley *et al.*, 1992).

1. Introduction

Furthermore, in pancreatic islet β -cells glucose stimulates a Cdc42-Pak1-Rac1 module that regulates insulin granule exocytosis through the reorganization of the actin cytoskeleton (reviewed in Kalwat & Thurmond, 2013). Another example of the involvement of Rho-GTPases in actin organization comes from mice, where colocalization of Rac3 with F-actin at pericellular sites regulates actin dynamics at axonal terminals (Bolis *et al.*, 2003).

Another prominent function of many Rac homologues is the regulation of ROS production and oxidative stress response. For example, in human phagocytes Rac regulates the production of ROS by interaction with the NCF2 subunit of the NADPH oxidase and in mice it was shown, that inhibition of Rac1 by the lethal toxin of *Clostridium sordellii* leads to diminished NADPH oxidase activity, resulting in reduced vascular oxidative stress (Diekmann *et al.*, 1994; Zimmer *et al.*, 2021). Furthermore, in the rice fungal pathogen *Magnaporthe grisea* MgRac1 interacts with MgNox1 and MgNox2 and promotes superoxide production. It also activates the kinase activity of MgChm1 via its PBD domain, which in turn could regulate actin organization and polarized cell growth during conidiogenesis (Chen *et al.*, 2008).

Rac homologues also act in signal transduction pathways governing nuclear gene expression. HsRac1 and HsCdc42 regulate the activity of the c-Jun N-terminal kinase (JNK). JNK phosphorylates the transcription factor c-Jun which regulates the expression of various target genes (Coso *et al.*, 1995). Additionally, Rac homologues have been shown to be important regulators of cell survival and apoptosis. In human lymphoma cells Rac inhibits apoptosis by stimulating retention of the proapoptotic Bcl-2 family member Bad and in mice down-regulated expression of Rac1 promotes apoptosis in the epithelial cells of the airways (Zhang *et al.*, 2004; Wan *et al.*, 2019). Further, in mice, double knock-out mutants of Rac1 and Rac2 encoding genes display strong phenotypes in chemotaxis, chemokinesis, interstitial motility, adhesion, and actin polymerization (Faroudi *et al.*, 2010).

Like all small GTPases, the members of the Rho-family are regulated by GEFs, GAPs and GDIs. Most Rho GEFs fall into one of three categories: the Dbl homology (DH) domain-containing, the DOCK and the PRONE GEFs. Of the three GEF categories the DOCK group is of special interest for this thesis. The members of this dedicators of cytokinesis (DOCK) family, are related to DOCK180, a specific activator of Rac1, and are characterized by two

1. Introduction

highly conserved regions. These regions are designated Dock-homology region-1 and -2 (DHR1 and DHR2). DHR2 mainly functions in the nucleotide exchange, while DHR1 is responsible for directing the GEF to membranes. Many DOCK family proteins interact with proteins of the engulfment and cell motility (ELMO) family and form a bipartite GEF (Brugnera *et al.*, 2002; Meller *et al.*, 2005). DOCK and ELMO proteins feature many domains that are involved in their regulation and interactions with their GTPases as well as other effector proteins. These are best studied for Rac1, DOCK180 and ELMO1-3, but were also shown to apply to other homologues. The PH-domain of ELMO is essential for the formation of a trimeric Rac/ELMO/DOCK-complex, necessary for Rac activation, and can function *in trans* to optimally activate the GTPase. Some ELMO- and DOCK-domains like the PxxP motif, the ELMO inhibitory domains (EID), the ELMO autoregulatory domains (EAD), the SH3 domain, the ELMO binding domain (EBD) and the DHR2 domain are involved in the autoregulation of the bipartite GEF (Figure 2). Others like the Ras binding domain (RBD) of ELMO1 interact with proteins, e.g. the binding of RhoG to the RBD is necessary for activation of Rac1 (Gumienny *et al.*, 2001; Brugnera *et al.*, 2002; Gasteier *et al.*, 2003; Katoh & Negishi, 2003; Lu *et al.*, 2004, 2005; Patel *et al.*, 2011).

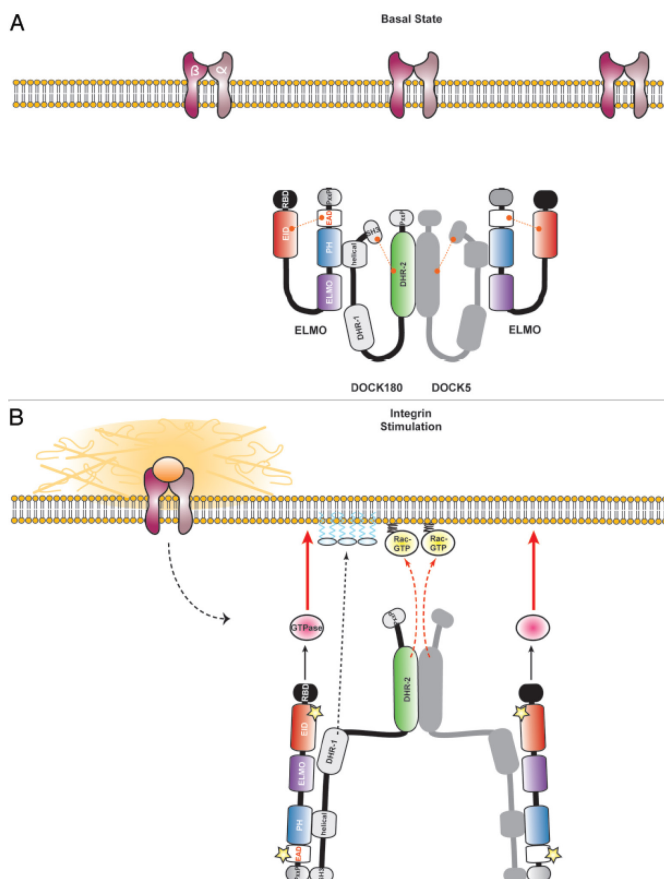


Figure 2: Model of DOCK/ELMO autoregulation upon integrin stimulation in mammalian cells. The model was proposed by Patel *et al.*, 2011. A) At basal levels DOCK and ELMO are autoinhibited, forming a consecutive complex where ELMO is autoinhibited by EID/EAD interaction and DOCK GEF activity is autoinhibited by DHR-2/SH3 interaction. B) Upon a stimulus autoinhibition is relieved. ELMO RBD/GTPase interaction promotes conformational changes and facilitates DOCK SH3/ELMO PxxP interaction. DOCK associates with membranes and recruits the GTPase. Proposed interactions with yet unknown partners with ELMO domains EAD and EID are indicated by yellow stars (from Patel *et al.*, 2011).

1.2.2.2 Cdc42 homologues and their function

The small GTPase Cdc42 displays similar and overlapping functions to Rac1. These are mostly connected to the regulation of actin dynamics, polarity establishment and oxidative stress. For example in mammalian epithelial cells Rac1 and Cdc42 activate the phosphatidylinositol-3-OH-Kinase, resulting in altered actin organisation and subsequently increased cell motility and invasiveness (Keely *et al.*, 1997). In mice both Rac1 and Cdc42 are necessary to control actin assembly and myoblast fusion (Vasyutina *et al.*, 2009). Cdc42 also shares common downstream effectors with Rac1, like the p21-activated protein kinase (PAK2), which plays important roles in stress signalling. Cdc42 mediated activation of PAK2 has also been related to the oxidative stress response in mammalian tissue (Huang *et al.*, 2020). Furthermore, in the filamentous fungus *Neurospora crassa* Cdc42 and Rac1 homologues have been found to mediate polarized growth and morphology. Interestingly, it was suggested that Cdc24, the GEF for Cdc42, also acts on Rac1 in these processes (Araujo-Palomares *et al.*, 2011).

While Cdc42 and Rac1 may act together in various signalling pathways of some organisms and cell types, in others Cdc42 acts exclusively and independent of Rac1. For example, in mouse oocytes and during embryotic development Cdc42 is an upstream regulator of IQGAP1, a central component which promotes cytokinesis (Bielak-Zmijewska *et al.*, 2008). In *Caenorhabditis elegans* and *Drosophila melanogaster* Cdc42 homologues regulate polarity through the asymmetrical localization of PAR (partitioning-defective) proteins (Kay & Hunter, 2001; Gotta *et al.*, 2001; Pichaud *et al.*, 2019). In the yeast *Saccharomyces cerevisiae* Cdc42 mediates actin polymerization and thus both shmoo formation and polarized budding. In order to fulfil this function, its GEF Cdc24 and the scaffold protein Bem1 are required for proper localization and function of Cdc42 (Ziman *et al.*, 1994; Leeuw *et al.*, 1995; Sheu *et al.*, 1998; Butty *et al.*, 2002). This function is conserved in other yeasts, so that in *Schizosaccharomyces pombe* homologues of Cdc42, Cdc24 and Bem1 are also involved in polarized growth (Chang *et al.*, 1994). On the other hand, in *Candida albicans*, Cdc42 regulates the production of reactive oxygen species through the NADPH oxidase Fre8 (Kowalewski *et al.*, 2021).

1.3 The different functions of Rho5 in *Saccharomyces cerevisiae*

Rho5 was first characterized through sequence comparison and later, through phylogenetic analyses, identified as a Rac1 homologue (Garcia-Ranea & Valencia, 1998; Eliáš & Klimeš, 2012). It has been studied extensively in the past two decades and participates in the regulation of a variety of stress responses pathways in *S. cerevisiae*, including the reactions to cell wall damage, medium osmolarity, oxidative and nutrient stress. It has thus been suggested to serve as central signalling hub in the coordination of the underlying signalling pathways (Figure 3, reviewed in Hühn *et al.*, 2020).

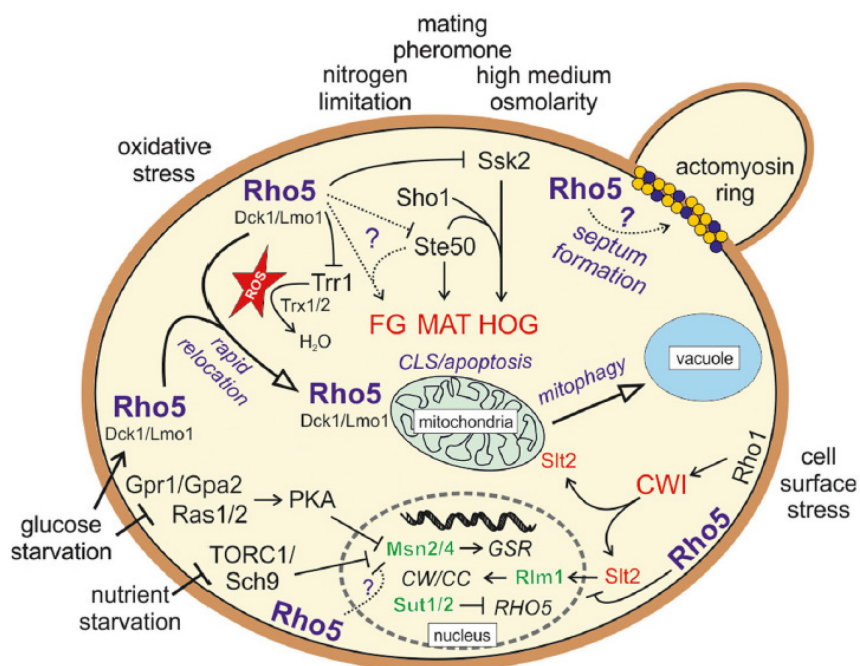


Figure 3: Overview on the different functions of Rho5 in yeast. Active Rho5 is highlighted in bold, dark blue letters, associated with its dimeric GEF Dck1/Lmo1. Biological processes are indicated in light blue and italics, MAPK pathways and their components in red (FG = filamentous growth, MAT = mating pheromone pathway, HOG = high osmolarity glycerol pathway, CWI = cell wall integrity pathway). Transcription factors are shown in green. Arrows indicate activation, lines with bars inhibition. Dotted lines and question marks are used for proposed interactions, for which little experimental evidence has been provided so far (from Hühn *et al.*, 2020).

1.3.1 Structure and distribution of Rho5 and its GEF

Yeast Rho5 retains the general features described above in chapter 1.2 for small GTPases and their Rho-type subfamily. Thus, the PBR and CAAX-motifs are essential for its proper localization and physiological function, as constructs lacking either of them did not

1. Introduction

complement the deletion phenotypes. In addition to these common features a comparison of Rho5 and Rac1 revealed a sequence of 98 amino acids in the yeast protein, preceding the C-terminal PBR/CAAX-motifs (Figure 4). This was designated as a yeast-specific extension and is required but not sufficient for proper localization and physiological function of the small GTPase (Sterk *et al.*, 2019). Moreover, Rho5 was shown to be subject to post-translational modifications. Thus, it appears to be ubiquitinated at several lysine residues, triggering its degradation by proteasomes. Ubiquitination depends on the phosphorylation state, which is mediated by the serine/threonine kinase Npr1 targeting the PEST sequence of Rho5, and Msi1, which inhibits and sequesters Npr1 (Annan *et al.*, 2008).



Figure 4: Alignment of ScRho5 and HsRac1. Identical amino acids are depicted in blue, conserved ones in gray. The orange box designates the 98 amino acid yeast-specific extension. Domains relevant for activation of the GTPase (P-loop, switch I and II, PBR and CAAX box) are highlighted (from Sterk *et al.*, 2019).

Schmitz *et al.* (2015) described the *Saccharomyces cerevisiae* homologues of DOCK and ELMO, designated as Dck1 and Lmo1, respectively. They showed that the domain structure was similar (Figure 5) and demonstrated their interaction. Dck1 and Lmo1 were thus deduced to act as a bipartite GEF of Rho5. This was supported by similar phenotypes of deletion mutants in the three encoding genes (*RHO5*, *DCK1*, *LMO1*), e.g. sensitivity towards hydrogen peroxide and Calcofluor white, as well as by the rapid translocation of all three proteins to mitochondria upon exposure to oxidative stress. Furthermore, deletions of *DCK1* or *LMO1* prevented the latter translocation of Rho5 (Schmitz *et al.*, 2015). This was later shown to also be the case for the translocation of Rho5 to the mitochondria under glucose starvation (Schmitz *et al.*, 2018).

1. Introduction

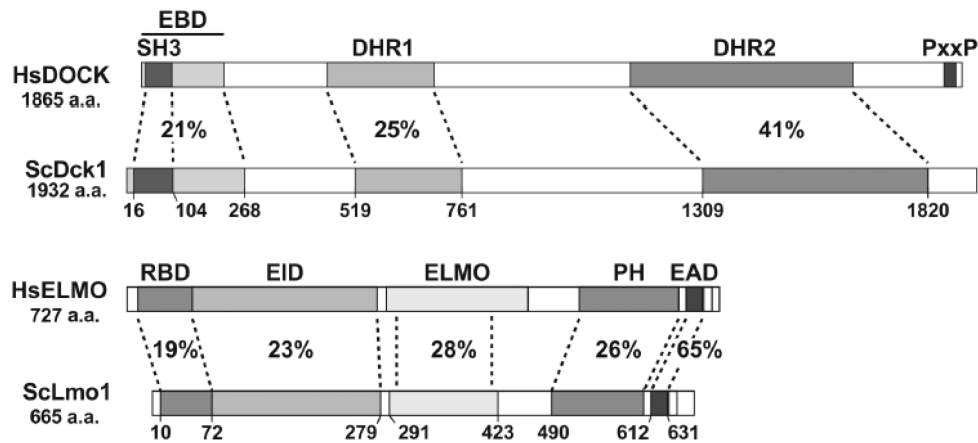


Figure 5: Comparison of the domain structures of DOCK to Dck1 and of ELMO to Lmo1. The domains are indicated by different shadings and are annotated according to Komander *et al.*, (2008). Numbers below indicate the amino acid positions in the yeast proteins. Percentages give the degree of identity among the indicated domains (from Schmitz *et al.*, 2015). Hs = *Homo sapiens*, Sc = *S. cerevisiae*

1.3.2 Physiological functions of Rho5 in yeast

Rho5 was first identified as a negative regulator of the Pkc1 mediated cell wall integrity (CWI) pathway (Figure 6). The latter is predominantly regulated by another small GTPase, Rho1, which is activated by the GEFs Rom1 and Rom2, and downregulated by different GAPs, which include Bem2 and Sac7. Rom 2 is believed to be activated after interaction with the cytosolic domain of one of the five surface receptors Wsc1-Wsc3, Mid2 and Mtl1, upon distortions at the cell surface. Rho1 then interacts with and activates the protein kinase C (Pkc1), which triggers a MAPK cascade consisting of the MAPKKK Bck1, the MAPKKs Mkk1 and Mkk2, and the MAPK Slt2 (Mpk1). Slt2 in turn phosphorylates and activates, among other target proteins, the transcription factor Rlm1, which promotes the transcription of the majority of CWI genes (reviewed in Levin, 2005). While a *rho5* deletion led to an increased level of dually phosphorylated Slt2, believed to

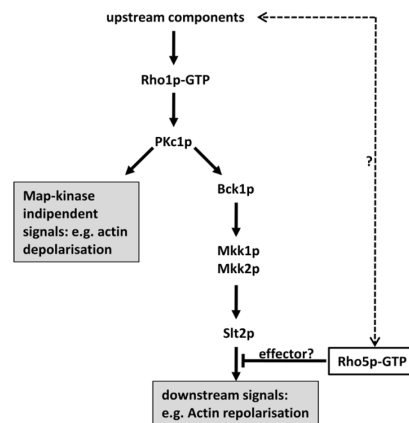


Figure 6: Rho5 as negative regulator of the CWI pathway. Model for ScRho5 action, created by Schmitz *et al.*, based on their findings (from Schmitz *et al.*, 2002).

1. Introduction

correlate with a rise in kinase activity, this did not cause an increase in Rlm1-dependent transcription of a target reporter gene. This suggested that Rho5 at least partially repressed Pkc1 signalling. This notion was supported by the observation that a *rho5* deletion also enhanced the resistance against cell wall stressors like Congo red and Calcofluor white. Epistasis analysis showed that a *rho5* deletion alleviated the necessity for osmotic stabilization in growing *bck1* and *slt2* deletions, indicating that Rho5 acts downstream in the CWI pathway. On the other hand, a lack of Rho5 exacerbated the temperature sensitive phenotype of a *bck1* deletion, which hints to a role upstream of Bck1 (Schmitz *et al.*, 2002).

Rho5 was also found to interact with the Sho1 branch of the high osmolarity glycerol (HOG) pathway. Sho1 is a membrane associated protein that activates the mitogen activated protein kinase kinase kinase (MAPKKK) Ste11, which then signals down the HOG-MAPK cascade to activate specific stress related genes. Hyperactive mutants of Rho5, in which a glutamine was exchanged for a histidine (Rho5^{Q91H}), showed an increased sensitivity towards osmotic stress in a $\Delta ste50$ background. This led to the assumption that Rho5 has a negative effect on the Sho1 branch of the HOG signalling pathway. In this pathway Ste50 interacts with Ste11 and Opy2 through the sterile alpha motif (SAM) and the Ras associated (RA) domain. This leads to the recruitment of Ste11 to the plasma membrane, which then activates the MAPKK Pbs2, which activates the MAPK Hog1, triggering a proper osmotic stress response. Rho5 can also interact with the RA domain of Ste50. In this context, Rho5 activity is diminished by the GAP Rgd2. Overexpressed from high copy number vectors *RGD2* suppresses the osmotic sensitivity displayed in the $\Delta ste20$ *RHO5*^{Q91H} double deletion. Further regulatory mechanisms are the abovementioned ubiquitination and phosphorylation. In strains with a defective proteasome the expression of *RHO5* leads to growth defects and the expression of *RHO5*^{Q91H} exacerbates these defects (Levin, 2005; Annan *et al.*, 2008).

Rho5 also seems to play a role in oxidative stress induced apoptosis. Thus, *rho5* deletions show a higher activity of the thioredoxin reductase Trr1 as compared to the wild-type cells. More importantly, the lack of Rho5 drastically increased the survival rate of cells under oxidative stress (Singh *et al.*, 2008; Schmitz *et al.*, 2015). The two observations have been interpreted as Rho5 causing the accumulation of reactive oxygen species (ROS) and

1. Introduction

cell death by inhibiting their detoxification by Trr1 (Singh *et al.*, 2008). Rho5, as well as its GEF subunits Dck1 and Lmo1, also rapidly translocated to the mitochondria upon treatment of cells with H₂O₂. Moreover, a colocalization of Dck1 and Lmo1 with Atg8, a common marker for autophagic structures, was observed under nitrogen limitation (Schmitz *et al.*, 2015). This hinted to a relation to mitophagy, which is a specialised type of macroautophagy for recycling defective mitochondria, that for example could be caused by increased ROS concentrations. During this process, the autophagy components Atg8 and Atg11 are localized to the mitochondria *via* interaction with the organelle-specific receptor Atg32 (Kanki *et al.*, 2009; Okamoto *et al.*, 2009; Klionsky *et al.*, 2010). Under nitrogen starvation, mitophagy was reduced in *rho5*, *dck1* and *lmo1* deletions, indicating that Rho5 is required for efficient turnover of mitochondria (Schmitz *et al.*, 2015). Interestingly, MAP kinases of the HOG and CWI pathways also have been related to mitophagy, the latter substantiating previous results relating Rho5 to CWI signalling (Schmitz *et al.*, 2002; Mao *et al.*, 2011). In line with a function in mitophagy, BiFC assays with different Rho5 variants, like a GTP-locked and a GDP- or nucleotide free locked version, showed that Atg21 interacted as a putative downstream effector preferably with GTP-Rho5. Atg21 mediates cell death induced by oxidants and it is a key component of the cytoplasm to vacuole targeting pathway in mitophagy. In fact, cells lacking either Atg21 or Rho5 displayed a drastically reduced mortality under oxidative stress as compared to the wild type. This was also observed for a constitutively active Rho5^{G12V} variant in the background of an *atg21* deletion (Singh *et al.*, 2019).

Another role of Rho5 has been found in relation to carbohydrate metabolism. Thus, under glucose starvation a reversible translocation of Rho5 and Dck1 to mitochondria was observed. Epistasis analyses revealed that *rho5 sch9* double deletions are not viable and that double deletions of *rho5* with *gpr1* or *gpa2* are likewise synthetically lethal or synthetically sick (Schmitz *et al.*, 2018). Gpr1 is a glucose sensor, which in the presence of sugar, activates the small GTPase Gpa2. Another GTPase, Ras2, is also activated in the presence of glucose, albeit more indirectly (reviewed in Conrad *et al.*, 2014). Both GTPases target the PKA/cAMP glucose signalling pathway, repressing the utilization of alternate carbon sources. On the other hand, Sch9 is a protein kinase, acting downstream of TORC1 signalling and has been connected to nitrogen starvation (reviewed in Broach, 2012). While *ras2 sch9* double deletions are synthetically lethal or synthetically sick, *rho5*

1. Introduction

ras2 double deletions as well as *rho5 snf1* double deletions are perfectly viable. Deletions of *SCH9*, *GPA2*, *GPR1* and *RAS2* all share an increased resistance towards oxidative stress with the phenotype of a *rho5* deletion. From these data, a model was proposed (Figure 7) in which Rho5 would contribute to the sequestration of the Rim15 kinase to the cytoplasm. Glucose or oxidative stress in triggering the translocation of Rho5 to mitochondria would thus relieve the inhibition of Rim15, which in turn would phosphorylate Msn2/4, transcription factors mediating the general stress response, thus leading to stress related gene expression (Schmitz *et al.*, 2018).

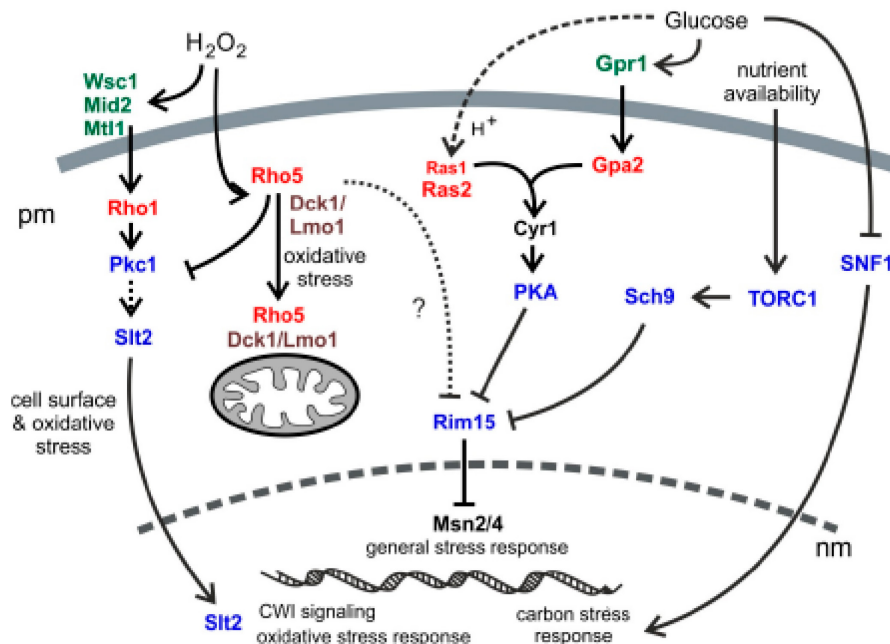


Figure 7: Rho5 and its dimeric GEF in potential interactions with other small GTPases in *S. cerevisiae*. Arrows indicate activation, lines with bars indicate inhibition of the effectors/pathways. pm = plasma membrane, nm = nuclear membrane (from Schmitz *et al.*, 2018).

Further functions of Rho5 seem to be a more indirect involvement in the regulation of the actin cytoskeleton and a function connected to the chronological lifespan. In *rho5* deletions the depolarisation of the actin cytoskeleton upon heat shock was abolished, whereas it was enhanced by overexpression of a hyper active *RHO5* allele. Moreover, *dck1* and *lmo1* deletions displayed an increase in the number of actin patches beneath the plasma membrane, as well as a moderate resistance towards Latrunculin A, an inhibitor of actin polymerization. This suggested that Dck1 and Lmo1 may interact with

1. Introduction

other GTPases in regulating of the actin cytoskeleton dynamics, and that the contribution of Rho5 may be comparatively small and rather indirect (Schmitz *et al.*, 2002, 2018). Studies on the chronological lifespan in a *rho5* deletion strain showed a reduced survival timer compared to the wild-type control (Cao *et al.*, 2016). The Authors also reported on a significant decrease in the expression of starvation-specific genes in a *rho5* deletion.

Altogether, the large number of physiological effects observed in the mutants led to the hypothesis that Rho5 acts as a central signalling hub, integrating multiple stress signals into an appropriate cellular response, by fine-tuning a multitude of different signalling pathways (Hühn *et al.*, 2020).

1.4 Aim of this thesis

The role of the small Rho-GTPase Rho5 and its bipartite GEF ScDck1/ScLmo1 has been primarily studied in the yeast *Saccharomyces cerevisiae*, so far. Rho5, proposed to be a homologue of the human Rac1, other fungal homologues of which were shown to regulate ROS homeostasis, as well as the actin cytoskeleton dynamics and related cellular processes, such as cytokinesis and polarized growth.

In the current work, the small GTPase *K/Rho5* was to be studied for its roles in stress response and the regulation of the actin cytoskeleton in the diary yeast *Kluyveromyces lactis*. This included microscopic examination of the of *Klrho5* deletions in budding cells, as well as the investigations of cross-species complementation between *K. lactis* and *S. cerevisiae* homologues. In addition, the responses of different deletion mutants to the presence of stressors were to be investigated by automated growth assays. To gain more insight into genetic interactions, epistasis analyses with candidate gene deletions would also be performed. Given reports on overlapping functions in other fungi, the relation between Rho5 and Cdc42 was of special interest in this context. Moreover, microscopic approaches were used to study the spatio-temporal distribution of GFP-tagged *K/Rho5*, *K/Dck1* and *K/Lmo1* under standard growth conditions and different stresses in live cell microscopy. These studies were to be complemented by TEM microscopy and time-lapse imaging of wild-type and mutant cells.

2. Material and Methods

2.1 Materials

2.1.1 Media

For standard solid media 1.5 % (m/v) agar were added to prepare plates. All synthetic media were adjusted to pH 6.2 with NaOH. Glucose and agar were added before autoclaving (121 °C, 20 min). Antibiotics and other agents were added after the media had cooled down to approximately 50 °C. Deionised water was used for all media and buffer preparations.

Rich medium (Yeast extract, peptone, dextrose = YEPD)

1 % (w/v) yeast extract (Becton, Dickinson and company, New Jersey, USA), 2 % (w/v) bacto peptone (Becton, Dickinson and company, New Jersey, USA) and 2 % (w/v) glucose. 200 mg/l of G418 were added from a stock solution, if required.

Synthetic media

For basic synthetic media 0.67 % (w/v) yeast nitrogen base without amino acids but with ammonium sulphate (Becton, Dickinson and company, New Jersey, USA) and 2 % (w/v) glucose were used (synthetic minimal medium = SMD). For preparation of synthetic complete medium (SCD) 0.06 % (w/v) of complete supplement mixture (lacking histidine, tryptophan, uracil and leucine; Mp Biomedicals, Germany) and 1 % (v/v) 100x stock solutions were added, as required (20 mg/l histidine, 20 mg/l uracil, 100 mg/l leucine, 20 mg/l tryptophan). G418 was added to a final concentration of 200 mg/l to select for the *kanMX* marker, if necessary.

Malt extract agar

For crossing of *K. lactis* strains, plates containing 5 % (w/v) malt extract and 3 % (w/v) agar were prepared.

2. Material and Methods

Sporulation media

K. lactis and *S. cerevisiae* diploids were sporulated on medium with 1 % (w/v) potassium acetate and 3 % (w/v) agar.

Luria broth (LB)

Medium for growth of *E. coli* contained 1 % (w/v) select peptone or bacto tryptone (Becton, Dickinson and company, New Jersey, USA), 0.5 % (w/v) yeast extract (Becton, Dickinson and company, New Jersey, USA) and 1 % (w/v) sodium chloride. For selection of antibiotic resistances either ampicillin or kanamycin were added from stock solutions to a final concentration of 100 mg/L or 50 mg/L, respectively. For blue white screening selective plates were prepared by plating a mix of 100 µl sterile water with 40 µl X-Gal stock solution (20 mg in 1 ml DMSO) approximately 30 min prior to the *E. coli* cells.

2.1.2 Strains, plasmids and oligonucleotides

Yeast strains employed in this thesis are listed in Table 2. For work with *E. coli*, the strain DH5α (*F*- Φ 80*lacZ*Δ*M15* Δ(*lacZ*YA-*argF*) *U169 recA1 endA1 hsdR17 (rK*-, *mK*+) *phoA supE44 λ*-*thi-1 gyrA96 relA1*; GIBCO BRL,USA) was used throughout. Plasmids are listed in Table 3 and oligonucleotides in Table 4.

Table 1: Yeast strains used in this thesis

Strain	Genotype	Source
<i>Kluyveromyces lactis</i> strains ¹		
CBS2359	<i>MATa</i>	Kooistra <i>et al.</i> , 2004
KHO46-6C/2751	<i>MATa ura3 leu2::pJJH2751-LEU2</i>	obtained from integration of pJJH2751 into KHO46-6C
KHO139-1C	<i>MATalpha ade2::loxP ku80::loxP</i>	J. J. Heinisch
KHO139-2B	<i>MATa ade2::loxP KU80wt</i>	J. J. Heinisch
KHO199-2A	<i>MATalpha ura3 leu2 ku80::loxP hof1::ScURA3</i>	J. J. Heinisch
KHO208-8A	<i>MATalpha ura3 leu2 his3::loxP ku80::loxP</i>	J. J. Heinisch
KHO208-8B	<i>MATalpha ura3 leu2 his3::loxP rho5::kanMX ku80::loxP</i>	J. J. Heinisch
KHO217-9B	<i>MATa ura3 his3::loxP rho5::kanMX</i>	J. J. Heinisch
KHO218-9A	<i>MATa ura3 leu2 his3::loxP dck1::kanMX</i>	J. J. Heinisch
KHO218-2A	<i>MATa ura3 leu2 dck1::kanMX</i>	J. J. Heinisch
KHO224-1C	<i>MATalpha ura3 leu2 his3::loxP ade2::loxP tal1::ScLEU2 KU80-wt</i>	J. J. Heinisch

2. Material and Methods

KHO254-1A	<i>MATalpha ura3 leu2 dck1::kanMX</i>	obtained from crossing KHO139-1C x KHO218-2A
KHO254-5D	<i>MATalpha</i>	obtained from crossing KHO139-1C x KHO218-2A
KHO254-11A	<i>MATa dck1::kanMX ku80::loxP</i>	obtained from crossing KHO139-1C x KHO218-2A
KHO255-1B	<i>MATalpha ura3 leu2 lmo1::kanMX ku80::loxP</i>	J. J. Heinisch
KHO255-3A	<i>MATalpha ura3 leu2 his3::loxP lmo1::kanMX ku80::loxP</i>	J. J. Heinisch
KHO256-13B	<i>MATalpha leu2 lmo1::kanMX KU80wt</i>	Obtained from crossing KHO255-1B x KHO139-2B
KHO259-7A	<i>MATa</i>	obtained from crossing KHO139-1C x KHO217-9B
KHO262-5D	<i>MATa trp1::kanMX KU80wt</i>	J. J. Heinisch
KHO264-3D	<i>MATa ade4::loxP KU80wt</i>	J. J. Heinisch
KHO277-3D	<i>MATalpha ura3 leu2 rho5::kanMX</i>	J. J. Heinisch
KHO336-1B	<i>MATalpha ura3 leu2 his3::loxP KU80 DCK1-GFP-SkHIS3</i>	J. J. Heinisch
KHO337-1C	<i>MATalpha ura3 leu2 his3::loxP KU80 LMO1-GFP-SkHIS3</i>	J. J. Heinisch
KHO343-8B	<i>MATalpha ura3 leu2 his3::loxP KU80wt GFP-RHO5-SkHIS3</i>	J. J. Heinisch
KHO346-7B	<i>MATa ura3 his3::loxP IDP1-mRuby-kanMX KU80wt</i>	J. J. Heinisch
KHO347-2B	<i>MATa ura3 leu2 his3::loxP KU80wt DCK1-GFP-SkHIS3 IDP1-mRuby-kanMX</i>	J. J. Heinisch
KHO348-2B	<i>MATa ura3 his3::loxP LMO1-GFP-SkHIS3 IDP1-mRuby-kanMX</i>	J. J. Heinisch
KHO276-2A	<i>MATa ura3 his3::loxP rho5::kanMX</i>	J. J. Heinisch
KDR38-1D	<i>MATa ura3 leu2 his3::loxP myo1::kanMX</i>	Rippert <i>et al.</i> , 2014
KDR40-8A	<i>MATa ura3 leu2 his3::loxP Myo1-mCherry-ScURA3</i>	Rippert <i>et al.</i> , 2014
KMO01-14C	<i>MATa dck1::kanMX</i>	obtained from crossing KHO254-11A x KHO254-5D
KMO03-1D	<i>MATalpha lmo1::kanMX</i>	obtained from crossing KHO256-13B x KHO259-7A in this thesis
KMO05-12C	<i>MATalpha rho5::kanMX leu2 ura3 his3::loxP</i>	obtained from crossing KHO277-3D x KDR40-8A
KMO06-23	<i>MATalpha ura3 leu2 myeGFP-RHO5-SkHIS3 ku80::loxP</i>	obtained from integration of <i>mye-GFP-RHO5 SkHIS3</i> cassette into KHO208-8B
KMO16-27A	<i>MATa leu2 rho5::kanMX</i>	obtained from crossing KMO05-12C x KHO262-5D
KMO16-34D	<i>MATa ura3 rho5::kanMX</i>	obtained from crossing KMO05-12C x KHO262-5D
KMO21-7B	<i>MATalpha ade4::loxP rho5::kanMX</i>	obtained from crossing KHO277-3D x KHO264-3D
KMO23-2D	<i>MATa rho5::kanMX myo1::kanMX his3::loxP</i>	obtained from crossing KDR38-1D x KMO21-7B
KMO30-4A	<i>MATalpha ura3 leu2 MYO1-mCherry-ScURA3 GFP-RHO5-SkHIS3</i>	obtained from crossing KDR40-8A x KHO343-8B
KMO30-6D	<i>MATa ura3 leu2 his3::loxP MYO1-mCherry-ScURA3</i>	obtained from crossing

2. Material and Methods

	<i>GFP-RHO5-SkHIS3</i>	KDR40-8A x KHO343-8B
KMO31-4B	<i>MATa ura3 leu2 his3::loxP GFP-RHO5-SkHIS3 IDP1-mRuby-kanMX</i>	obtained from crossing KMO06-23 x KHO346-7B
KMO32-5D	<i>MATalpha ura3 his3::loxP leu2::pRRO297-LEU2 DCK1-GFP-SkHIS3</i>	obtained from integration of pRRO297 into KHO336-1B
KMO33-8A	<i>MATalpha ura3 his3::loxP leu2::pRRO297-LEU2 LMO1-GFP-SkHIS3</i>	obtained from integration of pRRO297 into KHO337-1C
KHO70	<i>MATa/MATalpha ura3/ura3 leu2/leu2 his3::loxP/HIS3 ade2::loxP/ADE2 ku80::loxP/ku80::loxP</i>	Heinisch <i>et al.</i> , 2010
KHO70/cdc42	<i>MATa/MATalpha ura3/ura3 leu2/leu2 his3::loxP/HIS3 ade2::loxP/ADE2 ku80::loxP/ku80::loxP CDC42/cdc42::kanMX</i>	Substitution of <i>CDC42</i> by <i>kanMX</i> marker through homologous recombination
KMO17	<i>MATa/alpha ura3/ura3 leu2/LEU2 rho5::kanMX/RHO5 hof1::ScURA3/hof1</i>	obtained from crossing KHO199-2A x KMO16-34D
KMO23	<i>MAT a/alpha ura3/URA3 leu2/LEU2 his3/HIS3 ade4/ADE4 rho5::kanMX/RHO5 myo1::kanMX/MYO1</i>	obtained from crossing KDR38-1D x KMO21-7B
KMO24	<i>MATa/alpha URA3/ura3 leu2/leu2 HIS3/his3::loxP ADE2/ade2::loxP RHO5/rho5::kanMX TAL1/tal1::ScLEU2</i>	obtained from crossing KHO224-1C x KMO16-27A
KHO276	<i>MATa/alpha URA3/ura3 LEU2/leu2 his3::loxP /his3::loxP RHO5/rho5::kanMX PIL1/pil1::ScHIS3</i>	J. J. Heinisch
KHO277	<i>MATa/alpha URA3/ura3 leu2/leu2 HIS3/his3::loxP RHO5/rho5::kanMX LSP1/lsp1::ScLEU2</i>	J. J. Heinisch
KHO291	<i>MATa/alpha ura3/ura3 leu2/leu2 HIS3/his3::loxP RHO5/rho5::kanMX GPR1/gpr1::kanMX</i>	J. J. Heinisch
KHO293	<i>MATa/alpha ura3/ura3 leu2/leu2 RHO5/rho5::kanMX SCH9/sch9::ScLEU2</i>	J. J. Heinisch
KHO314	<i>MATa/alpha leu2/leu2 HIS3/his3::loxP RHO5/rho5::kanMX SOD1/sod1::SpHIS5</i>	J. J. Heinisch
KHO316	<i>MATa/alpha ura3/ura3 leu2/leu2 HIS3/his3::loxP RHO5/rho5::kanMX GPR1/gpr1::kanMX</i>	J. J. Heinisch
KHO341	<i>MATa/alpha leu2/leu2 his3::loxP /his3::loxP RHO5/rho5::kanMX SOD1/sod1::ScLEU2</i>	J. J. Heinisch
KHO344	<i>MATa/alpha URA3/ura3 LEU2/leu2 HIS3/his3::loxP RHO5/rho5::kanMX RPE1/rpe1::kanMX</i>	J. J. Heinisch
KHO354	<i>MATa/alpha URA3/ura3 leu2/leu2 HIS3/his3::loxP ADE2/ade2::loxP RHO5/rho5::kanMX ZWF1/zwf1::ScLEU2</i>	J. J. Heinisch
KHO368	<i>MATa/alpha ura3/ura3 leu2/leu2 HIS3/his3::loxP ADE2/ade2::loxP RHO5/rho5::kanMX TDP1/tdp1::ScLEU2</i>	J. J. Heinisch
KHO377	<i>MATa/alpha ura3/ura3 leu2/leu2 HIS3/his3::loxP ADE2/ade2::loxP RHO5/rho5::kanMX MPK1/mpk1::ScLEU2</i>	J. J. Heinisch
KHO278	<i>MATa/alpha ura3/ura3 LEU2/leu2 his3::loxP/his3::loxP RHO5/rho5::kanMX RLM1/rlm1::ScURA3</i>	J. J. Heinisch

2. Material and Methods

KHO379	<i>MATa/alpha URA3/ura3 LEU2/leu2 his3::loxP /his3::loxP LAC4/lac4::loxP RHO5/rho5::kanMX BCK1/bck1::kanMX</i>	J. J. Heinisch
KHO381	<i>MATa/alpha ura3/ura3 his3::loxP /his3::loxP RHO5/rho5::kanMX POR1/por1::SkHIS3</i>	J. J. Heinisch
<i>Saccharomyces cerevisiae</i> strains²		
DAJ138	<i>MATa/MATalpha ura3-52/ura3-52 leu2-3,112/leu2-3,112 his3-11,15/his3-11,15 sch9::SkHIS3/SCH9 rho5::kanMX/RHO5</i>	Schmitz <i>et al.</i> , 2015
HD56-5A	<i>MATalpha ura3-52 his3-11,15 leu2-3,112</i>	Kirchrath <i>et al.</i> , 2000
HAJ216-A	<i>MATa ura3-52 his3-11,15 leu2-3,112 rho5::kanMX</i>	Schmitz <i>et al.</i> , 2018
HAJ03-B	<i>MATalpha ura3-52 his3-11,15 leu2-3,112 dck1::kanMX</i>	Schmitz <i>et al.</i> , 2018
HAJ201-B	<i>MATalpha ura3-52 his3-11,15 leu2-3,112 lmo1::kanMX</i>	Schmitz <i>et al.</i> , 2018

¹ The prefix “*Kl*” was omitted for all *K. lactis* genes in the genotype. Rather, only heterologous genes employed for manipulations in *K. lactis* are designated by the prefix indicating the source species (*Sc* = *Saccharomyces cerevisiae*, *Sp* = *Schizosaccharomyces pombe*, *Sk* = *Saccharomyces kluyveri*)

² The prefix “*Sc*” was omitted for all *S. cerevisiae* genes in the genotype. Rather, only heterologous genes employed for manipulations in *S. cerevisiae* are designated by the prefix indicating the source species (*Sk* = *Saccharomyces kluyveri*).

Table 2: Plasmids used

Pre-existing plasmids		
Name	Features	Source
pCse24	<i>Klori, ori, CEN4/ARS1 ScLEU2, bla</i>	Heinisch <i>et al.</i> , 2010
pCXJ18	<i>Klori, ori, KICEN2, ScURA3, lacZα</i>	Chen, 1996
pCXs22	<i>Klori, ori, CEN4/ARS1 ScURA3, bla</i>	Heinisch <i>et al.</i> , 2010
pFA6a-kanMX	<i>kanMX bla ori</i>	Bähler <i>et al.</i> , 1998
pFA6a-GFP-SKHIS3	<i>GFP SkHIS kanMX bla ori</i>	Longtine <i>et al.</i> , 1998
pJJH2357	<i>KILEU2 kan ori</i>	J. J. Heinisch
pJJH2600L	<i>KILEU2 kan ori</i>	J. J. Heinisch
pRRO297	<i>KILEU2 bla ori PFK2p-NLS-mCherry</i>	Rosaura Rodicio (University of Oviedo/Spain)
YCplac111	<i>ScLEU2 CEN4/ARS1 bla ori</i>	Gietz & Akio, 1988
YEpl181JJH	<i>2μ LEU2 bla ori lacZα</i>	J. J. Heinisch
Plasmids constructed for this study¹		
Name	Backbone	Genes inserted
pMHO011	pJJH2357	<i>KIRHO5</i>
pMHO012	pJJH2357	<i>ScRHO5</i>
pMHO013	pJJH2357	<i>HsRac1</i>
pMHO014	pJJH2357	<i>ScRHO5^{Δloop}</i>
pMHO015	pJJH2357	<i>ScRHO5^{G12V}</i>
pMHO016	pJJH2357	<i>ScRHO5^{Q91H}</i>
pMHO017	pJJH2357	<i>KIRHO5^{Sc222-331}</i>
pMHO018	pJJH2357	<i>HsRAC1^{G12V}</i>

2. Material and Methods

pJH2751	pJH2600L	<i>GFP-RHO5 KIABP140frag-mRuby</i>
pJH2789	YCplac111	<i>KIRHO5</i>
pJH2790	YEP181	<i>KIRHO5^{Q91H}</i>
pJH2917L	pJH2600L	<i>KIDC42^{G12V}</i>
pJH2918	pJH2600L	<i>KIDC42</i>
pMMO05	pJH2357	<i>KIRHO5</i>
pMMO06	pJH2357	<i>KILMO1</i>
pMMO07	pJH2357	<i>KIDCK1</i>
pMMO27	pJH2357	<i>HsRac1^{K1200-254}</i>
pMMO22	pJH2357	<i>GFP-CDC42</i>

¹ Plasmids pMHO011-pMHO018 were constructed by Miriam Hegemanns in the course of her Bachelor thesis, plasmids with the prefix “pJH” were provided by J. J. Heinisch.

Table 3: Oligonucleotides used in this study

Number	Name	Sequence (5' → 3')
03.45	KanMX-5'out	GGAATTTAATCGCGCCTCG
03.44	KanMX-3'out	GTATTGATGTTGGACGAGTCGG
05.135	ScMAT1	AGTCACATCAAGATCGTTTATGG
05.136	ScMAT2	GCACGGAATATGGGACTACTTCG
05.137	ScMAT3	ACTCCACTTCAAGTAAGAGTTTG
06.54	KISla2	GTATTCAACAACAGGAAATGGAAAAGG
06.55	KIMATa1	GGAGTCATGTGCGACAATGATATGGCAG
06.56	KIMATalpha1	GTAGATAAACAGACAAGAAAGAATTGGG
11.233	KIDCK1del5'	TGCAACTATTTTCGTCACTATTGATTTAGTGGTGGTTTTTT GTACGACTTCGTACGCTGCAGGTCGAC
11.234	KIDCK1del3'	TACATGAGGTGAGAATTAGAACAGTTGCAGTGGGAGAAAGTT ATTCTATGCCGCATAGGCCACTAGTGGATCTG
11.244	KIDCK1_5-3	CTAAGTCCTTCCAGTAGAGC
11.245	KIDCK1_3-5	TCACCGACAGACTTGAGCTC
15.110	Kllmo1del5	TTCAAGAAAGCGACCAGCCATTTATTCTTCATACAGACTATTTT CATACTTCGTACGCTGCAGGTCGAC
15.111	Kllmo1del3	ATACTACATAAACGCAGTTGAGGTGTTATTACATAATCATCAA CTCTCAGCATAGGCCACTAGTGGATCTG
15.112	Klrho5del5	AAATATTAAGTAGGACCCAACCACAAAAAAAAAAAAAAAAATAATCA TAATACTTCGTACGCTGCAGGTCGAC
15.113	Klrho5del3	AACCAGGAAGTAAGGAACAAAAAAAAAAAAAAAAAGGAAATGAAT CCACTCTAGCATAGGCCACTAGTGGATCTG
15.156	KILMO1wvor	CAGTCATATTCAATCCATCTAC
15.157	KILMO1wnach	GGGACACGGGTTTCGATTCTCG
15.180	KIRHO5wvor	GGTAACTCGCATCACTTAGG
15.181	KIRHO5wnach	GGCGACTAACTACGCTGGTG
19.096	Klcdc42del5	AAAGGCCTGCAGTGATAGTAGTATAAAAGCAAGGAAGAAAG GAATTTAAAACCTTCGTACGCTGCAGGTCGAC
19.097	Klcdc42del3	CTGATACATGTAAGTAAATAAAAAAAAAAAAAAAAAATACAAGGCCG ATCACTTTTGCATAGGCCACTAGTGGATCTG
21.086	CDC42ww_for	TTTACCCTTTGTAGCCACA
21.087	CDC42ww_rev	CTGAGCCATCGTTCAGTGTT
18.260	KILMO1-GFPgenomfor	GCATTTTACTTGGAGAGTACAGAGAG

2. Material and Methods

18.261	KILMO1-GFPgenomrev	CTATGTTCTTAGTTTTGGCTTAATTATCAATGCGCATGAAAATT CATTATACTGGATGGCGGCGTTAGTA
18.258	KIDCK1-GFPgenomfor	GATCTGCTGGAAGTAACGGAAGTG
18.259	KIDCK1-GFPgenomrev	TACATGAGGTGAGAATTAGAACAGTTGCAGTGGGAGAAAGTT ATTCTATGACTGGATGGCGGCGTTAGTA
18.139	GFPRHO5SKHISindelrev	TGGTTTTCTGAGATGTTCCGACTCCTGCACAGCCTTTATAATG GGCCAATGAAT TCCACTTTGTAACCTA
18.140	GFPRHO5SkHISindelrev	TTAAACATCAGCATTATTCTTATCCCATACATCATGTATATAAG AACGAACTGGATGGCGGCGTTAGTAT
15.064	KILEU2intfor	GATCTAGAATAATGTGGCAAAGG
15.065	KILEU2intrev	TTTAGATTTAACACATTGCAGG
20.193	KICDC42forSal	GTGAGTCGACTATGCAAACCTCTTAAGTGTGTTG
20.194	KICDC42revSph	GAGCGCATGCGTAGTTTTAGGATGTTGGTTTAG

All oligonucleotides were custom synthesized by Biologio (Nijmegen, Netherlands).

2.2 Methods

2.2.1 Methods for *E. coli*

2.2.1.1 Freeze transformation of *E. coli* (Hanahan, 1983)

E. coli were incubated in 5 ml LB₀ medium with shaking at 180 rpm overnight at 37 °C. 100 ml of culture were then inoculated at a starting OD₆₀₀ of 0.1 and grown to reach an OD₆₀₀ of 0.4 to 0.6. Afterwards the cells were incubated for 30 min on ice, harvested at 11000 g and 4 °C, the pellet was resuspended in 40 ml RF1 (100 mM RbCl, 50 mM MnCl, 30 mM KAc, 10 mM CaCl₂, 15 % (v/v) glycerine, adjusting PH to 5.8 with acetic acid) solution, and incubated for one to two hours on ice. Cells were pelleted for 10 min at 11000 g and 4 °C, resuspended in 8 ml RF2 (10 mM MOPS, 10 mM RbCl, 75 mM CaCl₂, 15 % (v/v) glycerine, adjusting pH to 6.8 with acetic acid) solution and incubated on ice for 15 min. 100 µl aliquots were distributed in sterile 1,5 ml Eppendorf tubes under a clean bench and on ice. The aliquots were stored at -70 °C until use (up to several months).

For transformation, the frozen competent *E. coli* aliquots were thawed on ice for 10 min. Then 0.5 µl to 10 µl of plasmid-DNA or a ligation reaction were added and cautiously mixed with the tip of the pipette, followed by a 30 min incubation on ice. After a heat shock for 90 sec at 42 °C cells were put on ice for 1-2 min, and 800 µl LB₀ were added. To allow for the expression of the resistance gene and regeneration, cells were incubated for 45 min at 37 °C on a rotator at 120 rpm. Cells were collected by centrifugation at 2400 g and the supernatant was discarded. The pellet was resuspended in the remaining liquid and plated onto selective medium.

2. Material and Methods

2.2.1.2 Plasmid isolation from *E. coli* (with the GeneJET Plasmid Miniprep Kit from Thermo Scientific)

Purified plasmid DNA was prepared using the GeneJET Plasmid Miniprep Kit from Thermo Scientific. 2 ml of an overnight culture were centrifuged at 13800 g, the supernatant was discarded and the pellet resuspended in 250 μ l of resuspension buffer. 250 μ l lysis solution were added and the solution was gently mixed by inversion. Then, 350 μ l of neutralization solution were added and mixed by inversion, followed by a centrifugation step at 13800 g followed and the transfer of 800 μ l of the supernatant into the supplied GeneJET columns, which were centrifuged at 13800 g for 1 min. The flow-through was discarded followed by a washing step with 500 μ l washing solution and 1 min of centrifugation at 13800 g. This step was repeated and the columns were centrifuged dry at 13800 g for 1 min, put into a 1.5 ml Eppendorf cup and 50 μ l elution buffer were added to the columns, followed by an incubation for 2 min at room temperature and centrifugation at 13800 g for 2 min. The eluted plasmid DNA was stored at -20 °C.

2.2.2 Methods for yeasts

Yeasts were generally handled by standard procedures described in Methods in Yeast Genetics: A Cold Spring Harbor Laboratory Course Manual

2.2.2.1 Preparation of overnight cultures

3-5 ml of YEPD were inoculated with a yeast culture, either from a liquid culture or from a colony. They were then grown for approximately 16 h at 30 °C on a shaker set at 180 rpm. For selection, either SCD medium lacking certain bases or amino acids or YEPD medium containing G418 was used.

2.2.2.2 Growth curves

Overnight cultures were inoculated to an $OD_{600} = 0.3$ and then grown to an $OD_{600} = 1.0$. A 96 well plate with lid was prepared with 90 μ l YEPD per well with or without the agents in question, and each well was inoculated with 10 μ l of culture. Three technical replicas per condition at a starting OD_{600} of 0.1 were recorded. The blank and all empty wells were

2. Material and Methods

filled with 100 µl YEPD. All outside wells of the four borders were filled with 1.7 ml of sterile water to avoid desiccation. The OD₆₀₀ was recorded every 20-30 min, with shaking at 1024 rpm in 5 second intervals. Acquired data were transferred to an excel sheet and normalized by dividing the values by 0.282 (path length of the cell culture) to allow comparison with conventional photometer readings. The employed plate reader was the Varioskan Lux plate reader from Thermo Scientific (Waltham, USA) together with the SkanIt 6.1 software.

2.2.2.3 Determination of chronological lifespan (CLS)

For CLS measurements 50 ml SCD were inoculated with an overnight culture to a OD₆₀₀ of 0.1 and grown to stationary phase at 30 °C with shaking at 180 rpm. 150 µl of each culture were removed in regular intervals to determine the number of colony forming units (CFU, cells per undiluted ml). 50 µl (diluted 1:20) were used to measure the OD₆₀₀ and the remaining 100 µl were used for a serial dilution. Two of the dilutions, resulting in approximately 20-200 cells per plate, were plated on YEPD, incubated at 30 °C for 3 days and counted. Cell survival was followed until less than 20 CFUs could be observed for 100 µl of the undiluted culture.

2.2.2.4 Freeze-transformation of *K. lactis* (Klebe *et al.*, 1983)

Yeast cells were grown over night in liquid media, freshly inoculated in 50 ml YEPD at a starting density of OD₆₀₀ 0.2 and grown to an OD₆₀₀ between 0.6 - 1.0. After harvesting the cells by centrifugation at 900 g for 3 min, they were washed with 10 ml solution A (1 M Sorbit, 10 mM Bicine pH 8.35, 3 % (v/v) ethylenglycol) and centrifuged at 900 g for 3 min. The pellet was resuspended in 4 ml solution A and divided into 0.2 ml aliquots in sterile 1.5 ml Eppendorf tubes, which were stored at -70 °C for at least one day until use (up to 2 years).

For transformation, 20 µl of PCR product or 5 µl of plasmid DNA, were added directly onto the frozen cells, along with 5 µl of herring sperm DNA (5 µl of a sterile sonicated solution with 10 mg/ml) and 5 µl of a sterile CaCl₂ solution (2 M). After incubation with shaking at 37 °C for 5 min, 500 µl of solution B (40 % (v/v) PEG1000, 200 mM Bicine pH 8.35) were added and the cells were incubated for 1-2 hours at 30 °C. Afterwards, the

2. Material and Methods

cells were collected at 900 g for 3 min, and the supernatant was discarded. The cells were resuspended in the remaining liquid and plated onto selection medium and incubated for 2-3 days at 30 °C. For selection of G418 resistance, cells were incubated at least 3 h in liquid YEPD before plating, to allow for expression of the resistance cassette. At least three independent colonies were picked onto selective master plates, which were again incubated over night at 30 °C

2.2.2.5 Fast extraction of genomic DNA from yeast (Robzyk & Kassir, 1992)

A small amount of cells was picked from a plate and thoroughly suspended in 50 µl of a 20 mM NaOH solution in a 1.5 ml Eppendorf tube. After incubation for 2 min at room temperature, the reaction tube was placed into the microwave oven for 2 min at 600 W, mixed vigorously, and incubated for 5 min at room temperature. 2 µl were directly transferred into 50 µl of the PCR reaction mixture.

2.2.2.6 Medium-scale extraction of genomic DNA from yeast

1.5 ml of an overnight culture were transferred into a 1.5 ml Eppendorf tube, centrifuged at 900 g for 1 min and resuspended in 300 µl spheroplast buffer (0.9 M Sorbit, 0.1 M EDTA). After addition of 4 µl of Zymolyase 20T (12.5 mg/ml) and incubation at 37 °C for 1 hour, 50 µl SDS (10 %) and 50 µl EDTA (0.5 M, pH 8.0) were added, followed by an incubation at 65 °C for 5 min. Then the sample was incubated for 5 min at room temperature, before 150 µl KAc (5M, pH 8.6) were added and the cells were incubated for 1 hour on ice. Afterwards, the sample was centrifuged for 10 min at 4 °C and 10620 g and 500 µl of the supernatant were transferred to a new 1.5 ml Eppendorf tube. 340 µl of isopropanol were added, followed by a 5 min incubation at room temperature and centrifugation for 15 min at 4 °C and 17940 g. Then the pellet was washed with 1 ml 70 % (v/v) ethanol and centrifuged at 17940 g for 5 min. The ethanol was carefully decanted and the pellet dried. The dried pellet was resuspended in 50 µl sterile water and used either directly as template for PCR reactions or stored at -20 °C.

2. Material and Methods

2.2.2.7 Mating of yeast strains

Two strains with opposite mating types and complementary auxotrophies were streaked out against each other, on plates with either YEPD (*S. cerevisiae*) or malt extract agar (*K. lactis*). The plates were incubated at 30 °C over night. and replica-plated onto appropriate media for selection of diploids.

2.2.2.8 Sporulation and tetrad dissection

Diploid strains were grown over night in liquid YEPD, harvested by centrifugation for 3 min at 900 g and dropped onto a potassium acetate plate. After incubation for 2-3 days at 30 °C formation of asci was checked under the light microscope. A small amount of asci was then suspended in 100 µl of sterile water in a 1.5 ml Eppendorf tube and 4 µl of Zymolyase 20T (12.5 mg/ml) were added. The suspension was incubated for 10 min at room temperature and 15 µl were streaked onto a YEPD plate for tetrad dissection. Plates were incubated for 2-3 days at 30 °C to allow for the growth of the segregants. Colonies were either picked onto a masterplate or directly replica-plated on selective media for tetrad analysis. For tetrad dissection the micromanipulator (MSN system) from Singer Instruments (Mainz, Germany) with a Cassiopeia pocket pc from Casio was used.

2.2.2.9 Plasmid isolation from yeast

5 ml of an overnight culture of yeast cells grown on selective medium for plasmid-maintenance were centrifuged for 3 min at 900 g, the supernatant was discarded and the pellet resuspended in 400 µl resuspension buffer (Thermo scientific Plasmid isolation kit). 500 µl of glass beads (with a diameter of 0.3-0.5 mm, Roth, Karlsruhe, Germany) were added and vigorously shaken at 4 °C for at least half an hour. 250 µl of the solution without glass beads were transferred into a new 1.5 ml Eppendorf tube. The following steps followed the procedure for the plasmid isolation from *E. coli* (starting with the addition of lysis buffer), as described in 2.1.2. Plasmid DNA was eluted from the columns with 20 µl elution buffer, preheated to 50 °C. 10 µl of the isolated plasmid were employed to transform *E. coli*, as described in 2.1.1.

2. Material and Methods

2.2.2.10 Fluorescence microscopy (Schmitz *et al.*, 2015)

3 ml of overnight cultures were inoculated to an OD₆₀₀ 0.3 in synthetic medium and then grown for approximately 3-5 h at 30 °C to the logarithmic phase. For observation under standard conditions 2.5 µl of the culture were put on a slide, topped by with a cover slip, sealed with liquid glue if necessary, and then examined in the microscope.

For application of oxidative stress H₂O₂ was added at a final concentration of 4.4mM to the culture before preparation for microscopy. To study glucose starvation, cells were transferred to synthetic medium without carbon source and incubated with shaking at 30 °C for 30 min. Prior to examination of these samples, the remaining cells were re-inoculated in fresh SCD medium and again incubated for 30 min at 30 °C for comparison.

For time-lapse imaging, cells were diluted 1:5 in fresh medium and 2.5 µl of logarithmically growing cells were transferred to a slide containing freshly dried solid synthetic medium, prepared with 1 % agarose. They then were covered with a large cover slip and sealed by putting liquid adhesive around the edges of the cover slip. Slides were incubated for 45 min at 30 °C and then examined under the microscope, with images taken every 4-5 min for the next 18-20 h. If not stated otherwise brightfield images were exposed for 20 ms and fluorescent images for 500 ms.

For staining with Calcofluor white (CFW), cells were collected from 1 ml of logarithmically growing liquid cultures by centrifugation at 900 g for 3 min. The pellet was resuspended in 100 µl SCD and 1 µl CFW (10 mg/ml) was added. The cells were then incubated for 5 min in the dark, washed with 1 ml SCD and collected by centrifuged for 3 min at 900 g. The supernatant was discarded and the pellet resuspended in 100 µl SCD, 2.5 µl of which were then microscopically examined

Vacuoles were stained with CMAC (7-amino-4-chloromethylcoumarin) by harvesting 1 ml of logarithmically growing cells at 900 g for 3 min. The pellet was resuspended in 100 µl SCD and 1 µl CMAC (10 mM) was added. After incubation for 30-60 min at room temperature, the sample was washed with 1 ml SCD and again centrifuged for 3min at 900 g. The supernatant was discarded and the pellet resuspended in 100 µl SCD for microscopy.

2. Material and Methods

The microscope setup employed a Zeiss Axioplan 2 (Carl Zeiss, Jena, Germany) with a 100x alpha-Plan Fluor objective (numerical aperture 1.45) and differential interference contrast (DIC), equipped with a Hamamatsu digital camera C11440 ORCAFlash 4.0LT and a SPECTRA X light engine from Lumencor. The images were processed with the Metamorph program from the Universal Imaging Corporation and deconvolved with the Huygens Pro deconvolution program.

2.2.2.11 Transmission electron microscopy (Backhaus *et al.*, 2010)

TEM imaging was performed by Christian Meyer from the zoology department (University of Osnabrück). In preparation for TEM, 30 OD₆₀₀ units of exponentially growing cells were prefixed with 3xFIX (6 % Glutaraldehyde, 600 mM sorbitol, 300mM PIPES, 3 mM MgCl₂, 3 mM CaCl₂) for 5 min at room temperature. Therefore, the cells were harvested by centrifugation and then incubated for 30 min with 1xFIX at room temperature. Cells were then washed three times with water and fixed with freshly prepared KMnO₄ 3 % (w/v) for 15 hours at 8 °C. Then they were washed four times with water and incubated in 1 % (w/v) NaIO₃ for 15 min at room temperature. Cells were again washed with water, then resuspended in 50 mM (NH₄)₃PO₄ and incubated for another 15min at room temperature. The fixed cells were dehydrated by washing with increasing concentrations of ethanol (10-100 % v/v) and transferred to a 1:1 mixture of ethanol and acetone for 15 min, followed twice by incubation in acetone for 5 min. Next, the cells were incubated overnight in a 3:1 mixture of acetone:Epon812, which was then replaced by Epon812 for 7-8 h. Cells were then resuspended in fresh Epon812, which was polymerized for 72 h at 60 °C. Sections (70 nm thick) were cut with a diamond knife on a Leica Ultracut UC7 ultramicrotome. The cells were then transferred to single slot grids, stained with 2 % uranyl acetate and lead citrate and examined with a Zeiss TEM 902A electron microscope at 80 kV.

2. Material and Methods

2.2.3 Methods for DNA analysis

2.2.3.1 Agarose gel electrophoresis

For gel electrophoresis 1% agarose gels in 1x TAE buffer (1:50 diluted in sterile water from a 50x stock solution (24.2 % (m/v) Tris, 10 % (v/v) 0.5 M EDTA (pH 8.0), 5.72 % (v/v) acetic acid)) were used. Electrophoresis was run for 50-55 min at 90 V. For staining of DNA, the gel was incubated for 20 min in ethidium bromide (300 ml sterile water containing 100 μ l of a 1 % ethidium bromide solution). For

visualization of the bands, the Bio-Print gel documentation (Vilber Lourmat, Eberhardzell, Germany) was employed. The “GeneRuler 1 kb DNA Ladder” from Thermo Fisher (Waltham, USA) was used as size standard (Figure 8). For extraction of specific bands and their purification the “GeneJet Gel Extraction Kit” (Thermo Fisher Scientific, Waltham, USA) was employed, as specified by the manufacturer.

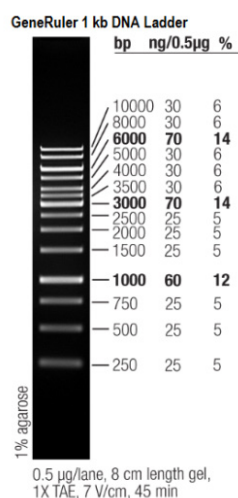


Figure 8: Pattern and concentration of the GeneRuler 1 kb DNA ladder. (taken from the Thermo Scientific user guide for the product, version of 2019).

2.2.3.2 Polymerase chain reaction (PCR)

For control PCRs 0.5 μ l DreamTaq polymerase (200 U/ μ l; Thermo Fisher Scientific) were used per. For all other reactions, either 0.5 μ l Phire Hot Start II DNA Polymerase (Thermo Fisher Scientific) or Phusion High-Fidelity DNA Polymerase (2 U/ μ l; Thermo Fisher Scientific) were used per reaction. PCRs were routinely prepared in 0.2 ml Eppendorf tubes, containing 0.5 μ l of the polymerase, 1 μ l each of the forward and backward primer (10 pmoles/ μ l), 3 μ l of plasmid or 5 μ l genomic DNA (corresponding to approximately 10 ng and 200 ng of DNA, respectively), 5 μ l of a 0.2 mM mixture of the four desoxyribose nucleotide triphosphates (dNTPs) and either 5 μ l of 10x concentrated buffer solution or 10 μ l of 5x concentrated buffer solution, as provided by the manufacturer, adjusted to a total volume of 50 μ l with sterile water. The PCR products were purified with the “GeneJet PCR purification Kit” (Thermo Fisher Scientific, Waltham, USA), following the manufacturers specifications. For determination of mating types, a mixture of three

2. Material and Methods

primers was employed (*S. cerevisiae*: 05.135, 05.136, 05.137; *K. lactis*: 06.54, 06.55, 06.56) for PCR reactions. Two representative PCR programs employed are given in Table 4.

Table 4: standard PCR programs

Routine programming for PCR reactions		
Steps	Temperature	Duration
Initial denaturation	95 °C	10 min
Denaturation	95 °C	45 sec
Annealing	Dependent on primers	30 sec
Elongation* ¹	68 °C /72 °C	1 min /20 sec per 1000 bp
Final elongation* ¹	68 °C / 72 °C	10 min
PCR programm for determination of mating types		
Steps	Temperature	Duration
First denaturation	96 °C	10 min
Second denaturation	50 °C	10 min
Denaturation	94 °C	30 sec
Annealing	55 °C	30 sec
Elongation* ²	72 °C	40 sec / 90 sec
Final elongation	68 °C	8 min

*¹ Dream Taq Polymerase: 68 °C and 1 min per 1000 bp; Phire Hot Start II DNA Polymerase or Phusion High-Fidelity DNA Polymerase: 72 °C and 20 sec per 1000 bp.

*² 40 sec for *S. cerevisiae* and 90 sec for *K. lactis*.

Expected PCR products for the mating types are: *S. cerevisiae* MAT_a = 544 bp and MAT_α = 404 bp; *K. lactis* MAT_a = 1.45 kbp and MAT_α = 1.13 kbp.

2.2.3.3 Use of restriction endonucleases

For verification of restriction sites and cloning, plasmids or PCR products were digested in a total volume of 20 µl, containing 4 µl of plasmid (approximately 20 ng), 0.6 µl of restriction enzyme (New England Biolabs, Ipswich, USA) and 2 µl 10x buffer solution, as provided by the manufacturer, adjusted with sterile water. If DNA fragments were to be exercised from plasmid for yeast transformation and homologous recombination 50 µl approaches were used and the volumes were adjusted accordingly. Furthermore, 1 µl alkaline phosphatase was added to inhibit relegation of the vector. The samples were digested for a minimum of 30 min at 37 °C, if not otherwise recommended by the manufacturer.

2. Material and Methods

2.2.3.4 Ligation

For subcloning, fragments with matching sticky ends were ligated *in vitro*. Ligations were carried out in a total volume of 20 μ l, in which plasmid backbone and DNA fragment to be inserted were mixed in an appropriate molar ratio of 1:10, with 1 μ l T4-DNA-Ligase (5 units), 2 μ l 10x ligase buffer (40 mM Tris/HCl, 10 mM DTT and 0.5 mM ATP, pH 7.4) and adjusted with sterile water. Ligations were incubated for 1 h at room temperature and then used to transform *E. coli* as described in 2.2.1.1.

2.2.3.5 Sequencing

Custom sequencing was performed by Microsynth/SeqLab (Göttingen, Germany) with plasmid DNA or PCR samples prepared with premixed primers as specified by the company

2.2.3.6 DNA synthesis

DNA synthesis was done by Thermo Fisher Scientific (Waltham, USA) with their “GeneArt String Synthesis” method

3. Results

In this thesis the role of the small GTPase Rho5 and its activating dimeric GEF (Dck1/Lmo1), further referred to as the DLR complex, were investigated in the yeast *Kluyveromyces lactis* by both genetic and cell biological approaches. The construction and physiological characterization of *Klrho5*, *Kldck1* and *Kllmo1* deletion mutants was instrumental for this purpose.

3.1 *In silico* analyses of the primary sequences of the DLR complex

The components of the DLR complex in *K. lactis* were first identified by their homology to their *S. cerevisiae* counterparts, which have been extensively studied. Alignments of the deduced amino acid sequences (Figure 9) revealed that the overall domain structure of the proteins was conserved. Thus, the amino acid identities between the yeast proteins were 47% for Rho5, 38% for Dck1 and 27% for Lmo1. Furthermore, the alignment shows that putative functional domains were conserved in all three proteins. This was the case for the Dck1 SH3, DHR1 and DHR2 domains, as well as for the Lmo1 PH, EAD and Elmo domains. For the Rho5 homologues a high conservation of the PBR and the switch I and II domains could be observed. The ScRho5 amino acid sequence displayed two extended regions that seemed to be absent or drastically shortened in the homologous proteins of *K. lactis* and humans. The first one consists of 22 amino acids located between the switch I and II regions. The second one extends from Pro221 to Asp320 prior to the PBR-CAAX regions and is necessary for proper function of ScRho5 (Sterk *et al.*, 2019). The lower amino acid identity between full-length *HsRac1* and ScRho5 (32%), compared to the one between *HsRac1* and *KlRho5* (43%), can also be attributed to the longer yeast-specific extensions of ScRho5.

3. Results

only aligned to their *S. cerevisiae* homologues. Conserved functional domains are indicated by boxes and designated. The *ScRho5*-specific extension, also indicated by a box, is not present in *HsRac1* and only as a shortened version in *K/Rho5* (from Musielak *et al.*, 2021).

3.2 Mutant and complementation analyses

The physiological importance of proteins in yeast is routinely assessed by construction of deletions in their encoding genes and determination of the associated phenotypes. These often provide a first hint for possible relations to signalling pathways and/or interaction partners that can be further examined. Moreover, pronounced phenotypes can be used for heterologous complementation and suppression studies, in order to elucidate protein functions and regulatory.

3.2.1 *K/DLR* mutants do not display pronounced growth defects under standard growth conditions

Previous tetrad analyses indicated that deletion mutants lacking either of the three *K/DLR* components did not display any growth defects on standard rich medium, compared to the wild type, neither in *K. lactis* nor *S. cerevisiae*.

However, synthetic growth defects or synthetic lethality was observed for *Scrho5* deletions with *Scsch9*, *Scgpa1*, *Scgpa2* and *Scras2* mutants (Schmitz *et al.*, 2018). In a search for a strong selectable phenotype in *K. lactis*, the *Klrho5* deletion strain was therefore crossed to several strains carrying deletions in a number of candidate genes expected to show synthetic phenotypes. Different physiological processes were targeted in this screen: i) Genes encoding components in the pentose phosphate pathway (*KIZWF1*, *KIRPE1*, *KITAL1*). ii) Genes for CWI signal transduction components (*KIMPK1*, *KIBCK1*, *KIRLM1*). iii) Genes encoding components of the budding and cytokinesis machinery (*KIMYO1*, *KIHOF1*). iv) Genes involved in oxidative stress response (*KISOD1*, *KISOD2*). v) Genes for eisosome formation (*KIPIL1*, *KILSP1*). vi) Genes encoding components involved in nutrient signalling (*KISNF1*, *KISCH9*, *KIGPR1*). Furthermore, *KIPOR1*, expressing a mitochondrial voltage-dependent ion channel (VDAC), and *KITDP1*, involved in DNA repair, were also tested in this screen. Tetrad analyses of the resulting

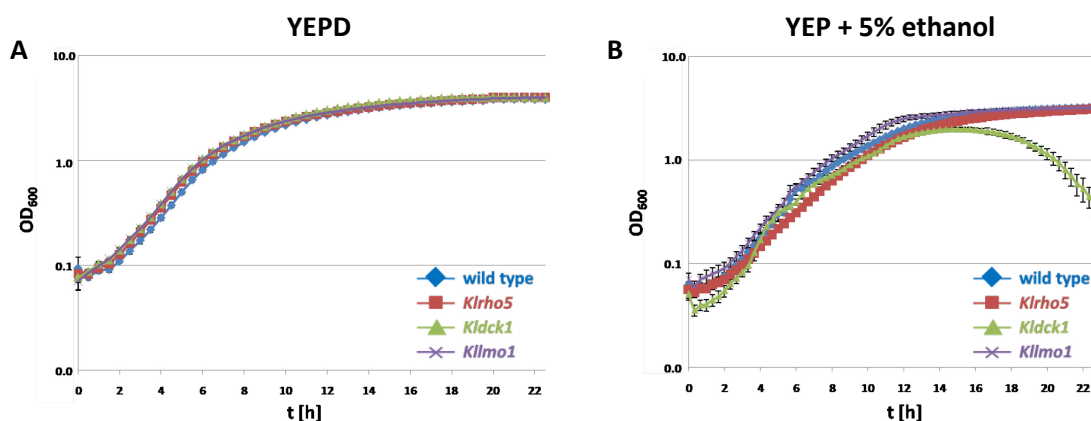
3. Results

diploids showed that none of the following genes appeared to genetically interact with *KIRHO5*.

3.2.2 Growth of *KIDL*R mutants upon application of different stresses

Scrho5 deletions, as well as strains lacking either of the two subunits of its GEF Dck1/Lmo1, are hyper-resistant to cell wall perturbing agents and oxidative stress (Schmitz *et al.*, 2002; Singh *et al.*, 2008). To test whether this is also true for *K. lactis*, growth curves of the respective deletions were recorded in different media (Figure 10)

Growth for all three deletions was indistinguishable from wild-type cells under standard conditions in rich medium with 2 % glucose as carbon source (Figure 10A). This was also generally observed when 5 % ethanol was employed as carbon source, with an unusual sensitivity only detected for the *Kldck1* deletion after reaching stationary phase (Figure 10B). In contrast, all the deletions were less sensitive towards hydrogen peroxide and also grew better than the wild type on acidic medium with 45 mM acetic acid (Figures. 10C and 10D). On the other hand, hyper-resistance of the deletions towards caffeine was comparatively marginal (Figure 10E). Finally, the wild type could cope better with the presence of the cell wall perturbing agent Calcofluor white, which more strongly reduced growth of the deletions (Figure 10F).



3. Results

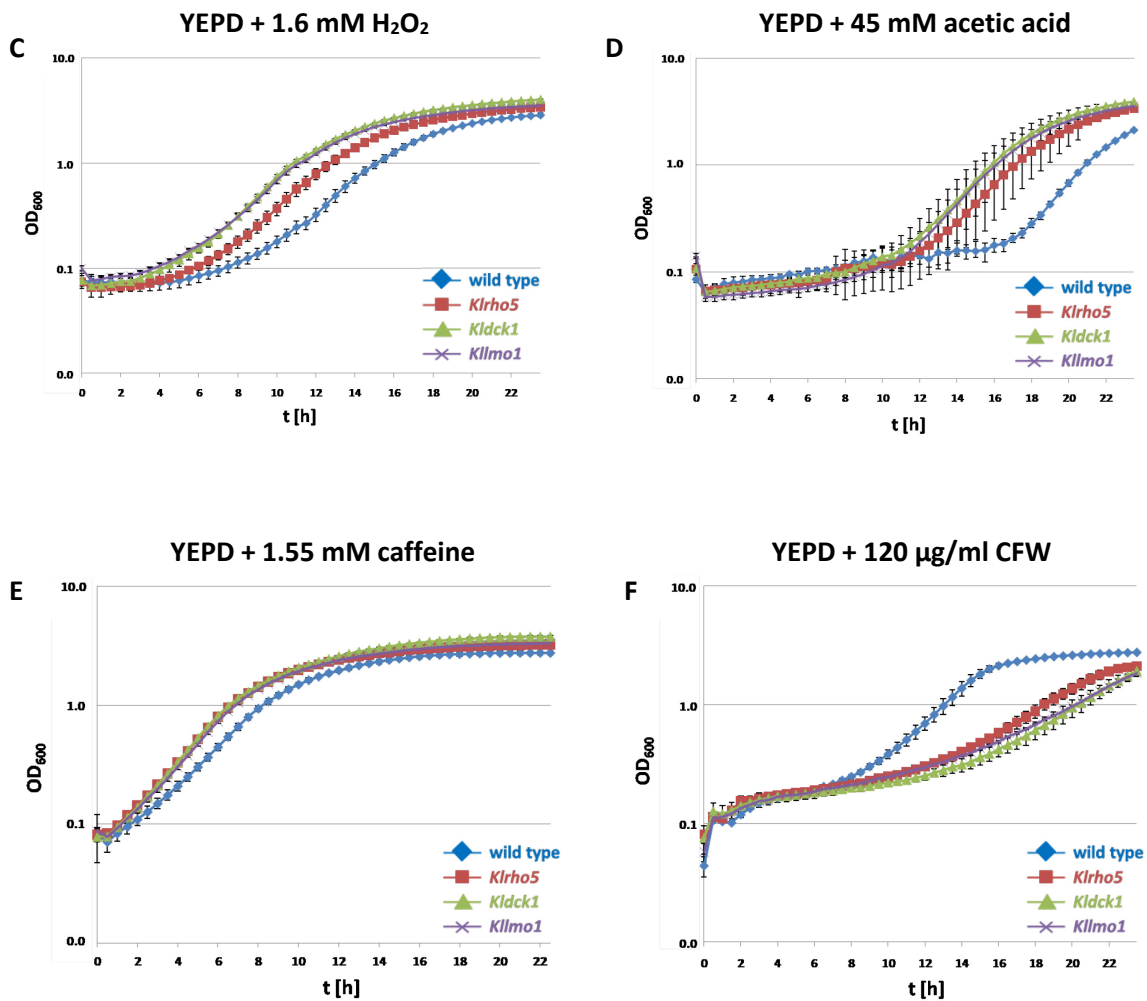


Figure 10: Comparative growth assays of wild-type and *K/DLR* deletion strains. The following strains were used for all depicted growth assays: KHO208-8B (*Klrho5*), KHO255-3A (*Kllmo1*), KHO218-9A (*Kldck1*) and KHO208-8A (wild type). Growth was followed in the indicated media for at least 23 h at 30 min intervals.

3.2.3 Effect of the *K/DLR* complex on the chronological lifespan

The chronological lifespan (CLS) is defined as the period of time non-dividing cells remain alive in stationary phase. Since *Scrho5* deletions were reported to have a shorter CLS than the wild type (Cao *et al.*, 2016), it was investigated in this thesis for *Klrho5*, *Kldck1* and *Kllmo1* deletion strains. As shown in Figure 11A, the number of colony forming units (CFU) decreased with a similar rate in all strains, including the wild type, leaving no detectable viability after 18 days. The apparent lack of an effect of *DLR* deletions in *K. lactis* on CLS prompted a similar investigation in *S. cerevisiae*. As evident from Figure 11B, and in contrast to the published data (Cao *et al.*, 2016), the CLS in the genetic background of our

3. Results

standard laboratory strain (DHD5) did not differ significantly between strains lacking either one of the ScDLR components and the wild type.

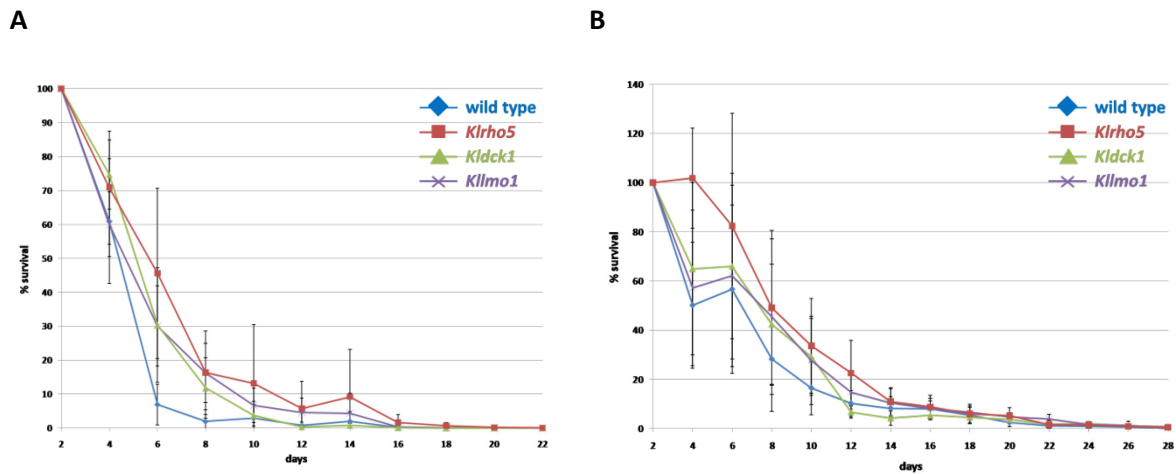


Figure 11: Chronological lifespan in yeasts lacking *K/DLR*-components. A) CLS in *K. lactis*. Three independent strains carrying the indicated deletion or being wild type were grown to stationary phase in synthetic complete medium. Samples were taken at the time points indicated, diluted to produce single colonies, plated on rich medium (YEPD), and incubated for three days to determine the number of colony forming units (CFU). CFUs were set at 100% at day 0, starting with approximately 4×10^8 viable cells/ml. Error bars give the standard deviations of % survivors in the three biological replicates. Strains employed were: wild types KHO208-8A, KHO254-5D, KHO259-7A; *Klrho5* deletions KHO208-8B, KHO276-2A, KHO277-3D; *Kldck1* deletions KHO218-9A, KMO01-14C, KHO254-1A; *Kllmo1* deletions KMO03-1D, KHO255-1B, KHO255-3A B) CLS in *S. cerevisiae*. Three independent cultures of the indicated deletions and wild-type strains were grown to stationary phase in synthetic complete medium. Samples were taken at the time points indicated, diluted to produce single colonies, plated on rich medium (YEPD) and incubated for three days to determine the number of colony forming units. CFUs were set at 100% at day 0, starting with approximately 7×10^7 viable cells/ml. Error bars give the standard deviations of % survivors in the three biological replicates. strains employed were: wild type HD56-5A; *Scrho5* deletion HAJ216-A; *Scdck1* deletion HAJ03-B; *Sclmo1* deletion HAJ201-B

3.2.4 *K. lactis* strains lacking DLR components display morphological defects

In previous works in this laboratory distinct morphological defects were noted in strains carrying a *Klrho5* deletion, which were addressed in the following. In fact, not only *Klrho5* deletions, but also strains with *Kldck1* and *Kllmo1* deletions, showed protrusions at their surface under the light microscope, which resembled an emerging bud (Figure 12). Staining with Calcofluor white (CFW), which stains chitin and therefore accumulates in

3. Results

and is used to visualize bud scars, showed that it uniformly distributed throughout the cell wall in all three mutants (Figure 12).

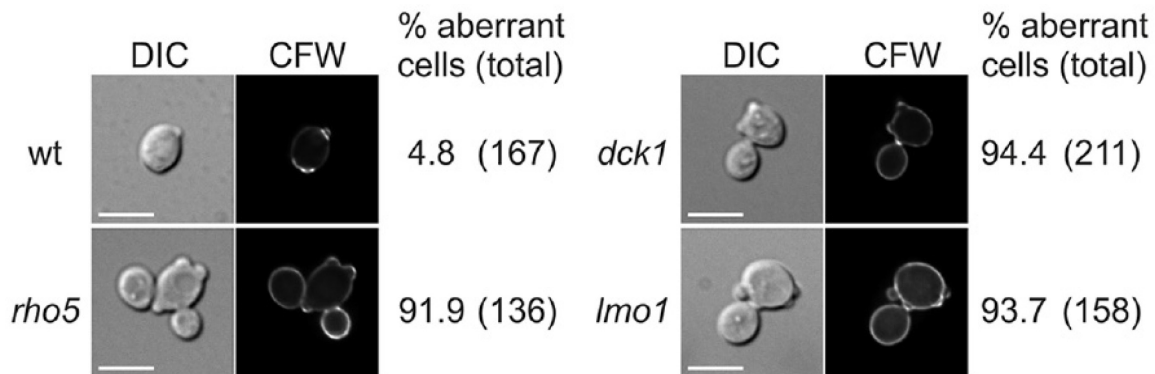


Figure 12: *K/DLR* deletion strains stained with Calcofluor white (CFW). Wild type (KHO208-8A) or a deletion strain lacking *KIRHO5* (KHO208-8B), *KIDCK1* (KHO218-9A) or *KILMO1* (KHO255-1B) were grown to logarithmic phase in SCD, stained with CFW and observed under the fluorescent microscope. Numbers to the right give the percentages of aberrant cells, i.e. with protruding bud scars and no normal bud scars, compared to the number of total cells counted (given in parenthesis). The scale bars correspond to 5 μ m (from Musielak *et al.*, 2021).

The number of protrusions varied and was apparent on the mother cells during all stages of the cell cycle that followed the budding of the daughter cell. To confirm that this phenotype was indeed caused by the deletions, first centromeric plasmids (based on pCse24, pCXJ18 and pCXs22) carrying the wild-type *KIRHO5*, *KIDCK1* and *KILMO1* genes were introduced into their respective deletion strains. This only led to a partial rescue of the protrusion phenotype, with approximately 65-75% of aberrant cells, as compared to strains carrying only the empty vector (94-97%). Since this may be due to a low mitotic stability of episomal vectors in *K. lactis*, the experiment was repeated with wild-type genes carried on plasmids which integrated into the *Klleu2* locus (*KIRHO5*=pMMO05, *KILMO1*=pMMO06, *KIDCK1*=pMMO07). This time 99% (n=209) of the *Klrho5*, 98% (n=103) of the *Kldck1* and 94% (n=118) of the *Kllmo1* strains with the integrated wild-type gene lacked apparent morphological defects. In contrast, more than 70% of the recipient strains or those carrying the empty vectors displayed aberrant protrusions.

To determine whether these protrusions were remnants after cytokinesis or due to an aborted budding mechanism, time-lapse images of growing cells were recorded

3. Results

(Figure 13). These clearly showed that cells budded normally, but left behind a protruding bud scar after cytokinesis was completed.

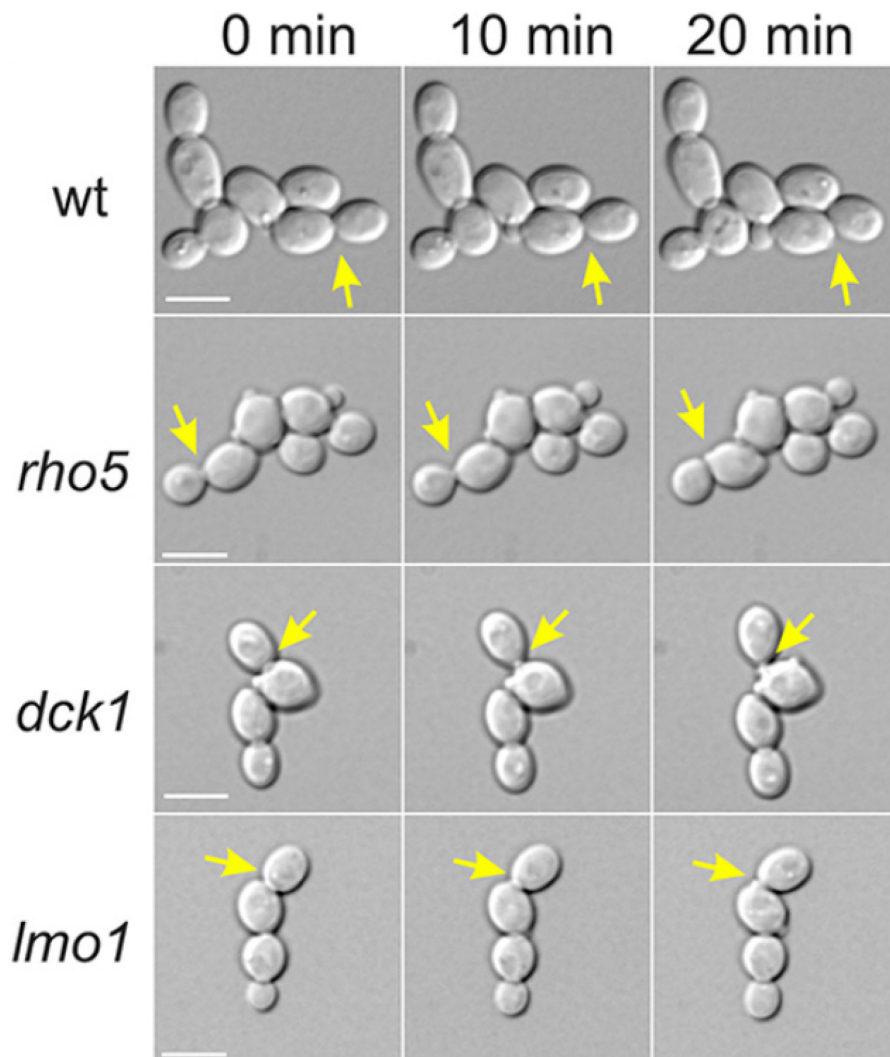


Figure 13: Frames from time-lapse imaging of wild-type and *KIDL*R deletion strains. Logarithmically growing cells were diluted 1:5 and transferred to a slide with SCD and 1% agarose. Slides were incubated for 45 min at 30 °C prior to microscopic examination for 18 hours. Images were recorded every 4 to 5 min. Depicted are selected images from a time-lapse series of a wild-type strain (KHO208-8A) and strains with deletions of either *KIRHO5* (KHO208-8A), *KIDCK1* (KHO208-9A) or *KILMO1* (KHO255-1B). The yellow arrows indicate active budding sites. The scale bar depicted in the right picture of every row resembles 5 μ m and is applicable to all pictures of the same row (from Musielak *et al.*, 2021).

3.2.4.1 TEM imaging of wild-type and *KIDL*R mutant cells

To further investigate the origin of the protrusions, transmission electron microscopy (TEM) was employed to examine the bud necks of cells undergoing cytokinesis. Whereas

3. Results

wild-type cells have a flat, slightly curved chitinous primary septum, cells from all three deletion mutants often displayed distorted primary septa, which were either extremely bent or did not even close properly (Figure 14). Multiple primary septae oriented towards the mother cell were also observed in some of the mutant cells.

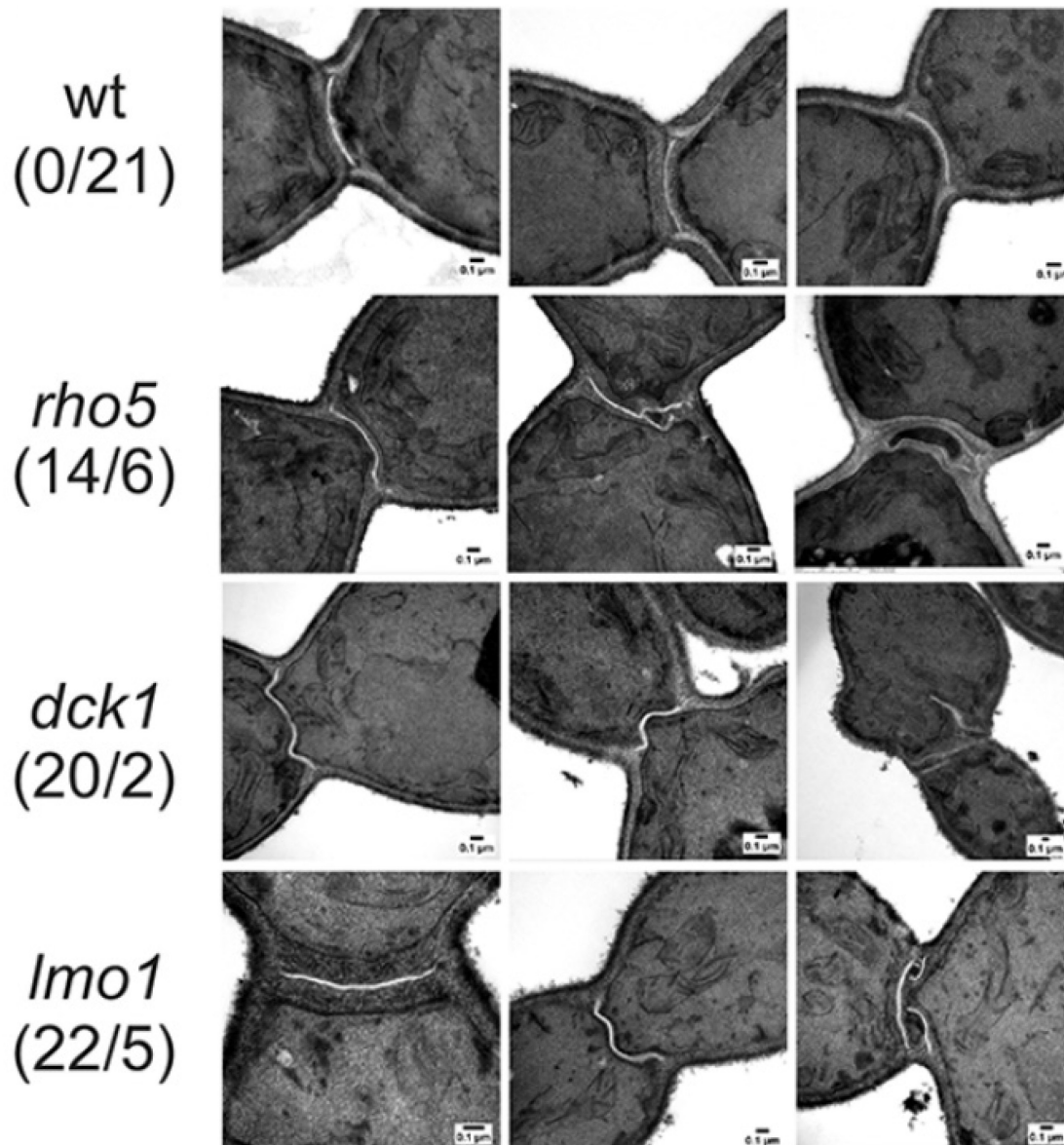
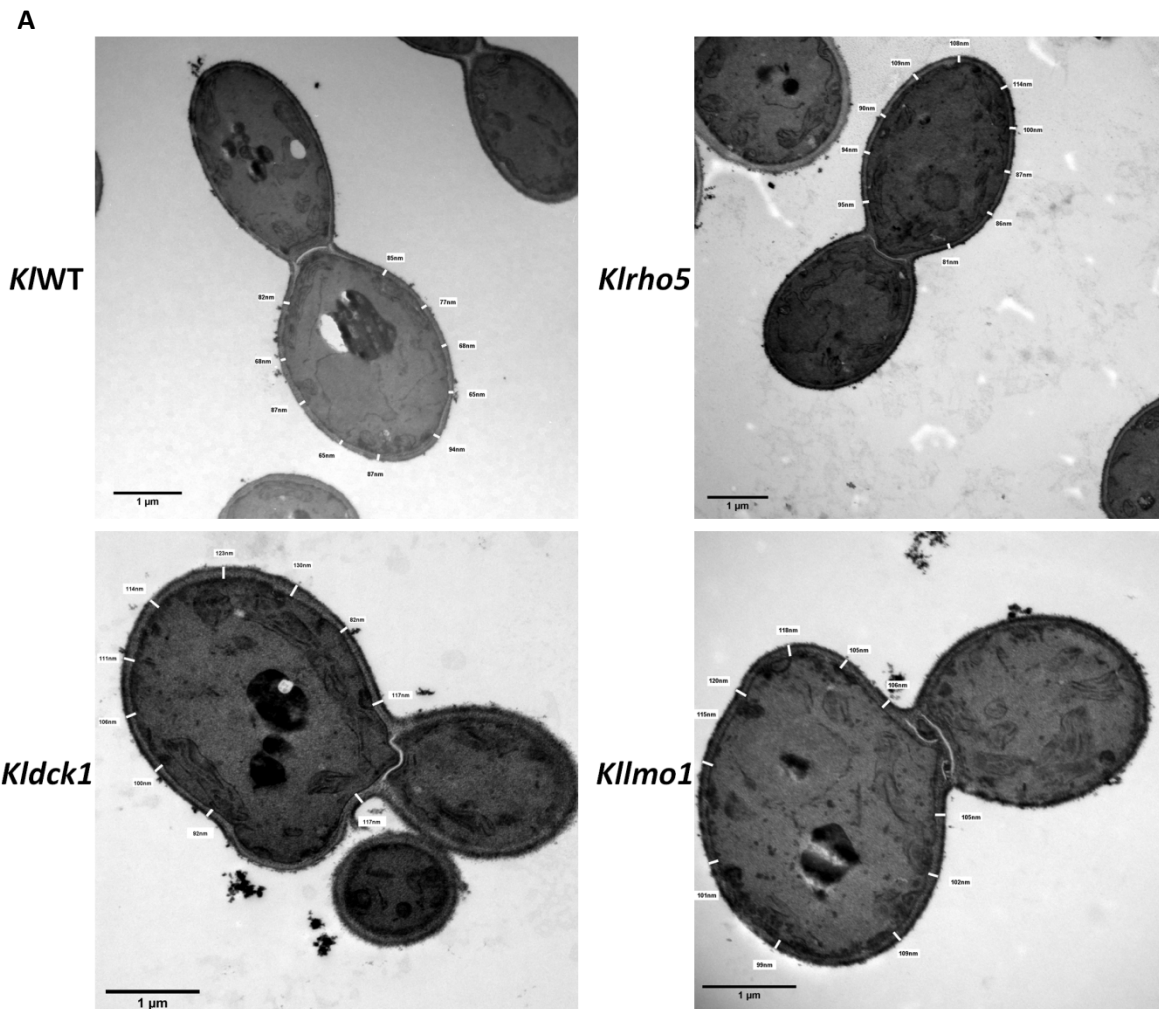


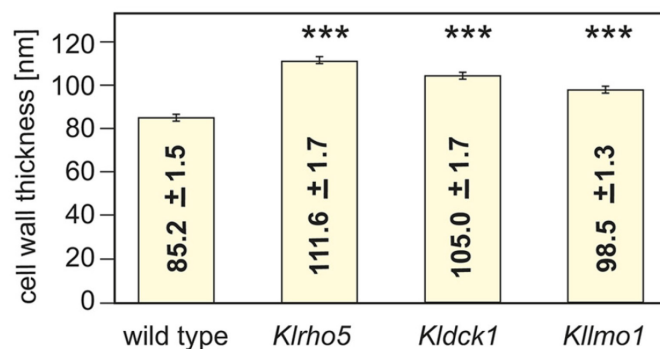
Figure 14: TEM images of wild-type and *K/DLR* deletion strains. Shown are three representative images, each, obtained from wild-type (CBS2359), *Klrho5* (KHO208-2B), *Kldck1* (KMO01-14C) or *Kllmo1* (KMO03-1D) deletion strains. The numbers in parenthesis indicate the ratio of aberrant cells versus normal cells. The scale bars depicted in the lower right corner of the images correspond to 0.1 μm (from Musielak *et al.*, 2021).

3. Results

The CWI pathway in *S. cerevisiae* governs cell wall maintenance and is required for proper cytokinesis. Since the sensitivity of *KIDLR* mutants to CFW and the morphological phenotype described above (chapter 3.2.2 and 3.2.4) suggested an involvement of *KIRho5* in CWI signalling and budding, it was investigated if it may also have an effect on the homeostasis of the cell wall. The average thickness of the cell wall was calculated from the TEM images (Figure 15) and revealed that *Klrho5*, *Kldck1*, *Kllmo1* deletion strains had a thicker cell wall compared to the wild-type controls.



B



3. Results

Figure 15: Measurement of the cell wall thickness in deletion and wild-type strains. A) Representative images for measuring cell wall thickness in wild-type (CBS2359), *Klrho5* (KHO208-2B), *Kldck1* (KMO01-14C) and *Klmyo1* (KMO03-1D) deletion strains. Cell wall thickness was measured at 10 points, each, in mother cells (white lines), intended to be equally distributed over the cell wall. Bud scars and the bud necks were excluded from measurements. Scale bars are 1 μm . B) Statistical analysis of cell wall thickness. Mean values and standard deviation are given for 10 measurement points per cell from 14 cells of each strain. P-values calculated using the two-sided *t*-test of Microsoft Excel showed the differences to be statistically significant, with values smaller than 0.001 (***) (from Musielak *et al.*, 2021).

3.2.4.2 GFP-*Klrho5* localizes to the bud neck during cytokinesis

The data reported above indicated that *Klrho5* may be involved in the regulation of budding and cytokinesis. It would thus be expected to appear at the bud neck of growing cells. To further investigate this hypothesis, a colocalization with known bud neck components was to be tested. In this context, *Klmyo1* encodes a central component of the actomyosin ring, which mediates the ingression of the plasma membrane during cytokinesis (Rippert *et al*, 2014). Since a *Klmyo1* deletion is temperature sensitive, but not lethal, a possible synthetic interaction with *Klrho5* was investigated, and the double deletion proved to be viable, as explained in chapter 3.2.1. In fact double deletions displayed both, the protrusion phenotype of *Klrho5* cells, and the multiple buds observed in *Klmyo1* deletions (Figure 16), indicating a lack of genetic interaction.

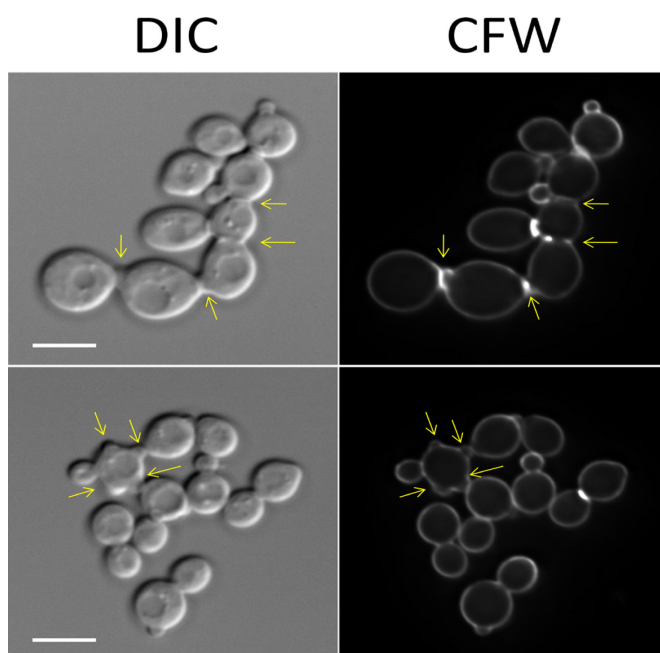
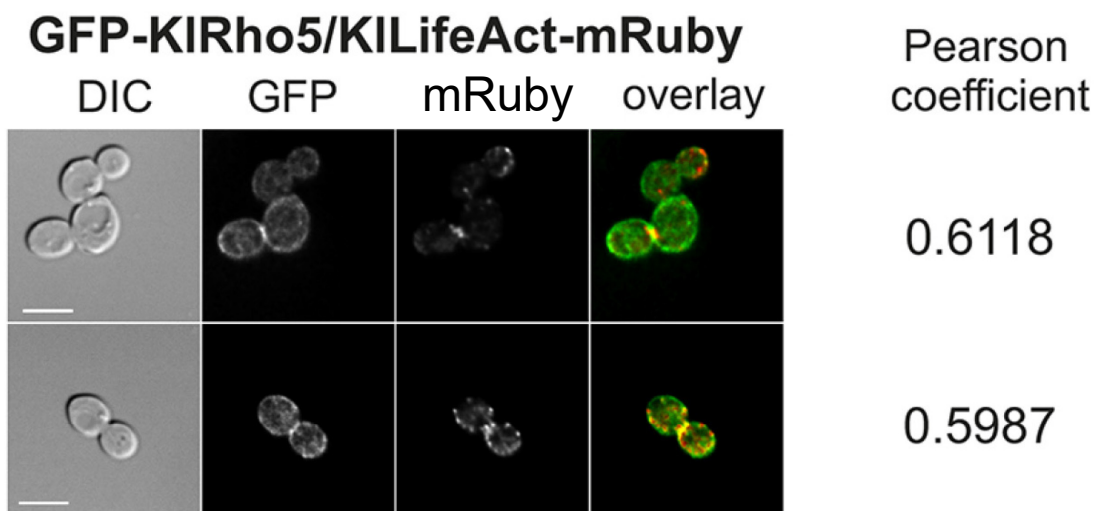


Figure 16: Microscopic images of the *Klrho5 Klmyo1* double deletion. Two representative images of haploid cells carrying the double deletion are shown (strain: KMO23-2D). The right hand images show cells stained with CFW. Yellow arrows point to phenotypes typical for a *Klmyo1* deletion (multiple budding; upper row) or a *Klrho5* deletion (surface protrusions; lower row). Scale bars are 5 μm .

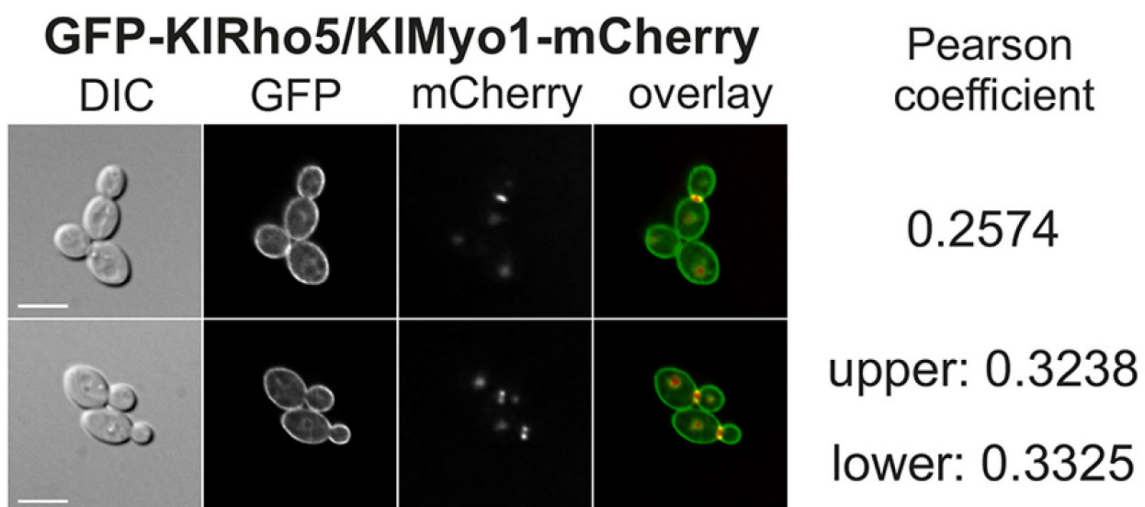
3. Results

To further investigate the function of *KIRho5* in cytokinesis, *KIMyo1-mCherry* and a *KLifeact* construct (*KIABP140frag-mRuby*) were employed for live cell fluorescence imaging. First, a plasmid containing *GFP-KIRHO5* and the gene encoding the *KLifeact-mRuby* fusion (pJJH2751) was integrated at the *KIleu2* locus of a wild-type strain (KHO46-6C). Second, a *KIMYO1-mCherry* gene fusion was combined by crossing and tetrad analysis with the *GFP-KIRHO5* gene fusion. Out of the 328 cells carrying the *KLifeact/GFP-KIRho5* combination 106 showed a colocalization of actin and *KIRho5* at the bud neck. The actin signal was also detected in membrane patches, as expected. In 20 cells that were examined in the later stages of cytokinesis, as indicated by their larger buds, *KIRho5* was still observed at the bud neck (Figure 17B upper row, lower cell), while actin was not detected and rather confined to patches of the lateral plasma membrane (Figure. 17A).

A



B



3. Results

Figure 17: Colocalization of *K/Rho5* with *K/Myo1* and actin at the bud neck. A) Representative images of 328 cells counted for KHO46-6D, containing *GFP-K/RHO5* and the gene expressing the *K/Lifeact* construct. Pearson coefficients are given for cells where both signals appear at the bud neck. B) Representative images of 238 cells counted for KMO30-4A (upper panel) and KMO30-6D (lower panel). Both contain *GFP-K/RHO5* and *K/Myo1-mCherry*. Pearson coefficients are given for each cell where both signals appear at the bud neck. The scale bars indicated on the left images of each panel correspond to 5 μm and are applicable to all pictures of the same row. In the overlay images, red indicates mCherry or mRuby signals, green GFP signals and yellow overlapping signals of both (from Musielak *et al.*, 2021).

K/Myo1 is one of the early proteins localizing to the bud neck (Rippert *et al.*, 2014). When checked for colocalization with *GFP-K/Rho5* it appeared primarily at the borders of the actomyosin ring, close to the plasma membrane. This was true for 157 out of 238 cells. Again in cells with larger buds that were in the later stages of cytokinesis, no *K/Myo1* could be observed, but *K/Rho5* accumulated at the bud neck (Figure 17B, upper row, lower cell). This was the case for 30 out of the 238 cells. To substantiate the observed colocalization, Pearson coefficients of both *K/Lifeact/GFP-K/Rho5* and *K/Myo1-mCherry/GFP-K/Rho5* were determined. On average, values of 0.44 +/- 0.22 were obtained for 22 cells with colocalization of *K/Myo1-mCherry* and *GFP-K/Rho5*. For the colocalization of *K/Lifeact-mRuby* and *GFP-K/Rho5* the average Pearson coefficient from 8 cells was 0.54 +/- 0.10. Furthermore, in deletion mutants of *K/RHO5*, *K/DCK1* and *K/LMO1*, both actin and *K/Myo1* localised in normal patterns at the bud neck (Data not shown).

3.2.5 Heterologous complementation of *rho5*-specific phenotypes in *S. cerevisiae* and *K. lactis*

A *Scrho5* deletion does not display strong phenotypes under standard growth conditions. However, it is synthetically lethal with a *Scsch9* deletion. Therefore, a diploid *S. cerevisiae* strain heterozygous for both deletion alleles (DAJ138) was used as a recipient to introduce the *K/RHO5* gene (pJJH2759) as well as the hyperactive allele *K/RHO5^{Q91H}*, followed by sporulation and tetrad analysis. As shown in Figure 18, both alleles rescued the growth defect of the double deletion, in contrast to those carrying the vector without any *RHO5* gene (YE_{p118JJH}).

3. Results

In contrast to *S. cerevisiae*, *Klrho5* deletions are not synthetically lethal with a *Klsch9* deletion (Musielak *et al.*, 2021), impeding a similar approach to test for heterologous complementation. Instead, *Klrho5* deletions display a distinct morphological defect with protruding bud scars on the cell surface (chapter 3.2.4). Since plasmids in *K. lactis* are also highly unstable and frequently lost during mitosis, stable inheritance can only be ensured by the use of integrative vectors. Thus, different *RHO5* variants, as well as the human *RAC1* gene, were integrated at the *Klleu2* locus and tested for their ability to restore a normal morphology to the growing yeast cells. As shown in Table 5, only the wild-type *KIRHO5* allele was able to complement the defect, whereas *ScrHO5*, its derivatives, or human Rac1 failed to do so.

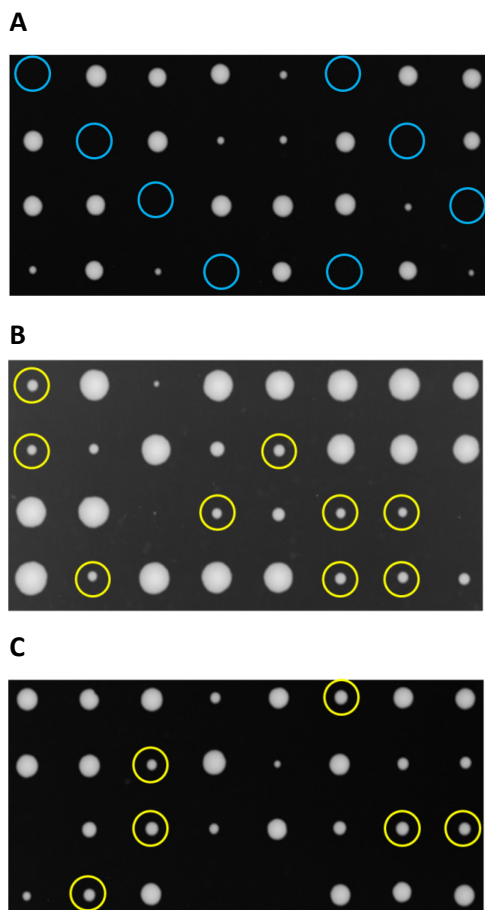


Figure 18: Complementation of the synthetic lethality of *Scrho5 Scsch9* double deletions. A) Tetrads of DAJ138 with the vector plasmid YEp118JJH. Blue circles mark the position of segregants deduced to carry a *Scrho5 Scsch9* double deletion. B) Tetrads of DAJ138 with the plasmid pJJH2759 (*KIRHO5*). Yellow circles mark colonies carrying the double deletion and the plasmid. C) Tetrads of DAJ138 with the plasmid pJJH2760 (*KIRHO5^{Q91H}*). Yellow circles mark colonies carrying the double deletion and the plasmid.

Note that small colonies are usually associated with the *Scsch9* deletion, whereas *Scrho5* deletions (not highlighted) do not display a pronounced growth defect as compared to wild-type segregants (Schmitz *et al.*, 2018).

Table 5: Complementation of the morphological defect of a *Klrho5* deletion with different homologues and alleles. The following plasmids were integrated into the recipient strain KHO208-8B: pJJH2357 (empty vector), pMHO011 (*KIRHO5* wild-type allele), pMHO017 (*KIRHO5^{Sc222-331}*, encoding *KIRho5* with its C-terminus exchanged for the one of *S. cerevisiae*), pMHO012 (*ScrHO5* wild-type allele), pMHO016 (constitutively active *ScrHO5^{Q91H}* allele), pMHO015 (constitutive active *ScrHO5^{G12V}* allele), pMHO014 (*ScrHO5^{Δ222-319}*, an allele missing the

3. Results

ScRho5-specific extension), pMHO013 (*HsRAC1* wild-type allele), pMHO018 (constitutively active *HsRAC1*^{G12V} allele), pMMO027 (*HsRAC1*^{K1200-254}, encoding *HsRac1* with the *KIRho5* C-Terminus from amino acid 200 onward cloned behind the Pro180 of *HsRac1*).

Integrated mutant allele	Frequency of aberrant cells [aberrant cells/total count]
none	119/123
<i>KIRHO5</i>	0/127
<i>KIRHO5</i> ^{Sc222-331}	120/125
<i>ScRHO5</i>	122/124
<i>ScRHO5</i> ^{Q91H}	126/128
<i>ScRHO5</i> ^{G12V}	119/121
<i>ScRHO5</i> ^{Δ222-319}	129/130
<i>HsRAC1</i>	119/120
<i>HsRAC1</i> ^{G12V}	119/123
<i>HsRAC1</i> ^{K1200-254}	126/127

3.3 Intracellular distribution of DLR components in *K. lactis*

For ScRho5 and its dimeric GEF a rapid translocation to the mitochondria could be observed under oxidative stress and glucose starvation (Schmitz *et al.*, 2015, 2018). In the following, the distribution of the homologues in *K. lactis* was investigated.

3.3.1 *KIRho5*, *KIDck1* and *KILmo1* associate with mitochondria upon oxidative stress

The increased resistance of the *Klrho5*, *Kldck1* and *Kllmo1* deletions against hydrogen peroxide suggested that the proteins in *K. lactis* encoded by the wild-type genes serve similar functions as their *S. cerevisiae* counterparts in the cellular response to oxidative stress. Since all three proteins translocate rapidly to the mitochondria upon exposure to H₂O₂ (Schmitz *et al.*, 2015), the distribution of their *K. lactis* homologues was investigated by fluorescent tags and live cell microscopy. For this purpose, C-terminal fusions of the *KIDCK1* and *KILMO1* open reading frames with the GFP coding sequence were constructed at their native loci, while an N-terminally tagged GFP-*KIRho5* was produced from a plasmid integrated at the *Klleu2* locus. The resulting three strains (*GFP-KIRHO5* =

3. Results

KMO06-23, *KIDCK1-GFP* = KHO336-1B, *KILMO1-GFP* = KHO337-1C) were crossed with a strain containing a genomic *KIIDP1-mRuby* allele (KHO346-7B), which encodes the mitochondrial NADP-specific isocitrate dehydrogenase fused to the red fluorescent tag mRuby. Sporulation of the resulting diploids and tetrad dissection yielded haploid strains containing the required combination of fluorescent labels, which were subjected to life cell imaging (Figure 19).

Inspection of the images revealed that GFP-*K/Rho5* was primarily associated with the plasma membrane under standard growth conditions in synthetic medium, while a minor fraction diffusely distributed in the cytosol. Note that the morphological defects with protruding bud scars discussed above in chapter 3.2.4 were occasionally observed, indicating that the fusion protein is not fully functional. For *K/Dck1-GFP* and *K/Lmo1-GFP* diffuse cytosolic distributions with occasional patches were observed under standard growth conditions. They were also observed associating with undefined intracellular structures. Less than 3 % of the GFP signals from the three protein fusions were associated with mitochondria under these conditions. In contrast, when exposed to H₂O₂ all three proteins translocated to the mitochondria within the two to three minutes required for sample preparation. While GFP-*K/Rho5* was clearly associated with mitochondria after addition of hydrogen peroxide, significant portions of the fusion protein also remained at the plasma membrane and in the cytosol. This was different for the fusions of the two GEF subunits, which appeared almost exclusively at the mitochondria after exposure to oxidative stress. Nevertheless, the translocation was evident, and for all three proteins 99-100 % of the observed cells showed a colocalization with the mitochondrial *KIIDP1-mRuby* marker.

3. Results

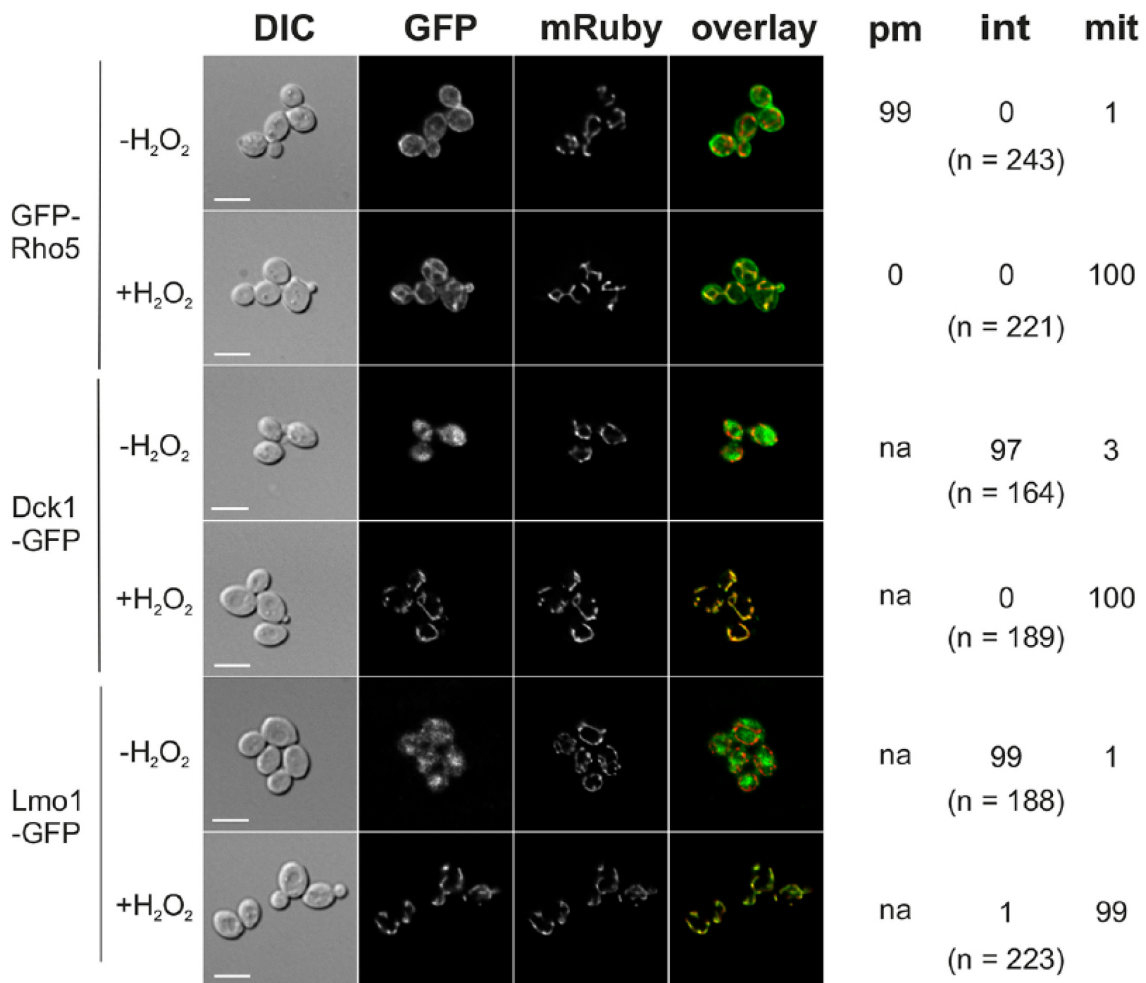


Figure 19: Translocation of the *K/DLR* components under oxidative stress. Haploid strains containing either GFP-*K/Rho5* (KMO31-4B), *K/Dck1*-GFP (KHO347-2B) or *K/Lmo1*-GFP (KHO348-2B) together with a mitochondrial *K/IDP1*-mRuby marker, were observed with live cell fluorescence microscopy. Cells were grown to logarithmic phase in synthetic medium and either examined without further treatment (upper panels) or within a maximum of 10 min after addition of 4.4 mM H₂O₂ (lower panels). The percentage of cells displaying signals at the plasma membrane (pm), intracellular in the cytosol (int) or colocalizing with the mitochondrial marker (mit) were calculated for the total number of cells counted (n). *K/Dck1*-GFP and *K/Lmo1*-GFP did not appear at the plasma membrane (na = not applicable). The scale bars correspond to 5 μm and are applicable to all images in the same row. In the overlay images, red indicates mRuby signals, green GFP signals and yellow overlapping signals of both (from Musielak *et al.*, 2021).

To determine which intracellular structures *K/Dck1*-GFP and *K/Lmo1*-GFP might associate with under standard growth conditions both the vacuole and the nucleus were stained. Therefore, a strain carrying a plasmid (pRRO297) with a nuclear localization sequence fused to mCherry, integrated into the *Klleu2* locus, was crossed with the strains carrying the GFP fusions of *KIDCK1* and *KILMO1*. These were then sporulated and subjected to

3. Results

tetrad analyses and segregants carrying both fusions were followed in life cell imaging. The vacuole was subsequently stained with CMAC, a dye that can be externally added and is transported into the yeast cells, where it accumulates in the vacuoles. No distinct colocalization with either nucleus or the vacuoles was detected in any of the cells examined for the two strains (Figure 20).

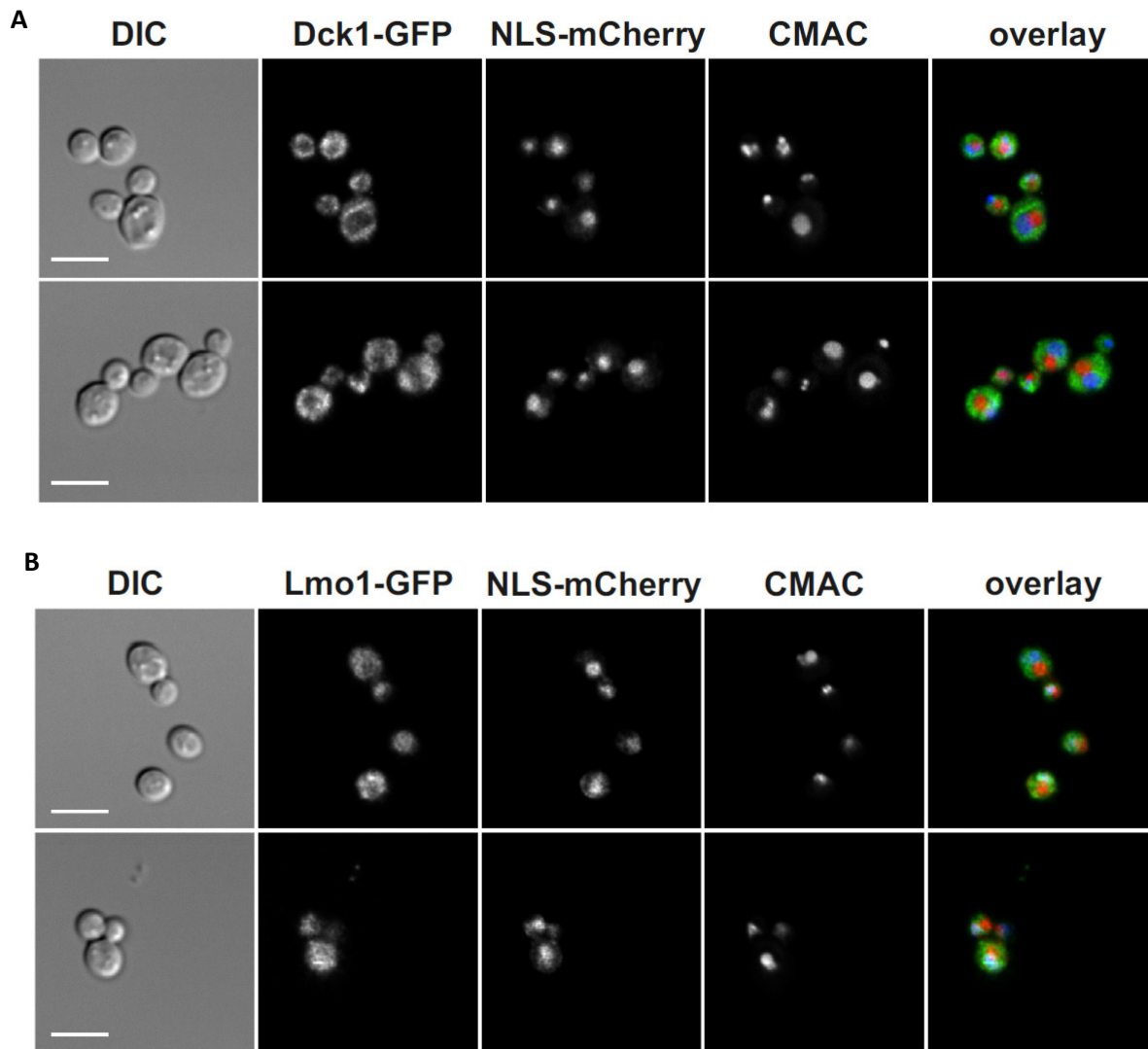


Figure 20: Life cell fluorescent imaging of *K/Dck1-GFP* and *K/Lmo1-GFP* together with a nuclear marker and vacuole staining. The cells were grown in SCD to logarithmic phase and observed directly after the staining with CMAC. Scale bars depicted in the left image of each row correspond to 5 μm and are applicable to all images in the same row. A) Localization of *K/Dck1-GFP* in combination with a nuclear marker and CMAC-stained vacuoles. B) Localization of *K/Lmo1-GFP* in combination with a nuclear marker and CMAC-stained vacuoles. In the overlay images red indicates mCherry signals, green GFP signals, blue CMAC staining, and white overlapping signals from all three (from Musielak *et al.*, 2021).

3.3.2 *KIRho5*, *KIDck1* and *KILmo1* associate with mitochondria upon glucose starvation

A rapid translocation of the *K/DLR* components to mitochondria was also observed in *S. cerevisiae* cells starved for glucose (Schmitz *et al.*, 2018). To investigate if this function is conserved in *K. lactis*, the distribution of the GFP fusion proteins studied above was determined upon glucose starvation. When grown in glucose containing medium, the three GFP-fusions localized as described above (chapter 3.3.1), with GFP-*KIRho5* associated to the plasma membrane and *KIDck1*-GFP and *KILmo1*-GFP in the cytosol. In contrast, after starvation for 30 min in medium without glucose, GFP signals largely colocalized with the mitochondrial *K/IDP1*-mRuby marker (Figure 21).

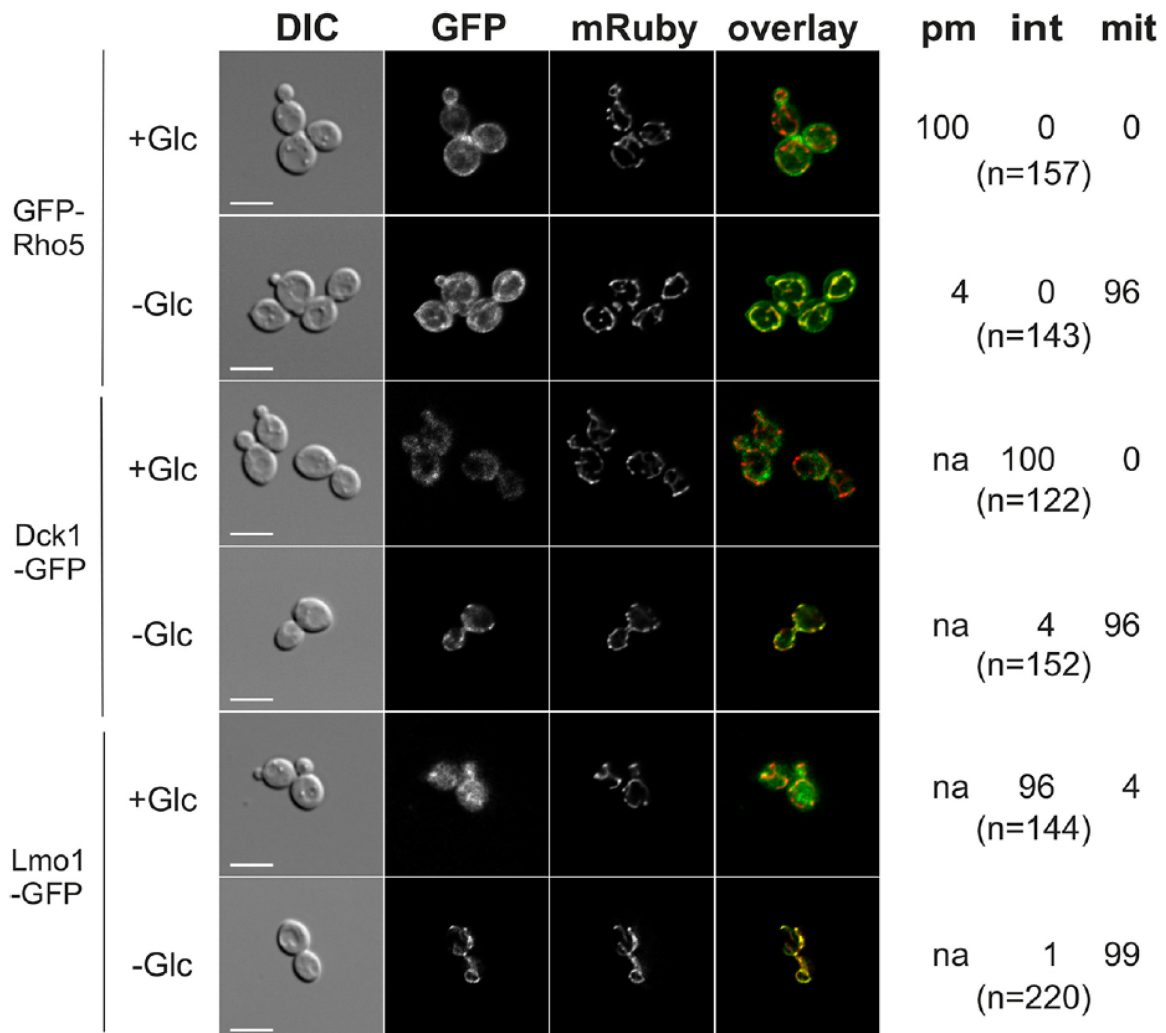


Figure 21: Translocation of the *K/DLR* components under glucose starvation. Haploid strains containing either GFP-*KIRho5* (KMO31-4B), *KIDck1*-GFP (KHO347-2B) or *KILmo1*-GFP (KHO348-2B) together with a mitochondrial *K/IDP1*-mRuby marker were observed with life cell fluorescence microscopy. Cells were grown to logarithmic phase in synthetic medium with glucose and either

3. Results

examined without further treatment (upper panels) or within 30 min of incubation in synthetic medium without glucose (lower panels). The percentage of cells displaying signals at the plasma membrane (pm), in the cytosol (int = intracellular, diffuse) or colocalizing with the mitochondrial marker (mit) were calculated for the total number of cells observed (n). *K/Dck1*-GFP and *K/Lmo1*-GFP did not appear at the plasma membrane (na = not applicable). The scale bars depicted in the left images correspond to 5 μ m and are applicable to all images in the same row. In the overlay images red indicates mRuby signals, green GFP signals and yellow overlapping signals of both (from Musielak *et al.*, 2021).

3.4 *KICdc42* localizations suggest shared functions with *KIRho5*

In many fungi Rac1 homologues share overlapping functions and/or collaborate in tandem with other small GTPases. A common partner of Rac1 and its homologues in the establishment of polarity and cytokinesis is Cdc42 (Virag *et al.*, 2007). Therefore, the *K. lactis* counterpart of the small GTPase was also investigated.

3.4.1 *KICDC42* is an essential gene

First, a *Klcdc42* deletion mutant was constructed by homologous recombination and substitution of the open reading frame for the *kanMX* marker in the diploid recipient strain KHO70. The heterozygous diploid strain KHO70/*cdc42* was subjected to tetrad analysis. No more than two viable segregants were produced in each of a total of 18 tetrads, indicating that *KICDC42* is an essential gene (Figure 22, left image). Accordingly none of the viable segregants carried the *kanMX* marker deduced from replica-plating onto plates containing G418. As expected, integration of a plasmid carrying the wild-type *KICDC42* gene, into the *Klleu2* locus of the heterozygous diploid, followed by tetrad analysis, complemented the lethality of the *Klcdc42* deletion (Figure 22, right image).

Interestingly, when a *KICDC42*^{G12V} allele on a plasmid (pJJH2917) was integrated into the *Klleu2* locus of a *Klrho5* deletion strain, it suppressed the morphological defects, since 18 out of 21 *Klrho5* deletion segregants from a tetrad analysis also carrying the *KICDC42*^{G12V} did not show aberrant protrusions on their surface.

3. Results

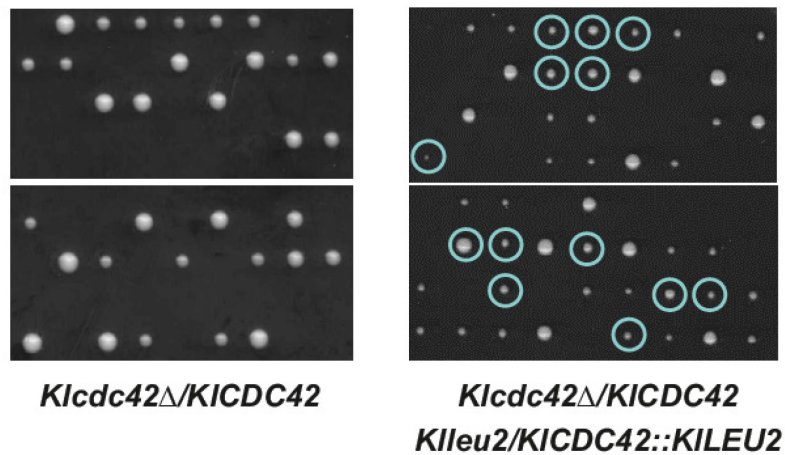


Figure 22: Complementation of the *Klcdc42* deletion by the wild-type gene. Depicted are the tetrads of KHO70/*cdc42* (left) and the same strain with pJH2918 (*KICDC42*), integrated into the *Klleu2* locus (right). Blue circles in the right picture indicate segregants with the *Klcdc42* deletion in conjunction with the integrated plasmid (from Musielak *et al.*, 2021).

3.4.2 GFP-*KICdc42* translocates to mitochondria under oxidative stress

Integration of the plasmid carrying the *GFP-CDC42* in the heterozygous diploid KHO70/*cdc42* strain followed by tetrad analysis, resulted in only two viable segregants per tetrad, suggesting that the fusion protein was not functional. Nevertheless, the intracellular distribution of the encoded fusion protein was determined in the heterozygous diploid strain. GFP-*KICdc42* signals appeared to be diffuse within the cytosol, with a distinct accumulation at the incipient bud site in the early stages of cytokinesis (Figure 23). Haploid strains also carrying the mitochondrial *KIIDP1-mRuby* construct (KHO346-7B) revealed that the GFP-*KICdc42* signals, besides their diffuse distribution in the cytosol, also appeared to be associated with internal structures, coinciding with the surface of vacuoles, as deduced from the brightfield images (Figure 24 upper two rows). GFP signals also accumulated in daughter cells, at the pole opposite to the bud neck (Figure 24 upper two rows). In contrast to GFP-*K/Rho5*, GFP-*KICdc42* did not appear at the bud neck itself during cytokinesis.

3. Results

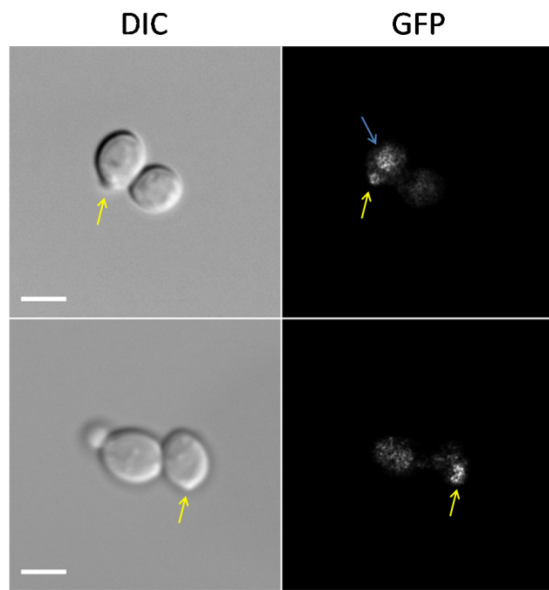


Figure 23: Localization of GFP-*Klc42* at early budding sites. *KHO70/cdc42* cells with pMMO22 (*GFP-KLCDC42*) integrated at the *Klleu2* locus, were grown in SCD without leucine to logarithmic phase and observed under the fluorescent microscope. The GFP signals were diffusely distributed in the cytosol and accumulated at incipient budding sites in the early stages (yellow arrows). Accumulation at internal structures was also detected (blue arrow). Scale bars correspond to 5 μ m.

In contrast to its distribution under standard growth conditions, the GFP-*Klc42* fusion protein colocalized with the mitochondrial *KlIDP1-mRuby* within minutes after exposure of the cells to hydrogen peroxide (Figure 24). This rapid translocation was reminiscent of the components of the *K/DLR* complex described above (chapter 3.3.1).

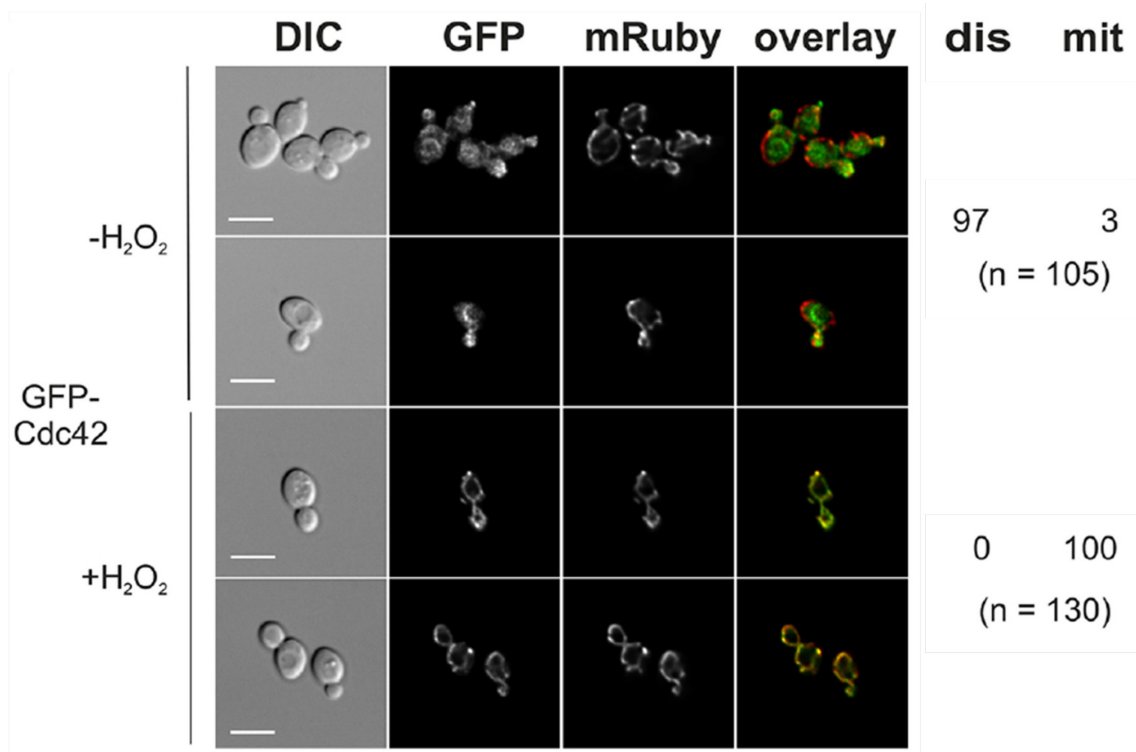


Figure 24: Translocation of GFP-*Klc42* to mitochondria upon oxidative stress. Representative pictures of the *KlIDP1-mRuby* strain (*KHO346-7B*) with pMMO22 (*GFP-KLCDC42*) integrated into

3. Results

the *Klleu2* locus. The strain was grown in SCD without leucine to logarithmic phase and examined either without further treatment (upper two panels) or after addition of 4.4 mM H₂O₂ (lower two panels). The numbers on the right give the percentages of signals distributing diffusely in the cytosol (dis) or colocalizing with the mitochondrial marker (mit), from total cell counts (n). The scale bars correspond to 5 μm and are applicable to all images of the same row. In the overlay images red represents the mRuby signals, green those of GFP and yellow overlapping signals of both (from Musielak *et al.*, 2021).

4. Discussion

In this thesis the small GTPase *K/Rho5* and its bipartite GEF consisting of *K/Dck1* and *K/Lmo1* were investigated for their *in vivo* functions and potential connections to different signal transduction pathways. Since in the last few years a lot of new discoveries were made for its closely related homologue *ScRho5*, *K/Rho5* was first checked for similarities.

4.1 Similarities between *ScRho5* and *K/Rho5*

In this thesis several similarities between *K/Rho5* and its *S. cerevisiae* homologue were uncovered. First, deletion of any of the *K/DLR*-components resulted in a heightened resistance to caffeine and hydrogen peroxide (chapter 3.2.2), suggesting similar roles as a negative regulator of CWI signalling and the thioredoxin reductase *Trr1*, as described for *ScRho5* (Schmitz *et al.*, 2002; Singh *et al.*, 2008). Furthermore, fusion proteins of GFP with either *K/Rho5*, *K/Dck1* or *K/Lmo1* displayed a rapid translocation to mitochondria under oxidative stress and glucose starvation. This was also found for their *S. cerevisiae* homologues (Schmitz *et al.*, 2015, 2018). This indicates similar functions for *K/Rho5* as those described for *ScRho5*, such as the induction of mitophagy and apoptosis as a response to oxidative stress (Singh *et al.*, 2008; Schmitz *et al.*, 2015).

4.1.1 Functionality of the *K/DLR* components fused to GFP and their localization under standard conditions

To determine the intracellular distribution of the *DLR* components, an N-terminal GFP-*K/Rho5* fusion was employed, while *K/Dck1* and *K/Lmo1* carried the fluorescence tag at their C-terminal ends. Whether these fusions are functional was only addressed for GFP-*K/Rho5*, as in the background of a *Klrho5* deletion some 10% of cells displayed the aberrant protrusions. This indicates that the GTPase was not fully functional when fused to the 27 kDa fluorescent tag, similar to the respective construct with the *S. cerevisiae* homologue (Sterk *et al.*, 2019). Recent studies in our laboratory with GFP-*ScRho5* fusions indicate that close to wild-type GTPase activity can be achieved by substitution of the linker sequence by PAPAP, as found in previous studies with other fusion proteins (Franziska Schweitzer, personal communication; Chen *et al.*, 2013).

4. Discussion

The functionality of the *K/Dck1*- and *K/Lmo1*-GFP fusions was not assessed, as no aberrant cells were observed and this would have required growth curves to determine the reactions towards stressors (as in chapter 3.2.2) in the background of the respective deletion strains. While the first fusion is not expected to affect Dck1 function, as deduced from the homologous construct with GFP-ScDck1, the C-terminal fusion of ScLmo1-GFP appeared to be completely non-functional (Sterk *et al.*, 2019). However, recent studies in our laboratory with a functional N-terminal GFP-ScLmo1 fusion showed that its intracellular distribution did not differ from that of the non-functional ScLmo1-GFP construct (Linnet Bischof, personal communication). It is thus likely that the data deduced from the three *K. lactis* fusions with regard to their intracellular distribution are valid, despite the lack of functional assays.

In contrast to its counterpart in *S. cerevisiae*, the GFP-*K/Rho5* signal, although primarily confined to the plasma membrane under standard growth conditions, was also detected in the cytosol to some extent. This could be due to a more frequent trafficking between membranes, commonly mediated by the GDP dissociation inhibitor (GDI; Golding *et al.*, 2019). The higher mobility of the GTPase in *K. lactis* may be necessary because of its additional functions as compared to ScRho5, e.g. its participation in cytokinesis, as discussed below.

Interestingly, *K/Dck1*-GFP and *K/Lmo1*-GFP both displayed a diffused cytosolic signal, as well as in some cases accumulation in intracellular patches (chapter 3.3.1 and 3.3.2), which clearly differed from the punctuate structures observed for their *S. cerevisiae* counterparts (Schmitz *et al.*, 2015, 2018). The patches did neither colocalize with vacuoles nor with nuclei (Figure 20, chapter 3.3.1), so that their structural basis remains to be determined. Nevertheless, it indicates that the GEF subunits are not subject to an efficient turnover by proteolytic degradation in the yeast vacuole, which is frequently observed for misfolded proteins, further supporting the functionality of the employed fusions (Hong *et al.*, 1996). Moreover, *K/Dck1* and *K/Lmo1* seem to have no nuclear function, as it was suggested for DOCK180/ELMO complexes in human cells (Yin *et al.*, 2004).

4.2 Several regions of *K/Rho5*, *ScRho5* and *HsRac1* may convey species-specific functions

As shown in chapter 3.1, an *in silico* analysis revealed strong structural conservations between the Rho5 homologues of *K. lactis*, *S. cerevisiae* and human Rac1. As expected, identities were not evenly distributed along the entire primary sequence, but a stronger conservation was observed between functional domains.

The latter include the switch I and II regions, which are known to act as recognition sites for regulators and effectors, as well as the PBR-CAAX region, proposed to mediate intracellular localization and geranyl-geranylation, respectively (Heo *et al.*, 2006; Mosaddeghzadeh & Ahmadian, 2021). With regard to the specific extension of *ScRho5* between Pro221 and Asp320, which is not found in the human Rac1, the *K/Rho5* homologue retained a shorter sequence, as do other fungal homologues (Figure 25, red box). Interestingly, this region seems to be highly variable in fungi, as sequences are much less conserved and their lengths differ greatly. Nevertheless, were longer extensions are present, they appear to be enriched in basic amino acid residues (Figure 25, highlighted in yellow). One may thus speculate that the PBR needs to be longer in the respective yeast species as compared to human Rac1 to fulfil its function. Furthermore, in *S. cerevisiae* the extension apparently lacks secondary structures and can be classified as an intrinsically disordered region (IDR) (PhD thesis Carolin Sterk, 2020). These regions fail to fold into stable, defined structures, but upon interaction with specific partners they are capable of ordering up, resulting in highly specific interactions (reviewed in Bondos *et al.*, 2022).



Figure 25: Amino acid sequence alignment of different fungal Rho5 homologues and *HsRac1*. Depicted from top to bottom are the Rho5 homologues of *Saccharomyces cerevisiae* (*ScRho5*;

4. Discussion

NCBI KZV08440), *Kluyveromyces lactis* (*KIRho5*; NCBI QEU60661), *Ashbya gossypii* (*AgRho5*; NCBI AAS50632), *Candida albicans* (*CaRac1*; NCBI AOW26329), *Yarrowia lipolytica* (*YIRac1*; NCBI AAF40311), *Aspergillus nidulans* (*AnRacA*; NCBI CBF76882), *Neurospora crassa* (*NcRac1*; NCBI EAA35283), *Cryptococcus neoformans* (*CnRac1*; NCBI DAA64539) and humans (*HsRac1*; NCBI NP_008839). Conserved amino acids are highlighted with blue background and basic amino acids in the yeast-specific extension and PBR in yellow. The conserved P-loop and the switch I region are located between amino acids 1-42, and the switch II region is localized at the beginning of the homology block between amino acids 85-113, as numbered in the *S. cerevisiae* sequence. Boxes highlight either specific amino acids (orange) referred to in the text and Table 6, or specific regions like the Rho-specific insert (yellow) and the yeast-specific extension (red). All protein sequences were obtained from the online ncbi database (<https://www.ncbi.nlm.nih.gov/protein/> accessed on 16.11.2021) and aligned to *ScRho5* by the respective function of the Clone Manager program (Sci Ed Software LLC, Westminster, CO, USA) with standard settings.

The necessity for an elongated PBR sequence in the yeast Rho5 homologues was also supported by heterologous complementation studies. Thus, while *HsRAC1* did not complement the synthetic lethality of a *Scsch9 Scrho5* double deletion, a hybrid of *HsRAC1* with the 3'-region of *ScRHO5*, including the sequence coding for the specific extension, at least partially restored growth (Sterk *et al.*, 2019). In addition, two *KIRHO5* alleles (*KIRHO5* and *KIRHO5^{Q91H}*), although carrying a much shorter extension as compared to *ScRho5*, were also able to complement the synthetic lethality (chapter 3.2.5). *Vice versa*, the *ScRHO5* homologue did not complement the morphological defects of a *Klrho5* deletion, indicating that other parts of the longer extension may interfere with this function in *K. lactis*. This is also supported by the failure of the hybrid *KIRHO5^{Sc222-331}* allele to suppress the morphological defect. It would be interesting to see, if this defect could be suppressed by a hybrid *ScKIRHO5* gene, encoding the C-terminal part of the *K. lactis* homologue. In *Candida albicans* neither *HsRac1* nor a hybrid construct with the last 14 residues of *CaRac1* were able to complement the *Carac1* deletion, underlining the importance of the full length extension (Vauchelles *et al.*, 2010).

In the light of this results it was not surprising that neither *HsRAC1* nor *HsRAC1^{G12V}*, lacking the yeast-specific extension, complemented the *Klrho5* morphological defects. That a hybrid construct of *HsRac1* with the last 54 amino acids of *KIRho5* (*HsRAC1^{K1200-254}*), still lacked complementation indicates that either the fusion may have impaired GTPase function or other regions are also necessary for proper function of *HsRac1* in *K. lactis*.

The lack of function of the hybrid GTPase in *K. lactis* could also be explained by an inability of the *KIDck1* and *KILmo1* variants to activate and/or contribute to the proper

4. Discussion

intracellular distribution of the human homologue. As an example for the latter, ScRho5 does not translocate to mitochondria under oxidative stress in the absence of either ScDck1 or ScLmo1 (Schmitz *et al.*, 2015). A similar lack of translocation would be expected if the yeast GEF homologues failed to interact with the (hybrid) human Rac1 GTPase.

In this context, amino acid substitution studies showed that several residues of *HsRac1* are important for proper interaction with specific DOCK proteins (Figure 25, orange boxes; Kukimoto-Niino *et al.*, 2021). As shown in Table 6, most of these residues are similar between *S. cerevisiae* and *K. lactis*, while some differ between the yeasts and human Rac1. These changes, e.g. the substitution of the hydrophobic, non-polar Ala27 to the hydrophilic, polar Thr27 or Ser27 could impact *HsRac1* interaction with DOCK and ELMO homologues. Furthermore, Trp56 may be conserved in the Rac1 homologues, but the interacting residues of the DOCK proteins (Met1529, Asn1532, Phe1598) are neither conserved in *K/Dck1* or *ScDck1* (Figure 9, chapter 3.1). Yet, these differences alone cannot explain the failure of *HsRAC1*^{K1200-254} to complement the morphological phenotype of *Klrho5* deletions, since substitution of the PBR/CAAX region of *HsRac1* by the C-terminal 110 residues of ScRho5 largely restored function, despite the same differences (Sterk *et al.*, 2019).

Table 6: Important amino acids for specific *HsRac1*-DOCK interaction and their conservation between *K. lactis*, *S. cerevisiae* and human Rho5 homologues

Amino acid and position in <i>HsRac1</i>	Conservation	Function
Alanine 3	Ala3 → <i>K.l.</i> Ser3, <i>S.c.</i> Ser3	Binding of switch I and DOCK
Alanine 27	Ala27 → <i>K.l.</i> Thr27, <i>S.c.</i> Ser27	Binding of switch I and DOCK
Glycine 30	Gly30 → <i>K.l.</i> Gln30, <i>S.c.</i> Thr30	Binding of switch I and DOCK
Isoleucine 33	Ile33 → <i>K.l.</i> Ile33, <i>S.c.</i> Val33	Binding of switch I and DOCK
Asparagine 52	Asn52 → <i>K.l.</i> Lys60, <i>S.c.</i> Lys82	DOCK selectivity
Tryptophan 56	Trp56 → <i>K.l.</i> Trp64, <i>S.c.</i> Trp86	Main determinant of DOCK selectivity through interaction with Met1529, Asn1532, Phe1598

In addition to the differences in specific amino acid residues, the so called Rho-specific insert region, localized between the G4 and G5 domain (Figure 25 yellow Box), is believed to confer effector specificity and to bind the GEF (Schaefer *et al.*, 2014). This region shows 60% amino acid identity between ScRho5 and *K/Rho5*, as compared to only 40% between

KlRho5 and *HsRac1*. The lower conservation could also result in a functional impairment of *HsRac1* in yeasts and explain its failure to complement.

As described above, the inability of any *ScRho5* variant to complement the *Klrho5* morphological phenotype is likely due to the yeast-specific extension of *ScRho5* interfering with the interaction with *K. lactis*-specific effectors. It should be tested whether this is also true for other *Klrho5* phenotypes, e.g. if *ScRho5* can complement the growth variations caused by H₂O₂, Calcofluor white (CFW), acetic acid and caffeine (chapter 3.2.2). Moreover, the construction of other hybrid *HsRac1* variants, with the exchange of specific domains or amino acid residues, and the assessment of their complementation capacity in *K. lactis* could be used to elucidate the exact structure-function relationship.

4.3 *KIDL*R mutants display a variety of phenotypes that can be linked to stress signalling

As one of the first steps in investigating the functions of a specific protein is the deletion of its encoding gene and a subsequent phenotypic analysis, this strategy was also followed for *KlRho5*. The deletion mutants were tested for genetic interactions previously established for its *S. cerevisiae* homologue, as well as other potential candidates. Other phenotypes tested included the reaction to different stressors and a possible effect on the chronological lifespan.

4.3.1 *KIRHO5* shows no genetic interactions with different signalling pathways

In *S. cerevisiae*, double deletions of *ScRHO5* and either *ScSCH9*, *ScGPR1* or *ScGPA2* were synthetically lethal or synthetically sick, whereas a double deletion of *ScRHO5* with *ScSNF1* showed no genetic interactions. Therefore, *ScRho5* was suggested to act in parallel to the TORC and PKA/cAMP glucose signalling pathways, but independent from *ScSnf1* signalling (Schmitz *et al.*, 2018). Contrary to *S. cerevisiae*, in *K. lactis* no synthetic phenotypes were observed in the double deletion of *KIRHO5* with either those of *KISCH9*, *KIGPR1* or *KIGPA2*. Neither could a genetic interaction between *KIRHO5* and *KISNF1* be shown (chapter 3.2.1), suggesting that in *K. lactis* Rho5 might not be directly involved in

4. Discussion

glucose signalling. Approximately 40% of the cells glucose intake is channelled through the pentose phosphate pathway in *K. lactis*, thus playing a more prominent role in the organism's metabolism, compared to the baker's yeast (Bertels *et al.*, 2021). It could be assumed, that instead of regulating the TORC and PKA/cAMP pathways, *KIRho5* acts on the pentose phosphate pathway. However, *Klrho5* showed no genetic interactions with *Klzwf1*, *Klrpe1* or *Kltal1* deletions in tetrad analyses. This again indicated that *KIRho5* may not be involved in the regulation of glucose metabolism, despite its translocation to mitochondria upon glucose starvation discussed above.

In addition to glucose signalling, roles for *ScRho5* were also suggested in CWI and oxidative stress response signalling (Schmitz *et al.*, 2002, 2015; Singh *et al.*, 2008), *KIRHO5* was therefore also tested for genetic interactions with several genes involved in these processes (chapter 3.2.1), without showing genetic interactions with any candidate. In *S. cerevisiae* *ScRHO5* and *ScPOR1* displayed genetic interactions, which were only revealed when the double deletions were grown in the presence of H₂O₂, or when the *Scpor1* deletion was combined with a hyper-active allele of *ScRHO5* (Carolin Sterk PhD thesis, 2020; Franziska Schweitzer personal communication). This emphasizes the need to test all the double mutants constructed for genetic interactions in the other than standard growth conditions, e.g. under oxidative stress, glucose starvation, or cell wall stress. These studies could not be performed in the frame of this thesis due to time limitations.

4.3.2 *KIDL*R-deletion mutants do not affect the chronological lifespan

A decrease of the chronological lifespan (CLS) in *Scrho5* deletions has been reported in the *S. cerevisiae* BY-strain series (Cao *et al.*, 2016). Moreover, glucose signalling has been related to CLS in *Schizosaccharomyces pombe* and in *S. cerevisiae* mutations causing an increased resistance to oxidative stress also expanded the CLS (Fabrizio *et al.*, 2001, 2003; Roux *et al.*, 2009). That no effect on CLS was observed (chapter. 3.2.3) in a *Klrho5* deletion could be explained by the fact that *KIRho5* lacks a relation to glucose metabolism, as judged by the lack of synthetic phenotypes discussed above, and shows only a moderate increase in its resistance to H₂O₂ (chapter 3.2.2). On the other hand, *DLR*-deletions in the *S. cerevisiae* strain DHD5 used in this thesis also lacked any effect on the CLS (chapter

4. Discussion

3.2.3). This may be attributed to the differences in the strains genetic backgrounds, but *Scrho5* deletions in the BY strain also showed no effect on the CLS in our laboratory (personal communication Jürgen Heinisch). This discrepancy to published data may be due to differences in the experimental setup, as many factors like the availability of nutrients, oxidative stress, autophagy and apoptosis affect the CLS (see Figure 26 for an overview of pathways involved in CLS; Longo *et al.*, 1996; Herker *et al.*, 2004; Alvers *et al.*, 2009; Sampaio-Marques *et al.*, 2011; Rizzetto *et al.*, 2012). Thus, differences in the nutrient availability of media or oxygenation of cells can cause disparate results in CLS assays (Smith *et al.*, 2016). In their experiments Cao *et al.* (2016), employed YEPD for their CLS-assays, while in this thesis SCD medium was used to generate more controlled circumstances and because it was suggested that synthetic medium, better mirrors the nutrient availability yeast cells face in their natural environment (Alvers *et al.*, 2009). Experiments employing different media may help to elucidate this matter.

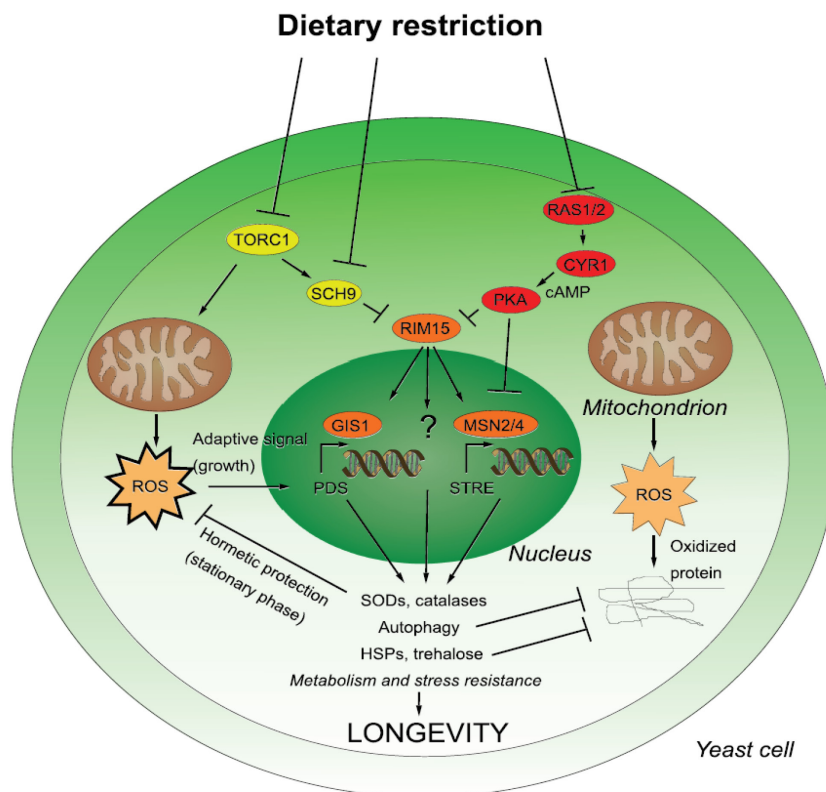


Figure 26: Major pathways driving chronological lifespan. Both the TORC1/Sch9 and PKA/cAMP pathways are responsive to the availability of nutrients in the environment. Upon nutrient restriction, they are downregulated and allow the central protein kinase Rim15 to activate the stress responsive transcription factors Gis1 and Msn2/4. Together, these pathways orchestrate the cellular stress responses through increased transcription of, among others, heat shock proteins, trehalose synthase, autophagy related genes, and detoxifying enzymes such as Sod2 and Ctt1. During growth, reduced TORC1/Sch9 signalling also upregulates mitochondrial respiration

and consequently increases the formation of ROS. This stimulates an adaptive response that decreases ROS production during chronological aging. Together, these cellular changes result in an increased chronological lifespan (from Wauters *et al.*, 2021)

4.3.3 Possible functions of the *K/DLR* complex in mediating the response to different stressors in the medium

In this thesis it was shown, that deletions of *KIRHO5*, *KIDCK1*, and *KILMO1* are more resistant than the wild type to the presence of hydrogen peroxide, caffeine and acetic acid, and more sensitive to Calcofluor white (Figure 10D, chapter 3.2.2). The resistance towards oxidative stress may be linked to the DLR functions in mitophagy and apoptosis, similar to what was postulated in *S. cerevisiae* (Schmitz *et al.*, 2015). In this context, both processes still need to be assessed in the *K. lactis* mutants as compared to wild type.

This may also be related to the effects of acetic acid, since it has been found to lead to either apoptosis, or at higher concentrations, necrosis in yeast cells (Ludovico *et al.*, 2001). Interestingly, for programmed cell death, both a ROS-dependent and a ROS-independent pathway triggered by acetic acid have been suggested. Activation of apoptosis by the ROS-dependent functions can be inhibited by the addition of the antioxidant N-acetyl-L-cysteine (NAC; Guaragnella *et al.*, 2007; Guaragnella *et al.*, 2010a; Guaragnella *et al.*, 2010b). This could be worth testing for its effects on growth of the DLR mutants, as ROS production is also related to mitochondrial malfunctions (Yi *et al.*, 2018) and strains with a high tolerance to acetic acid produce considerably lower levels of ROS compared to control strains (Lee *et al.*, 2015; Zheng *et al.*, 2013), one may envision the following interactions: In *S. cerevisiae*, ScRho5 has been reported to inhibit the thioreductase Trr1, which in turn is involved in the detoxification of ROS (Singh *et al.*, 2008). *Klrho5* mutants may thus alleviate the inhibition of *K/Trr1*, reducing the amount of intracellular oxidative stress and thus contribute to cell survival in the presence of acetic acid.

Furthermore, in *S. cerevisiae* several studies showed the activation of genes from the general stress response (GSR), also called environmental stress response (ESR), upon exposure to acetic acid (Mira *et al.*, 2010a, 2010b; Li & Yuan, 2010). The GSRs main transcription factors are Msn2 and Msn4, which get activated by a multitude of protein kinases involved in different stress response pathways like the in nutritional stress

4. Discussion

involved Rim15 or Hog1, which is involved in the osmotic stress response (Sadeh *et al.*, 2011; Heinisch & Rodicio, 2017). ScRho5 was suggested to play a role in sequestration of ScRim15 to the cytoplasm and upon its translocation to the mitochondria this regulation would be relieved and result in phosphorylation of ScMsn2 and ScMsn4 (Schmitz *et al.*, 2018). A similar effect of *K/Rho5* on a protein kinase activating the GSR in the context of acetic acid could be possible.

Another mechanism with which *S. cerevisiae* counteracts acetic acid stress is by changing the composition of its plasma membrane and its cell wall. As a response to acetic acid the turgor is increased and causes a reinforcement of the cell wall, while the permeability of the membrane for acetic acid is reduced (Ullah *et al.*, 2013; Lucena *et al.*, 2020; Ribeiro *et al.*, 2021). Therefore, the thicker cell wall observed in DLR-deletions (chapter 3.2.4.1) likely contributed to this resistance.

A considerable increase in cell wall thickness was also observed in *K. lactis* grown on ethanol as compared to glucose (Backhaus *et al.*, 2010). This may explain the lack of a growth phenotype of *K/DLR* mutants (Figure 10D), as they may not additionally contribute to strengthen the cell wall on this carbon source. Interestingly, the *Kldck1* deletions appeared to have a reduced viability in stationary phase, in contrast to *Klrho5* and *Kllmo1* deletions. This indicates a role for *K/Dck1* independent of its activation of *K/Rho5*. In fact, for mammalian Dock1 a role in trafficking of proteins from the endosome to the *trans*-Golgi network independent from Rac1 has been found (Hara *et al.*, 2008). Whether *K/Dck1* affects a similar network in *K. lactis* remains to be determined.

The thickening of the cell wall under standard growth conditions may be explained by the role of Rho5 in CWI signalling suggested in *S. cerevisiae* (Schmitz *et al.*, 2002). ScRho5 was suggested to be a negative regulator of the pathway, acting downstream of ScSlr2 and being regulated by components acting upstream of ScRho1. Its constitutively active mutant (*ScRHO5^{Q91H}*) was more sensitive than the wild type towards known cell wall stressors like caffeine, Congo red and CFW, whereas the *Scrho5* deletion mutants were hyper-resistant (Schmitz *et al.*, 2002). In contrast, the *Klrho5* deletion was highly sensitive to CFW (Figure 10F). This is quite surprising as it may indicate that *K/Rho5* is a positive regulator of the CWI pathway. On the other hand the slight resistance towards caffeine (Figure 10E) and the thickened lateral cell wall (chapter 3.2.4.1) observed in *Klrho5*

deletions suggest it to be a negative CWI regulator. The deletion would fail to block the MAPK signalling downstream of *K/Rho1*, resulting in a more sensible activation of stress response and subsequently, activation of chitin and glucan synthases, resulting for example in the observed thicker cell wall

These contradictions might be attributed to the regulation of Rho5 activity by upstream components. As cross-talk between CWI and other pathways like the TOR and PKA/cAMP pathways may differ between the two yeasts, Rho5 may react differently to deregulation by caffeine than by direct interactors of the cell wall, like CFW. Differences in CWI signalling between *K. lactis* and *S. cerevisiae* have been previously found with *bck1* deletions. A deletion in *S. cerevisiae* leads to temperature sensitivity and hypersensitivity towards caffeine, while in *Klbck1* strains no apparent CWI-related phenotypes were observed (Jacoby *et al.*, 1999). Moreover, the thickened cell wall observed in *Klrho5* deletions may interfere with their reaction to CFW, since it intercalates with chitin (Roncero & Durán, 1985; Ketela *et al.*, 1999). Analyses of the cell wall composition in *Klrho5* deletions would be required to show if the chitin content is increased, as would be expected, which could explain a stronger binding of and the higher sensitivity towards CFW.

4.4 The *K/DLR*-complex regulates cytokinesis

Previous works in this laboratory showed distinct morphological defects in *Klrho5* deletion strains and *Scrho5* deletions were reported to exhibit a higher proportion of budded cells in late exponential and transition phase, compared to the wild type (Cao *et al.*, 2016). Therefore, the effects of *K/DLR*-deletions, as well as the spatiotemporal localization of DLR- and components of the actomyosin ring, were examined through microscopic approaches.

In budding yeasts cytokinesis follows a conserved pattern which involves the constriction of the actomyosin ring (AMR) accompanied by the formation of a primary septum. Onto this chitinous structure glucans and mannoproteins are deposited to form secondary septa from both the mother and daughter cells (reviewed in Roncero & Sánchez, 2010; Bi & Park, 2012). *Klrho5*, *Kldck1* and *Kllmo1* deletions form specific protrusions on the cell

4. Discussion

surface, which are accompanied by aberrant primary septae in the ultrastructure of the bud neck (Figure 14, chapter 3.2.4.1), suggesting an effect of *Klrho5* on the cytokinesis machinery.

A likely candidate for a *Klrho5* effector in this context would be *KlMyo1*. *ScMyo1*, the sole myosin II heavy chain in budding yeast, is recruited early during cytokinesis in a septin and *lqg1*-dependent manner. It is required for AMR assembly, but also for AMR-independent cytokinesis, as its deletion is lethal in some *S. cerevisiae* strains and impairs proper cell separation in others (Rodriguez & Paterson, 1990; Schmidt *et al.*, 2002; Fang *et al.*, 2010; Rippert *et al.*, 2014; Feng *et al.*, 2015). The *Myo1* homologue is not essential in *K. lactis*, but rather shows a temperature-sensitive growth defect with the formation of aberrant primary septae, resembling the ones observed in this thesis for *K/DLR* mutants (Figure 27; Rippert *et al.*, 2014)

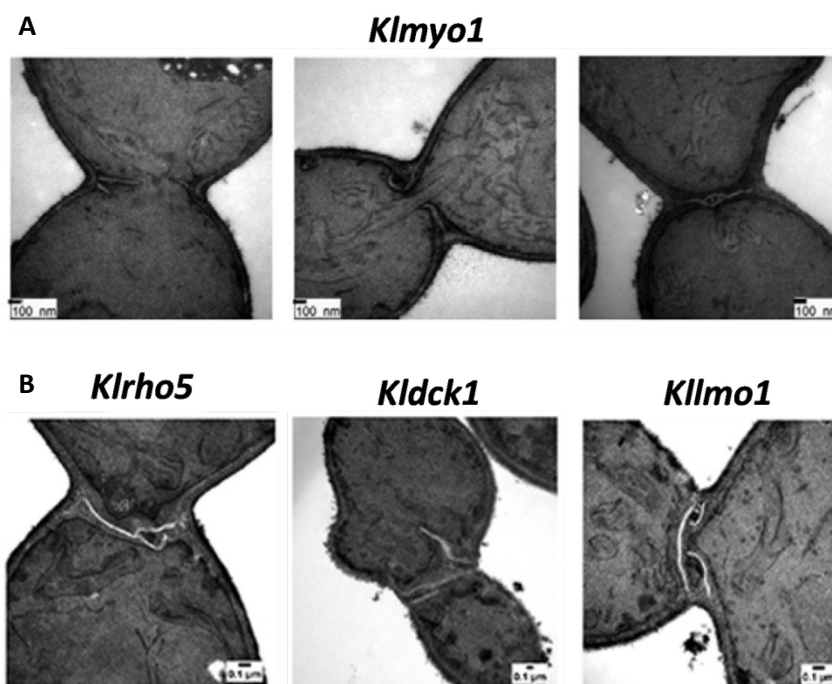


Figure 27: Comparison of primary septae in *Klmyo1* deletions and in *Klrho5*, *Kldck1* and *Kllmo1* deletions. Scale bars are 100 nm. A) TEM images of aberrant primary septae in *Klmyo1* deletions (from Rippert *et al.*, 2014). B) TEM images of *Klrho5*, *Kldck1* and *Kllmo1* deletions (copied from Figure 14)

Unlike the *Klrho5* deletion, a *Klmyo1* deletion produced multiple buds, rather than the protruding bud scars observed herein. On one hand, double deletions of *KIRHO5* and *KIMYO1* are neither synthetically lethal nor have additive growth defects in tetrads growing on standard YEPD medium at 30°C (chapter 3.2.1). On the other hand, when observed under the microscope, the double deletions cells showed only either the *Klmyo1* or the *Klrho5* phenotype (chapter 3.2.4.2). This indicates that both proteins

4. Discussion

participate in the same sequence of events regulating cytokinesis. A detailed analysis of the ultrastructure of the bud neck and the morphological phenotypes in the double mutants would be required to elucidate the exact epistatic relationship.

Other known regulators in *S. cerevisiae* are Iqg1, Inn1 Hof1 and Cyk3, all of which are represented by homologues in *K. lactis* (Rippert *et al.*, 2014). They could be interaction partners for *K/Rho5*. In *S. cerevisiae* Iqg1 is required for the targeting of Myo1, the regulation of actin, as well as in the contraction of the AMR. Furthermore, it colocalized with actin in ring like structures at the bud neck (Epp & Chant, 1997; Shannon & Li, 1999, 2000). Supporting an interaction between *K/Rho5* and *K/Iqg1* is on one hand, that in humans IQGAP1 is able to interact with Rac1 and Cdc42 (Ozdemir *et al.*, 2018; Nouri *et al.*, 2020). On the other hand, colocalization experiments with *K/Myo1* and actin had average pearson coefficients of 0.54 +/- 0.10 for actin compared to 0.44 +/- 0.22 for *K/Myo1* (chapter 3.2.4.2), which suggests a more likely colocalization with actin, resembling the localization pattern of Iqg1. However, in *K/DLR* deletions the localization pattern of actin and *K/Myo1* was similar to wild-type cells, suggesting that the AMR is not absent or aberrant and that *K/Rho5* may affect only some of the *K/Iqg1* functions in later stages of cytokinesis, when both are localized to the bud neck.

ScInn1 controls *ScChs2* activation and/or precise localization, but is not involved in the formation or contraction of the AMR (Sanchez-Diaz *et al.*, 2008; Nishihama *et al.*, 2009). It was shown to localize to the bud neck only shortly before *K/Myo1* could not be detected anymore, which would match the observed localization pattern for *K/Rho5* in this thesis (Rippert *et al.*, 2014). Interestingly, it was shown that the C2 domain of *ScInn1* is mostly responsible for its function during cytokinesis, as the C2 domain fused to *ScMyo1*, *ScHof1* or *ScChs2* could compensate for a *Scinn1* deletion. Furthermore, the C2 domain seems to confer species specificity. *K/Inn1* was unable to complement for a *Scinn1* deletion and *vice versa*, but when hybrid proteins with the native C2 domain were introduced complementation was achieved (Sanchez-Diaz *et al.*, 2008; devrekanli sadli *et al.*, 2012; Rippert *et al.*, 2014). *ScHof1* is responsible for the distribution of septins and *ScInn1*, regulates actin filaments and is involved in septum formation by restricting chitin to the neck region (Kamei *et al.*, 1998; Vallen *et al.*, 2000; Nishihama *et al.*, 2009; Graziano *et al.*, 2014; Garabedian *et al.*, 2020). *ScCyk3* is part of a circular structure, independent of the

4. Discussion

AMR that also constricts and is responsible for septum formation. Furthermore, ScCyk3 seems to share several functions with other cytokinesis regulators like ScHof1, ScIqg1 and ScMyo1, making it a central regulator of cytokinesis in yeast (Korinek *et al.*, 2000; Ko *et al.*, 2007; Wloka & Bi, 2012; Nishihama *et al.*, 2009; Jendretzki *et al.*, 2009).

All three proteins, Inn1, Cyk3 and Hof1, share suggested functions of *K/Rho5* in regulation of actin and construction of the primary septum. The three proteins interact in a complex, which could provide domains to facilitate interaction with the DLR-complex. ScInn1 has multiple PxxP motifs in its C-terminus that interact with the SH3 domains of ScCyk3 and ScHof1 (Nishihama *et al.*, 2009). One could suspect that in *K. lactis* these domains are possible interaction partners for *K/Dck1*, which also possesses a SH3 domain. Moreover, it was shown that the PBR of human Rac1 is able to directly bind the SH3 motive of β -pix, suggesting a mode of interaction were *K/Rho5* could itself directly interact with *K/Cyk3* and *K/Hof1* (Akakura *et al.*, 2005; ten Klooster *et al.*, 2006). Additionally, it was shown in human cells that the C2 domain of Smurf1 is necessary and sufficient to bind RhoA and the C2 domains of phospholipase C- β 1 and - β 2 mediate specific association to $G\alpha_q$ subunits (Wang *et al.*, 1999; Tian *et al.*, 2011). This opens up the possibility that the C2 domain of *K/Inn1* can be a binding partner for *K/Rho5*. A possible model could be that *K/Inn1*, through its C2-domain is responsible for the correct spatiotemporal localisation of *K/Rho5* at the later stages of cytokinesis, where the small GTPase then has regulatory effects on the components responsible for the synthesis of the primary septum, e.g. *K/Iqg1*, *K/Chs2*, *K/Hof1* and/or *K/Cyk3*. A possible interaction between the C2 domain of *K/Inn1* and for example the yeast-specific extension would also contribute to the species-specific role of *K/Rho5* in cytokinesis, suggested by the inability of ScRho5 to complement a *Klrho5* deletion. However, since most components of the cytokinesis machinery influence each other, it is not possible to exactly pinpoint the interaction partners of *K/Rho5* with the data acquired in this thesis, but colocalization and coimmunoprecipitation experiments could help elucidate this matter.

4.6 *K/Cdc42* has overlapping functions with *K/Rho5*

In many fungi homologues of Cdc42 and Rac1 display interchangeable functions and embedment in signalling pathways (reviewed in Harris, 2011), prompting an investigation

4. Discussion

of *KlCdc42* in this thesis. Tetrad analysis revealed that *KlCDC42* is essential and complementation of the *Klcdc42* lethality through the wild-type gene confirmed this (Figure 22, chapter 3.4.1).

To elucidate the roles of *KlCdc42* a GFP-*KlCdc42* fusion protein was created and its localization was observed under different conditions (Figures 23 and 24, chapter 3.4.2). Since the *GFP-KlCDC42* was unable to complement the deletion mutant in tetrad analysis the observed localization has to be taken with caution. Even if not functional it stands to reason that the observed localization could be similar to the wild-type alleles because Sterk *et al.*, (2019) showed that a dominant negative *ScRho5* localized like the wild type under oxidative stress. However, an interference of the GFP with the binding capacities of *KlCdc42* towards its GEF and other potential effectors that might be responsible for its correct spatiotemporal localization cannot be ruled out with the data acquired in this thesis.

When observed under the fluorescent microscope GFP-*KlCdc42* localized to some part in the cytoplasm, but also accumulated at internal membranes, some were identifiable as vacuole membranes in the brightfield channel, and the tips of emerging and growing daughter cells (Figures 23 and 24, chapter 3.4.2). These localization patterns are in line with some of the functions known for Cdc42 homologues, as *ScCdc42* was shown to be involved in vacuole membrane fusion and in *S. pombe* *SpNrf1*, which is involved in vacuolar fusion, was shown to be a negative regulator of *SpCdc42* (Murray & Johnson, 2000; Müller *et al.*, 2001). Based on *KlCdc42s* localization to vacuolar membranes, a similar function in vacuole fusion is imaginable, but to elucidate their exact role in this context further research would be necessary.

In *S. cerevisiae* Cdc42 is important for polarization and the determination of the budding site. After budding the *ScCdc42* GEF *ScBud3* remains at the budding site, activating *ScCdc42* in early G1 phase and thus accounts for polarization soon after cytokinesis. The GAP *ScRga1* prevents budding at the exact same site by inactivating *ScCdc42*. The temporal control in this process is mainly regulated by *ScRsr1*, a Ras-type GTPase, and the scaffold protein *ScBem1* (reviewed in Miller *et al.*, 2020). A similar localization of *KlCdc42* was observed in cells in the earliest budding stages, where it accumulated at sites of the emerging bud (Figure 23, chapter 3.4.1). This suggests a conserved function of *KlCdc42* in

4. Discussion

bud site selection and early budding stages. Moreover, the complementation of the morphological phenotype of *Klrho5* deletions in 18 out of 21 segregants carrying the *Klrho5* deletion and the constitutively active *KICDC42*^{G12V} mutant suggests a shared function of *KICdc42* and *KIRho5* in later stages of cytokinesis (chapter 3.4.1).

In many fungi, like *Numuraea rileyi*, *Aspergillus nidulans* and *Candida albicans* Cdc42 plays mayor role in polarized growth, often in tandem with a Rac1 homologue and through controlling ROS production (Virag *et al.*, 2007; Semighini & Harris, 2008; Jiang *et al.*, 2014; Kowalewski *et al.*, 2021). This involvement of Cdc42 in ROS regulation might be preserved in some form in *K. lactis*, since when stressed with H₂O₂ the GFP-*KICdc42* construct displayed a rapid translocation to mitochondria (Figure 24, chapter 3.4.2), similar to the one observed for GFP-*KIRho5* constructs (Figure 19, chapter 3.3.1).

In rhabdomyosarcoma cells it was shown that specific inhibition of either Rac1 or Cdc42 increased autophagy and apoptosis. Moreover it was shown that *HsCdc42* is important for actin cage formation during mitophagy (Kruppa *et al.*, 2018; Li *et al.*, 2021). Together with the translocation of *KICdc42* to mitochondria this could suggest an additional function of *KICdc42* in mitophagy and ROS homeostasis. To find out in more detail if and in what capacity this might be true will be an interesting prospect for future research.

5. Summary

Small GTPases are important signalling hubs which coordinate extra and intracellular cues with a proper adaptive response, and thereby ensure the survival of cells and organisms. In the model yeast *S. cerevisiae* the small GTPase Rho5, a homologue of the well studied human Rac1, mediates the response to both low and high medium osmolarity (CWI- and HOG-pathway, respectively), oxidative stress and nutrient availability. Here the roles of its homologue *KIRho5*, from the dairy yeast *Kluyveromyces lactis*, in these and other signalling pathways were assessed. First, *in silico* analyses including sequence alignments were employed to identify the homologues of *RHO5* and the genes encoding the subunits of its dimeric GEF, *DCK1* and *LMO1*, in the *K. lactis* genome. Upon cloning and heterologous expression, *KIRHO5* complemented the phenotypes of a *Scrho5* deletion. Deletion mutants in either of the three genes altered their sensitivities to oxidative and cell wall stress conditions. Moreover, *KIRho5* and its bipartite GEF *KIDck1/KILmo1* showed similar intracellular distributions as their *S. cerevisiae* counterparts. Thus both oxidative stress and glucose starvation caused a rapid translocation of the proteins to the mitochondria. A novel function for *KIRho5* was discovered in the regulation of cytokinesis, as deletion mutants displayed protruding bud scars, aberrant primary septa and a thickened cell wall. *KICdc42*, another protein of the same small GTPase subfamily, participates in yeast bud site selection and was found to largely complement the morphological defects of *Klrho5* deletions, indicating overlapping functions. *KICd42* also shares the rapid translocation to mitochondria under oxidative stress. Thus, *KIRho5* was found to regulate oxidative stress response, adaption to glucose starvation and cytokinesis. Whereas the first two functions are apparently shared with its homologue in *S. cerevisiae*, the latter seems to be specific for *K. lactis*

6. References

- Akakura S, Kar B, Singh S, Cho L, Tibrewal N, Sanokawa-Akakura R, Reichman C, Ravichandran KS & Birge RB (2005)** C-terminal SH3 domain of CrkII regulates the assembly and function of the DOCK180/ELMO Rac-GEF. *J Cell Physiol* 204: 344–351
- Alvers AL, Fishwick LK, Wood MS, Hu D, Chung HS, Dunn WA & Aris JP (2009)** Autophagy and amino acid homeostasis are required for chronological longevity in *Saccharomyces cerevisiae*. *Aging Cell* 8: 353–369
- Annan RB, Wu C, Waller DD, Whiteway M & Thomas DY (2008)** Rho5p Is Involved in Mediating the Osmotic Stress Response in *Saccharomyces cerevisiae*, and Its Activity Is Regulated via Msi1p and Npr1p by Phosphorylation and Ubiquitination. *Eukaryot Cell* 7: 1441–1449
- Araujo-Palomares CL, Richthammer C, Seiler S & Castro-Longoria E (2011)** Functional characterization and cellular dynamics of the CDC-42 - RAC - CDC-24 module in *Neurospora crassa*. *PLoS One* 6: e27148
- Aronheim A, Engelberg D, Li N, al-Alawi N, Schlessinger J & Karin M (1994)** Membrane targeting of the nucleotide exchange factor Sos is sufficient for activating the Ras signaling pathway. *Cell* 78: 949–961
- Aspenström P, Fransson A & Saras J (2004)** Rho GTPases have diverse effects on the organization of the actin filament system. *Biochem J* 377: 327–337
- Backhaus K, Buchwald U, Heppeler N, Schmitz H-P, Rodicio R & Heinisch JJ (2011)** Milk and sugar: regulation of cell wall synthesis in the milk yeast *Kluyveromyces lactis*. *Eur J Cell Biol* 90: 745–750
- Backhaus K, Heilmann CJ, Sorgo AG, Purschke G, de Koster CG, Klis FM & Heinisch JJ (2010)** A systematic study of the cell wall composition of *Kluyveromyces lactis*. *Yeast* 27: 647–660
- Bähler J, Wu J-Q, Longtine MS, Shah NG, Mckenzie III A, Steever AB, Wach A, Philippsen P & Pringle JR (1998)** Heterologous modules for efficient and versatile PCR-based gene targeting in *Schizosaccharomyces pombe*. *Yeast* 14: 943–951
- Bertels L-K, Fernández Murillo L & Heinisch JJ (2021)** The Pentose Phosphate Pathway in Yeasts—More Than a Poor Cousin of Glycolysis. *Biomolecules* 11: 725
- Bi E & Park H-O (2012)** Cell polarization and cytokinesis in budding yeast. *Genetics* 191: 347–387
- Bielak-Zmijewska A, Kolano A, Szczepanska K, Maleszewski M & Borsuk E (2008)** Cdc42 protein acts upstream of IQGAP1 and regulates cytokinesis in mouse oocytes and embryos. *Dev Biol* 322: 21–32
- Biou V & Cherfils J (2004)** Structural Principles for the Multispecificity of Small GTP-Binding Proteins †. *Biochemistry* 43: 6833–40
- Bolis A, Corbetta S, Cioce A & de Curtis I (2003)** Differential distribution of Rac1 and Rac3 GTPases in the developing mouse brain: implications for a role of Rac3 in Purkinje cell differentiation. *Eur J Neurosci* 18: 2417–2424
- Bondos SE, Dunker AK & Uversky VN (2022)** Intrinsically disordered proteins play diverse roles in cell signaling. *Cell Commun Signal* 20: 20

6. References

- Boriack-Sjodin PA, Margarit SM, Bar-Sagi D & Kuriyan J (1998)** The structural basis of the activation of Ras by Sos. *Nature* 394: 337–343
- Bos JL, Rehmann H & Wittinghofer A (2007)** GEFs and GAPs: critical elements in the control of small G proteins. *Cell* 129: 865–877
- Boulter E, Garcia-Mata R, Guilluy C, Dubash A, Rossi G, Brennwald PJ & BurrIDGE K (2010)** Regulation of RhoGTPase crosstalk, degradation and activity by RhoGDI1. *Nat Cell Biol* 12: 477–483
- Boureaux A, Vignal E, Faure S & Fort P (2007)** Evolution of the Rho family of ras-like GTPases in eukaryotes. *Mol Biol Evol* 24: 203–216
- Bourne HR, Sanders DA & McCormick F (1990)** The GTPase superfamily: a conserved switch for diverse cell functions. *Nature* 348: 125–132
- Bourne HR, Sanders DA & McCormick F (1991)** The GTPase superfamily: conserved structure and molecular mechanism. *Nature* 349: 117–127
- Broach JR (2012)** Nutritional Control of Growth and Development in Yeast. *Genetics* 192: 73–105
- Brugnera E, Haney L, Grimsley C, Lu M, Walk SF, Tosello-Trampont A-C, Macara IG, Madhani H, Fink GR & Ravichandran KS (2002)** Unconventional Rac-GEF activity is mediated through the Dock180-ELMO complex. *Nat Cell Biol* 4: 574–582
- Butty A-C, Perrinjaquet N, Petit A, Jaquenoud M, Segall JE, Hofmann K, Zwahlen C & Peter M (2002)** A positive feedback loop stabilizes the guanine-nucleotide exchange factor Cdc24 at sites of polarization. *EMBO J* 21: 1565–1576
- Cabib E, Drgonová J & Drgon T (1998)** Role of small G proteins in yeast cell polarization and wall biosynthesis. *Annu Rev Biochem* 67: 307–333
- Canagarajah B, Leskow F, Ho J, Mischak H, Saidi L, Kazanietz M & Hurley J (2004)** Structural Mechanism for Lipid Activation of the Rac-Specific GAP, β 2-Chimaerin. *Cell* 119: 407–18
- Cao L, Tang Y, Quan Z, Zhang Z, Oliver SG & Zhang N (2016)** Chronological Lifespan in Yeast Is Dependent on the Accumulation of Storage Carbohydrates Mediated by Yak1, Mck1 and Rim15 Kinases. *PLoS Genet* 12: e1006458
- Chang EC, Barr M, Wang Y, Jung V, Xu HP & Wigler MH (1994)** Cooperative interaction of S. pombe proteins required for mating and morphogenesis. *Cell* 79: 131–141
- Chen J, Zheng W, Zheng S, Zhang D, Sang W, Chen X, Li G, Lu G & Wang Z (2008)** Rac1 is required for pathogenicity and Chm1-dependent conidiogenesis in rice fungal pathogen *Magnaporthe oryzae*. *PLoS Pathog* 4: e1000202
- Chen X, Zaro J & Shen W-C (2013)** Fusion Protein Linkers: Property, Design and Functionality. *Adv Drug Deliv Rev* 65: 1357–1369
- Chen XJ (1996)** Low- and high-copy-number shuttle vectors for replication in the budding yeast *Kluyveromyces lactis*. *Gene* 172: 131–136
- Chen XJ & Clark-Walker GD (1993)** Mutations in MGI genes convert *Kluyveromyces lactis* into a petite-positive yeast. *Genetics* 133: 517–525

6. References

- Colicelli J (2004)** Human RAS Superfamily Proteins and Related GTPases. *Science's STKE* 2004: re13–re13
- Conrad M, Schothorst J, Kankipati HN, Van Zeebroeck G, Rubio-Teixeira M & Thevelein JM (2014)** Nutrient sensing and signaling in the yeast *Saccharomyces cerevisiae*. *FEMS Microbiol Rev* 38: 254–299
- Coso OA, Chiariello M, Yu J-C, Teramoto H, Crespo P, Xu N, Miki T & Silvio Gutkind J (1995)** The small GTP-binding proteins Rac1 and Cdc42 regulate the activity of the JNK/SAPK signaling pathway. *Cell* 81: 1137–1146
- Cullen PJ & Lockyer PJ (2002)** Integration of calcium and Ras signalling. *Nat Rev Mol Cell Biol* 3: 339–348
- Delprato A (2012)** Topological and functional properties of the small GTPases protein interaction network. *PLoS One* 7: e44882
- devrekanli sadli A, Foltman M, Roncero C, Sanchez-Diaz A & Labib K (2012)** Inn1 and Cyk3 regulate chitin synthase during cytokinesis in budding yeasts. *J Cell Sci* 125:5453-5466
- Diekmann D, Abo A, Johnston C, Segal AW & Hall A (1994)** Interaction of Rac with p67phox and regulation of phagocytic NADPH oxidase activity. *Science* 265: 531–533
- Dujon B, Sherman D, Fischer G, Durrens P, Casaregola S, Lafontaine I, De Montigny J, Marck C, Neuvéglise C, Talla E, *et al* (2004)** Genome evolution in yeasts. *Nature* 430: 35–44
- Eliáš M & Klimeš V (2012)** Rho GTPases: deciphering the evolutionary history of a complex protein family. *Methods Mol Biol* 827: 13–34
- Epp JA & Chant J (1997)** An IQGAP-related protein controls actin-ring formation and cytokinesis in yeast. *Curr Biol* 7: 921–929
- Fabrizio P, Liou L-L, Moy VN, Diaspro A, Valentine JS, Gralla EB & Longo VD (2003)** SOD2 functions downstream of Sch9 to extend longevity in yeast. *Genetics* 163: 35–46
- Fang X, Luo J, Nishihama R, Wloka C, Dravis C, Travaglia M, Iwase M, Vallen EA & Bi E (2010)** Biphasic targeting and cleavage furrow ingression directed by the tail of a myosin II. *J Cell Biol* 191: 1333–1350
- Faroudi M, Hons M, Zachacz A, Dumont C, Lyck R, Stein JV & Tybulewicz VLJ (2010)** Critical roles for Rac GTPases in T-cell migration to and within lymph nodes. *Blood* 116: 5536–5547
- Fauré J, Vignais PV & Dagher MC (1999)** Phosphoinositide-dependent activation of Rho A involves partial opening of the RhoA/Rho-GDI complex. *Eur J Biochem* 262: 879–889
- Feng Z, Okada S, Cai G, Zhou B & Bi E (2015)** Myosin-II heavy chain and formin mediate the targeting of myosin essential light chain to the division site before and during cytokinesis. *Mol Biol Cell* 26: 1211–1224
- Fransson Å, Ruusala A & Aspenström P (2006)** The atypical Rho GTPases Miro-1 and Miro-2 have essential roles in mitochondrial trafficking. *Biochem Biophys Res Commun* 344: 500–10

6. References

- Freeman JL, Abo A & Lambeth JD (1996)** Rac 'insert region' is a novel effector region that is implicated in the activation of NADPH oxidase, but not PAK65. *J Biol Chem* 271: 19794–19801
- Fukuhara H (2003)** The Kluver effect revisited. *FEMS Yeast Res* 3: 327–31
- Garabedian MV, Wirshing A, Vakhrusheva A, Turegun B, Sokolova OS & Goode BL (2020)** A septin-Hof1 scaffold at the yeast bud neck binds and organizes actin cables. *Mol Biol Cell* 31: 1988–2001
- Garcia-Ranea JA & Valencia A (1998)** Distribution and functional diversification of the ras superfamily in *Saccharomyces cerevisiae*. *FEBS Lett* 434: 219–225
- Gasteier JE, Madrid R, Krautkrämer E, Schröder S, Muranyi W, Benichou S & Fackler OT (2003)** Activation of the Rac-binding partner FHOD1 induces actin stress fibers via a ROCK-dependent mechanism. *J Biol Chem* 278: 38902–38912
- Gietz RD & Akio S (1988)** New yeast-*Escherichia coli* shuttle vectors constructed with in vitro mutagenized yeast genes lacking six-base pair restriction sites. *Gene* 74: 527–534
- Goldberg J (1998)** Structural basis for activation of ARF GTPase: mechanisms of guanine nucleotide exchange and GTP-myristoyl switching. *Cell* 95: 237–248
- Golding AE, Visco I, Bieling P & Bement WM (2019)** Extraction of active RhoGTPases by RhoGDI regulates spatiotemporal patterning of RhoGTPases. *eLife* 8: e50471
- Gotta M, Abraham MC & Ahringer J (2001)** CDC-42 controls early cell polarity and spindle orientation in *C. elegans*. *Curr Biol* 11: 482–488
- Graziano BR, Yu H-YE, Alioto SL, Eskin JA, Ydenberg CA, Waterman DP, Garabedian M & Goode BL (2014)** The F-BAR protein Hof1 tunes formin activity to sculpt actin cables during polarized growth. *Mol Biol Cell* 25: 1730–1743
- Guaragnella N, Antonacci L, Passarella S, Marra E & Giannattasio S (2007)** Hydrogen peroxide and superoxide anion production during acetic acid-induced yeast programmed cell death. *Folia Microbiol (Praha)* 52: 237–240
- Guaragnella N, Bobba A, Passarella S, Marra E & Giannattasio S (2010a)** Yeast acetic acid-induced programmed cell death can occur without cytochrome c release which requires metacaspase YCA1. *FEBS Lett* 584: 224–228
- Guaragnella N, Passarella S, Marra E & Giannattasio S (2010b)** Knock-out of metacaspase and/or cytochrome c results in the activation of a ROS-independent acetic acid-induced programmed cell death pathway in yeast. *FEBS Lett* 584: 3655–60
- Gumienny TL, Brugnera E, Tosello-Trampont AC, Kinchen JM, Haney LB, Nishiwaki K, Walk SF, Nemergut ME, Macara IG, Francis R, Schedl T, Qin Y, Van Aelst L, Hengartner MO & Ravichandran KS (2001)** CED-12/ELMO, a novel member of the CrkII/Dock180/Rac pathway, is required for phagocytosis and cell migration. *Cell* 107: 27–41
- Gureasko J, Galush WJ, Boykevich S, Sondermann H, Bar-Sagi D, Groves JT & Kuriyan J (2008)** Membrane-dependent signal integration by the Ras activator Son of sevenless. *Nat Struct Mol Biol* 15: 452–461

6. References

- Gureasko J, Kuchment O, Makino DL, Sondermann H, Bar-Sagi D & Kuriyan J (2010)** Role of the histone domain in the autoinhibition and activation of the Ras activator Son of Sevenless. *Proc Natl Acad Sci U S A* 107: 3430–3435
- Hall A (1998)** Rho GTPases and the actin cytoskeleton. *Science* 279: 509–514
- Hanahan D (1983)** Studies on transformation of *Escherichia coli* with plasmids. *J Mol Biol* 166: 557–580
- Hancock JF & Hall A (1993)** A novel role for RhoGDI as an inhibitor of GAP proteins. *EMBO J* 12: 1915–1921
- Hara S, Kiyokawa E, Iemura S, Natsume T, Wassmer T, Cullen PJ, Hiai H & Matsuda M (2008)** The DHR1 Domain of DOCK180 Binds to SNX5 and Regulates Cation-independent Mannose 6-phosphate Receptor Transport. *Mol Biol Cell* 19: 3823–3835
- Harris S (2011)** Cdc42/Rho GTPases in fungi: Variations on a common theme. *Molecular Microbiology* 79: 1123–7
- Heinisch JJ, Buchwald U, Gottschlich A, Heppeler N & Rodicio R (2010)** A tool kit for molecular genetics of *Kluyveromyces lactis* comprising a congenic strain series and a set of versatile vectors. *FEMS Yeast Res* 10: 333–342
- Heinisch JJ & Rodicio R (2017)** Stress Responses in Wine Yeast. In *Biology of Microorganisms on Grapes, in Must and in Wine*, König H, Uden G & Fröhlich J (eds) pp 377–395. Cham: Springer International Publishing
- Heo WD, Inoue T, Park WS, Kim ML, Park BO, Wandless TJ & Meyer T (2006)** PI(3,4,5)P3 and PI(4,5)P2 Lipids Target Proteins with Polybasic Clusters to the Plasma Membrane. *Science* 314: 1458–1461
- Herker E, Jungwirth H, Zweig K, Maldener C, Fröhlich K-U, Wissing S, Büttner S, Fehr M, Sigrist S & Madeo F (2004)** Chronological aging leads to apoptosis in yeast. *J Cell Biol* 164: 501–7
- Hodge RG & Ridley AJ (2016)** Regulating Rho GTPases and their regulators. *Nat Rev Mol Cell Biol* 17: 496–510
- Hoffman GR, Nassar N & Cerione RA (2000)** Structure of the Rho Family GTP-Binding Protein Cdc42 in Complex with the Multifunctional Regulator RhoGDI. *Cell* 100: 345–356
- Hong E, Davidson AR & Kaiser CA (1996)** A pathway for targeting soluble misfolded proteins to the yeast vacuole. *J Cell Biol* 135: 623–633
- Huang J, Huang A, Poplawski A, DiPino F, Traugh JA & Ling J (2020)** PAK2 activated by Cdc42 and caspase 3 mediates different cellular responses to oxidative stress-induced apoptosis. *Biochim Biophys Acta Mol Cell Res* 1867: 118645
- Hühn J, Musielak M, Schmitz H-P & Heinisch JJ (2020)** Fungal homologues of human Rac1 as emerging players in signal transduction and morphogenesis. *Int Microbiol* 23: 43–53
- Innocenti M, Tenca P, Frittoli E, Faretta M, Tocchetti A, Di Fiore PP & Scita G (2002)** Mechanisms through which Sos-1 coordinates the activation of Ras and Rac. *J Cell Biol* 156: 125–136

6. References

- Inoki K, Zhu T & Guan K-L (2003)** TSC2 Mediates Cellular Energy Response to Control Cell Growth and Survival. *Cell* 115: 577–90
- Itzen A, Pylypenko O, Goody R, Alexandrov K & Rak A (2006)** Nucleotide exchange via local protein unfolding—Structure of Rab8 in complex with MSS4. *EMBO J* 25: 1445–55
- Jacoby JJ, Kirchrath L, Gengenbacher U & Heinisch JJ (1999)** Characterization of KLBCK1, encoding a MAP kinase kinase kinase of *Kluyveromyces lactis*. *J Mol Biol* 288: 337–352
- Jendretzki A, Ciklic I, Rodicio R, Schmitz H-P & Heinisch JJ (2009)** Cyk3 acts in actomyosin ring independent cytokinesis by recruiting Inn1 to the yeast bud neck. *Molecular genetics and genomics : MGG* 282: 437–51
- Jiang S, Yin Y, Song Z, Zhou G & Wang Z (2014)** RacA and Cdc42 regulate polarized growth and microsclerotium formation in the dimorphic fungus *Nomuraea rileyi*. *Res Microbiol* 165: 233–242
- Kalwat MA & Thurmond DC (2013)** Signaling mechanisms of glucose-induced F-actin remodeling in pancreatic islet β cells. *Exp Mol Med* 45: e37
- Kamei T, Tanaka K, Hihara T, Umikawa M, Imamura H, Kikyo M, Ozaki K & Takai Y (1998)** Interaction of Bnr1p with a Novel Src Homology 3 Domain-containing Hof1p: IMPLICATION IN CYTOKINESIS IN SACCHAROMYCES CEREVISIAE *. *J Biol Chem* 273: 28341–28345
- Kanki T, Wang K, Cao Y, Baba M & Klionsky DJ (2009)** Atg32 is a mitochondrial protein that confers selectivity during mitophagy. *Dev Cell* 17: 98–109
- Katoh H & Negishi M (2003)** RhoG activates Rac1 by direct interaction with the Dock180-binding protein Elmo. *Nature* 424: 461–464
- Kay AJ & Hunter CP (2001)** CDC-42 regulates PAR protein localization and function to control cellular and embryonic polarity in *C. elegans*. *Current Biology* 11: 474–481
- Kazanietz MG & Caloca MJ (2017)** The Rac GTPase in Cancer: From Old Concepts to New Paradigms. *Cancer Res* 77: 5445–5451
- Keely PJ, Westwick JK, Whitehead IP, Der CJ & Parise LV (1997)** Cdc42 and Rac1 induce integrin-mediated cell motility and invasiveness through PI(3)K. *Nature* 390: 632–636
- Ketela T, Green R & Bussey H (1999)** *Saccharomyces cerevisiae* Mid2p Is a Potential Cell Wall Stress Sensor and Upstream Activator of the PKC1-MPK1 Cell Integrity Pathway. *J Bacteriol* 181: 3330–3340
- Kirchrath L, Lorberg A, Schmitz H-P, Gengenbacher U & Heinisch JJ (2000)** Comparative genetic and physiological studies of the MAP kinase Mpk1p from *Kluyveromyces lactis* and *Saccharomyces cerevisiae*. *J Mol Biol* 300: 743–758
- Klebe RJ, Harriss JV, Sharp ZD & Douglas MG (1983)** A general method for polyethylene-glycol-induced genetic transformation of bacteria and yeast. *Gene* 25: 333–341

6. References

- Klionsky DJ, Codogno P, Cuervo AM, Deretic V, Elazar Z, Fueyo-Margareto J, Gewirtz DA, Kroemer G, Levine B, Mizushima N, Rubinsztein DC, Thumm M, & Tooze SA (2010)** A comprehensive glossary of autophagy-related molecules and processes. *Autophagy* 6: 438–448
- ten Klooster JP & Hordijk PL (2007)** Targeting and localized signalling by small GTPases. *Biol Cell* 99: 1–12
- ten Klooster JP, Jaffer ZM, Chernoff J & Hordijk PL (2006)** Targeting and activation of Rac1 are mediated by the exchange factor beta-Pix. *J Cell Biol* 172: 759–769
- Ko N, Nishihama R, Tully GH, Ostapenko D, Solomon MJ, Morgan DO & Pringle JR (2007)** Identification of Yeast IQGAP (Iqg1p) as an Anaphase-Promoting-Complex Substrate and Its Role in Actomyosin-Ring-Independent Cytokinesis. *Mol Biol Cell* 18: 5139–5153
- Komander D, Patel M, Laurin M, Fradet N, Pelletier A, Barford D & Côté J-F (2008)** An alpha-helical extension of the ELMO1 pleckstrin homology domain mediates direct interaction to DOCK180 and is critical in Rac signaling. *Mol Biol Cell* 19: 4837–4851
- Kooistra R, Hooykaas PJJ & Steensma HY (2004)** Efficient gene targeting in *Kluyveromyces lactis*. *Yeast* 21: 781–792
- Korinek WS, Bi E, Epp JA, Wang L, Ho J & Chant J (2000)** Cyk3, a novel SH3-domain protein, affects cytokinesis in yeast. *Curr Biol* 10: 947–950
- Kowalewski GP, Wildeman AS, Bogliolo S, Besold AN, Bassilana M & Culotta VC (2021)** Cdc42 regulates reactive oxygen species production in the pathogenic yeast *Candida albicans*. *J Biol Chem* 297: 100917
- Kruppa AJ, Kishi-Itakura C, Masters TA, Rorbach JE, Grice GL, Kendrick-Jones J, Nathan JA, Minczuk M & Buss F (2018)** Myosin VI-Dependent Actin Cages Encapsulate Parkin-Positive Damaged Mitochondria. *Dev Cell* 44: 484-499.e6
- Kukimoto-Niino M, Ihara K, Murayama K & Shirouzu M (2021)** Structural insights into the small GTPase specificity of the DOCK guanine nucleotide exchange factors. *Curr Opin Struct Biol* 71: 249–258
- Lai C, Boguski M, Broek D & Powers S (1993)** Influence of Guanine Nucleotides on complex formation between Ras AND CDC25 proteins. *Mol Cell Biol* 13: 1345–52
- Lam BD & Hordijk PL (2013)** The Rac1 hypervariable region in targeting and signaling: a tail of many stories. *Small GTPases* 4: 78–89
- Lanning CC, Daddona JL, Ruiz-Velasco R, Shafer SH & Williams CL (2004)** The Rac1 C-terminal polybasic region regulates the nuclear localization and protein degradation of Rac1. *J Biol Chem* 279: 44197–44210
- Lee Y, Nasution O, Choi E, Choi I-G, Kim W & Choi W (2015)** Transcriptome analysis of acetic-acid-treated yeast cells identifies a large set of genes whose overexpression or deletion enhances acetic acid tolerance. *Appl Microbiol Biotechnol* 99: 6391–6403
- Leeuw T, Fourest-Lieuvain A, Wu C, Chenevert J, Clark K, Whiteway M, Thomas DY & Leberer E (1995)** Pheromone response in yeast: association of Bem1p with proteins of the MAP kinase cascade and actin. *Science* 270: 1210–1213

6. References

- Levin DE (2005)** Cell Wall Integrity Signaling in *Saccharomyces cerevisiae*. *Microbiol Mol Biol Rev* 69: 262–291
- Li B-Z & Yuan Y-J (2010)** Transcriptome shifts in response to furfural and acetic acid in *Saccharomyces cerevisiae*. *Appl Microbiol Biotechnol* 86: 1915–1924
- Li C, Li Z, Song L, Meng L, Xu G, Zhang H, Hu J, Li F & Liu C (2021)** GEFT Inhibits Autophagy and Apoptosis in Rhabdomyosarcoma via Activation of the Rac1/Cdc42-mTOR Signaling Pathway. *Front Oncol* 11: 656608
- Lin Q, Fuji RN, Yang W & Cerione RA (2003)** RhoGDI is required for Cdc42-mediated cellular transformation. *Curr Biol* 13: 1469–1479
- Llorca O, Arias-Palomo E, Zugaza JL & Bustelo XR (2005)** Global conformational rearrangements during the activation of the GDP/GTP exchange factor Vav3. *EMBO J* 24: 1330–1340
- Longo V, Gralla E & Valentine J (1996)** Superoxide dismutase activity is essential for stationary phase survival in *Saccharomyces cerevisiae*. Mitochondrial production of toxic oxygen species in vivo. *J Biol Chem* 271: 12275–80
- Longtine MS, Mckenzie III A, Demarini DJ, Shah NG, Wach A, Brachat A, Philippsen P & Pringle JR (1998)** Additional modules for versatile and economical PCR-based gene deletion and modification in *Saccharomyces cerevisiae*. *Yeast* 14: 953–961
- Lu M, Kinchen JM, Rossman KL, Grimsley C, deBakker C, Brugnera E, Tosello-Trampont A-C, Haney LB, Klingele D, Sondek J, Hengartner MO & Ravichandran KS (2004)** PH domain of ELMO functions in trans to regulate Rac activation via Dock180. *Nat Struct Mol Biol* 11: 756–762
- Lu M, Kinchen JM, Rossman KL, Grimsley C, Hall M, Sondek J, Hengartner MO, Yajnik V & Ravichandran KS (2005)** A Steric-inhibition model for regulation of nucleotide exchange via the Dock180 family of GEFs. *Curr Biol* 15: 371–377
- Lucena RM, Dolz-Edo L, Brul S, de Morais MA & Smits G (2020)** Extreme Low Cytosolic pH Is a Signal for Cell Survival in Acid Stressed Yeast. *Genes (Basel)* 11: E656
- Ludovico P, Sousa MJ, Silva MT, Leão CL & Côrte-Real M (2001)** *Saccharomyces cerevisiae* commits to a programmed cell death process in response to acetic acid. *Microbiology (Reading)* 147: 2409–2415
- Madaule P & Axel R (1985)** A novel ras-related gene family. *Cell* 41: 31–40
- Malaby AW, van den Berg B & Lambricht DG (2013)** Structural basis for membrane recruitment and allosteric activation of cytohesin family Arf GTPase exchange factors. *Proc Natl Acad Sci U S A* 110: 14213–14218
- Mao K, Wang K, Zhao M, Xu T & Klionsky DJ (2011)** Two MAPK-signaling pathways are required for mitophagy in *Saccharomyces cerevisiae*. *J Cell Biol* 193: 755–767
- McCallum SJ, Wu WJ & Cerione RA (1996)** Identification of a putative effector for Cdc42Hs with high sequence similarity to the RasGAP-related protein IQGAP1 and a Cdc42Hs binding partner with similarity to IQGAP2. *J Biol Chem* 271: 21732–21737

6. References

- Meller N, Merlot S & Guda C (2005)** CZH proteins: a new family of Rho-GEFs. *J Cell Sci* 118: 4937–4946
- Miller KE, Kang PJ & Park H-O (2020)** Regulation of Cdc42 for polarized growth in budding yeast. *Microb Cell* 7: 175–189
- Mira NP, Becker JD & Sá-Correia I (2010a)** Genomic Expression Program Involving the Haa1p-Regulon in *Saccharomyces cerevisiae* Response to Acetic Acid. *OMICS* 14: 587–601
- Mira NP, Palma M, Guerreiro JF & Sá-Correia I (2010b)** Genome-wide identification of *Saccharomyces cerevisiae* genes required for tolerance to acetic acid. *Microb Cell Fact* 9: 79
- Mistou M-Y, Jacquet E, Poulet P, Rensland H, Gideon P, Schlichting I, Wittinghofer A & Parmeggiani A (1992)** Mutations of Ha-ras p21 that define important regions for the molecular mechanism of the SDC25 C-domain, a guanine nucleotide dissociation stimulator. *EMBO J* 11: 2391–7
- Miura K, Jacques KM, Stauffer S, Kubosaki A, Zhu K, Hirsch DS, Resau J, Zheng Y & Randazzo PA (2002)** ARAP1: a point of convergence for Arf and Rho signaling. *Mol Cell* 9: 109–119
- Mosaddeghzadeh N & Ahmadian MR (2021)** The RHO Family GTPases: Mechanisms of Regulation and Signaling. *Cells* 10: 1831
- Müller O, Johnson DI & Mayer A (2001)** Cdc42p functions at the docking stage of yeast vacuole membrane fusion. *EMBO J* 20: 5657–5665
- Murray JM & Johnson DI (2000)** Isolation and characterization of Nrf1p, a novel negative regulator of the Cdc42p GTPase in *Schizosaccharomyces pombe*. *Genetics* 154: 155–165
- Musielak M, Sterk CC, Schubert F, Meyer C, Paululat A & Heinisch JJ (2021)** The small GTPase KIRho5 responds to oxidative stress and affects cytokinesis. *J Cell Sci* 134: jcs258301
- Naumov GI, Naumova ES, Glushakova AM, Kachalkin AV & Chernov IYu (2014)** Finding of dairy yeasts *Kluyveromyces lactis* var. *lactis* in natural habitats. *Microbiology* 83: 782–786
- Nimnual AS, Yatsula BA & Bar-Sagi D (1998)** Coupling of Ras and Rac guanosine triphosphatases through the Ras exchanger Sos. *Science* 279: 560–563
- Nishihama R, Schreiter J, Onishi M, Vallen E, Hanna J, Moravcevic K, Lippincott M, Han H, Lemmon M, Pringle J & Bi E (2009)** Role of Inn1 and its interactions with Hof1 and Cyk3 in promoting cleavage furrow and septum formation in *S. cerevisiae*. *J Cell Biol* 185: 995–1012
- Nouri K, Timson DJ & Ahmadian MR (2020)** New model for the interaction of IQGAP1 with CDC42 and RAC1. *Small GTPases* 11: 16–22
- Oishi A, Makita N, Sato J & Iiri T (2012)** Regulation of RhoA Signaling by the cAMP-dependent Phosphorylation of RhoGDI α . *J Biol Chem* 287: 38705–38715
- Okamoto K, Kondo-Okamoto N & Ohsumi Y (2009)** Mitochondria-Anchored Receptor Atg32 Mediates Degradation of Mitochondria via Selective Autophagy. *Developmental cell* 17: 87–97

6. References

- Olson MF, Ashworth A & Hall A (1995)** An Essential Role for Rho, Rac, and Cdc42 GTPases in Cell Cycle Progression Through G1. *Science* 269: 1270–1272
- Ozdemir ES, Jang H, Gursoy A, Keskin O, Li Z, Sacks DB & Nussinov R (2018)** Unraveling the molecular mechanism of interactions of the Rho GTPases Cdc42 and Rac1 with the scaffolding protein IQGAP2. *J Biol Chem* 293: 3685–3699
- Patel M, Pelletier A & Côté J-F (2011)** Opening up on ELMO regulation: New insights into the control of Rac signaling by the DOCK180/ELMO complex. *Small GTPases* 2: 268–275
- Pichaud F, Walther RF & Nunes de Almeida F (2019)** Regulation of Cdc42 and its effectors in epithelial morphogenesis. *J Cell Sci* 132: jcs217869
- Renault L, Kuhlmann J, Henkel A & Wittinghofer A (2001)** Structural Basis for Guanine Nucleotide Exchange on Ran by the Regulator of Chromosome Condensation (RCC1). *Cell* 105: 245–255
- Ribeiro RA, Vitorino MV, Godinho CP, Bourbon-Melo N, Robalo TT, Fernandes F, Rodrigues MS & Sá-Correia I (2021)** Yeast adaptive response to acetic acid stress involves structural alterations and increased stiffness of the cell wall. *Sci Rep* 11: 12652
- Ridley AJ, Paterson HF, Johnston CL, Diekmann D & Hall A (1992)** The small GTP-binding protein rac regulates growth factor-induced membrane ruffling. *Cell* 70: 401–410
- Rippert D & Heinisch JJ (2016)** Investigation of the role of four mitotic septins and chitin synthase 2 for cytokinesis in *Kluyveromyces lactis*. *Fungal Genet Biol* 94: 69–78
- Rippert D, Heppeler N, Albermann S, Schmitz H-P & Heinisch JJ (2014)** Regulation of cytokinesis in the milk yeast *Kluyveromyces lactis*. *Biochim Biophys Acta* 1843: 2685–2697
- Rizzetto L, Zanni E, Uccelletti D, Ferrero I & Goffrini P (2012)** Extension of Chronological Lifespan by Hexokinase Mutation in *Kluyveromyces lactis* Involves Increased Level of the Mitochondrial Chaperonin Hsp60. *J Aging Res* 2012: 946586
- Robzyk K & Kassir Y (1992)** A simple and highly efficient procedure for rescuing autonomous plasmids from yeast. *Nucleic Acids Res* 20: 3790
- Rodicio R & Heinisch JJ (2013)** Yeast on the milky way: genetics, physiology and biotechnology of *Kluyveromyces lactis*. *Yeast* 30: 165–177
- Rodriguez JR & Paterson BM (1990)** Yeast myosin heavy chain mutant: Maintenance of the cell type specific budding pattern and the normal deposition of chitin and cell wall components requires an intact myosin heavy chain gene. *Cell Motility* 17: 301–308
- Roncero C & Durán A (1985)** Effect of Calcofluor white and Congo red on fungal cell wall morphogenesis: in vivo activation of chitin polymerization. *J Bacteriol* 163: 1180–1185
- Roncero C & Sánchez Y (2010)** Cell separation and the maintenance of cell integrity during cytokinesis in yeast: the assembly of a septum. *Yeast* 27: 521–530
- Roux A, Leroux A, Alaamery M, Hoffman C, Chartrand P, Ferbeyre G & Luis R (2009)** Pro-Aging Effects of Glucose Signaling through a G Protein-Coupled Glucose Receptor in Fission Yeast. *PLoS Genet* 5: e1000408

6. References

- Sadeh A, Movshovich N, Volokh M, Gheber L & Aharoni A (2011)** Fine-tuning of the Msn2/4-mediated yeast stress responses as revealed by systematic deletion of Msn2/4 partners. *MBoC* 22: 3127–3138
- Salari R & Salari R (2017)** Investigation of the Best *Saccharomyces cerevisiae* Growth Condition. *Electronic physician* 9: 3592–3597
- Sampaio-Marques B, Felgueiras C, Silva A, Rodrigues F & Ludovico P (2011)** Yeast chronological lifespan and proteotoxic stress: is autophagy good or bad? *Biochem Soc Trans* 39: 1466–1470
- Sanchez-Diaz A, Marchesi V, Murray S, Jones R, Pereira G, Edmondson R, Allen T & Labib K (2008)** Inn1 couples contraction of the actomyosin ring to membrane ingression during cytokinesis in budding yeast. *Nature cell biology* 10: 395–406
- Saraste M, Sibbald PR & Wittinghofer A (1990)** The P-loop--a common motif in ATP- and GTP-binding proteins. *Trends Biochem Sci* 15: 430–434
- Schaefer A, Reinhard NR & Hordijk PL (2014)** Toward understanding RhoGTPase specificity: structure, function and local activation. *Small GTPases* 5: 6
- Scheffzek K, Ahmadian MR, Kabsch W, Wiesmüller L, Lautwein A, Schmitz F & Wittinghofer A (1997)** The Ras-RasGAP complex: structural basis for GTPase activation and its loss in oncogenic Ras mutants. *Science* 277: 333–338
- Schmidt M, Bowers B, Varma A, Roh D-H & Cabib E (2002)** In budding yeast, contraction of the actomyosin ring and formation of the primary septum at cytokinesis depend on each other. *J Cell Sci* 115: 293–302
- Schmitz H-P, Huppert S, Lorberg A & Heinisch JJ (2002)** Rho5p downregulates the yeast cell integrity pathway. *J Cell Sci* 115: 3139–3148
- Schmitz H-P, Jendretzki A, Sterk C & Heinisch JJ (2018)** The Small Yeast GTPase Rho5 and Its Dimeric GEF Dck1/Lmo1 Respond to Glucose Starvation. *Int J Mol Sci* 19: E2186
- Schmitz H-P, Jendretzki A, Wittland J, Wiechert J & Heinisch JJ (2015)** Identification of Dck1 and Lmo1 as upstream regulators of the small GTPase Rho5 in *Saccharomyces cerevisiae*. *Molecular Microbiology* 96: 306–324
- Sekiguchi T, Hirose E, Nakashima N, Ii M & Nishimoto T (2001)** Novel G Proteins, Rag C and Rag D, Interact with GTP-binding Proteins, Rag A and Rag B*. *J Biol Chem* 276: 7246–7257
- Semighini CP & Harris SD (2008)** Regulation of apical dominance in *Aspergillus nidulans* hyphae by reactive oxygen species. *Genetics* 179: 1919–1932
- Shannon KB & Li R (1999)** The Multiple Roles of Cyk1p in the Assembly and Function of the Actomyosin Ring in Budding Yeast. *Mol Biol Cell* 10: 283–296
- Shannon KB & Li R (2000)** A myosin light chain mediates the localization of the budding yeast IQGAP-like protein during contractile ring formation. *Current Biology* 10: 727–730
- Sheu Y-J, Fortin N, Costigan C & Snyder M (1998)** Spa2p Interacts with Cell Polarity Proteins and Signaling Components Involved in Yeast Cell Morphogenesis. *Mol Cell Biol* 18: 4053–69

6. References

- Singh K, Kang PJ & Park H-O (2008)** The Rho5 GTPase is necessary for oxidant-induced cell death in budding yeast. *Proc Natl Acad Sci U S A* 105: 1522–1527
- Singh K, Lee ME, Entezari M, Jung C-H, Kim Y, Park Y, Fioretti JD, Huh W-K, Park H-O & Kang PJ (2019)** Genome-Wide Studies of Rho5-Interacting Proteins That Are Involved in Oxidant-Induced Cell Death in Budding Yeast. *G3 (Bethesda)* 9: 921–931
- Smith DL, Maharrey CH, Carey CR, White RA & Hartman JL (2016)** Gene-Nutrient Interaction Markedly Influences Yeast Chronological Lifespan. *Exp Gerontol* 86: 113–123
- Snyder JT, Worthylake DK, Rossman KL, Betts L, Pruitt WM, Siderovski DP, Der CJ & Sondek J (2002)** Structural basis for the selective activation of Rho GTPases by Dbl exchange factors. *Nat Struct Biol* 9: 468–475
- Sor F & Fukuhara H (1989)** Analysis of chromosomal DNA patterns of the genus *Kluyveromyces*. *Yeast* 5: 1–10
- Sprang SR (1997)** G protein mechanisms: insights from structural analysis. *Annu Rev Biochem* 66: 639–678
- Sterk C, Gräber L, Schmitz H-P & Heinisch JJ (2019)** Analysis of Functional Domains in Rho5, the Yeast Homolog of Human Rac1 GTPase, in Oxidative Stress Response. *Int J Mol Sci* 20: E5550
- Sulciner DJ, Irani K, Yu ZX, Ferrans VJ, Goldschmidt-Clermont P & Finkel T (1996)** rac1 regulates a cytokine-stimulated, redox-dependent pathway necessary for NF-kappaB activation. *Mol Cell Biol* 16: 7115
- Thomas C, Fricke I, Scrima A, Berken A & Wittinghofer A (2007)** Structural Evidence for a Common Intermediate in Small G Protein-GEF Reactions. *Molecular Cell* 25: 141–149
- Tian M, Bai C, Lin Q, Lin H, Liu M, Ding F & Wang H-R (2011)** Binding of RhoA by the C2 domain of E3 ligase Smurf1 is essential for Smurf1-regulated RhoA ubiquitination and cell protrusive activity. *FEBS Lett* 585: 2199–2204
- Ugolev Y, Berdichevsky Y, Weinbaum C & Pick E (2008)** Dissociation of Rac1(GDP).RhoGDI complexes by the cooperative action of anionic liposomes containing phosphatidylinositol 3,4,5-trisphosphate, Rac guanine nucleotide exchange factor, and GTP. *J Biol Chem* 283: 22257–22271
- Ullah A, Chandrasekaran G, Brul S & Smits G (2013)** Yeast adaptation to weak acids prevents futile energy expenditure. *Frontiers in microbiology* 4: 142
- Vallen EA, Caviston J & Bi E (2000)** Roles of Hof1p, Bni1p, Bnr1p, and Myo1p in Cytokinesis in *Saccharomyces cerevisiae*. *Mol Biol Cell* 11: 593–611
- Vasyutina E, Martarelli B, Brakebusch C, Wende H & Birchmeier C (2009)** The small G-proteins Rac1 and Cdc42 are essential for myoblast fusion in the mouse. *Proc Natl Acad Sci U S A* 106: 8935–8940
- Vauchelles R, Stalder D, Botton T, Arkowitz R & Bassilana M (2010)** Rac1 Dynamics in the Human Opportunistic Fungal Pathogen *Candida albicans*. *PloS one* 5: e15400

6. References

- Vetter IR & Wittinghofer A (2001)** The guanine nucleotide-binding switch in three dimensions. *Science* 294: 1299–1304
- Virag A, Lee MP, Si H & Harris SD (2007)** Regulation of hyphal morphogenesis by cdc42 and rac1 homologues in *Aspergillus nidulans*. *Molecular Microbiology* 66: 1579–1596
- Wan J, Cao Y, Abdelaziz MH, Huang L, Kesavan DK, Su Z, Wang S & Xu H (2019)** Downregulated Rac1 promotes apoptosis and inhibits the clearance of apoptotic cells in airway epithelial cells, which may be associated with airway hyper-responsiveness in asthma. *Scand J Immunol* 89: e12752
- Wang T, Pentylala S, Elliott JT, Dowal L, Gupta E, Rebecchi MJ & Scarlata S (1999)** Selective interaction of the C2 domains of phospholipase C-beta1 and -beta2 with activated Galphaq subunits: an alternative function for C2-signaling modules. *Proc Natl Acad Sci U S A* 96: 7843–7846
- Wauters R, Britton SJ & Verstrepen KJ (2021)** Old yeasts, young beer-The industrial relevance of yeast chronological life span. *Yeast* 38: 339–351
- Williams CL (2003)** The polybasic region of Ras and Rho family small GTPases: a regulator of protein interactions and membrane association and a site of nuclear localization signal sequences. *Cellular Signalling* 15: 1071–1080
- Wloka C & Bi E (2012)** Mechanisms of cytokinesis in budding yeast. *Cytoskeleton* 69: 710–726
- Wolfe KH & Shields DC (1997)** Molecular evidence for an ancient duplication of the entire yeast genome. *Nature* 387: 708–713
- Worthylake DK, Rossman KL & Sodek J (2000)** Crystal structure of Rac1 in complex with the guanine nucleotide exchange region of Tiam1. *Nature* 408: 682–688
- Xiao Y, Lin VY, Ke S, Lin GE, Lin F-T & Lin W-C (2014)** 14-3-3 τ promotes breast cancer invasion and metastasis by inhibiting RhoGDI α . *Mol Cell Biol* 34: 2635–2649
- Yamada T, Sakisaka T, Hisata S, Baba T & Takai Y (2005)** RA-RhoGAP, Rap-activated Rho GTPase-activating protein implicated in neurite outgrowth through Rho. *J Biol Chem* 280: 33026–33034
- Yi D-G, Hong S & Huh W-K (2018)** Mitochondrial dysfunction reduces yeast replicative lifespan by elevating RAS-dependent ROS production by the ER-localized NADPH oxidase Yno1. *PLOS ONE* 13: e0198619
- Yin J, Haney L, Walk S, Zhou S, Ravichandran KS & Wang W (2004)** Nuclear localization of the DOCK180/ELMO complex. *Arch Biochem Biophys* 429: 23–29
- Zeeman A-M, Luttik MAH, Pronk JT, van Dijken JP & Steensma HY (1999)** Impaired growth on glucose of a pyruvate dehydrogenase-negative mutant of *Kluyveromyces lactis* is due to a limitation in mitochondrial acetyl-coenzyme A uptake. *FEMS Microbiology Letters* 177: 23–28
- Zhang B, Zhang Y & Shacter E (2004)** Rac1 Inhibits Apoptosis in Human Lymphoma Cells by Stimulating Bad Phosphorylation on Ser-75. *Mol Cell Biol* 24: 6205–6214

6. References

- Zheng D-Q, Wu X-C, Wang P-M, Chi X-Q, Tao X-L, Li P, Jiang X-H & Zhao Y-H (2011)** Drug resistance marker-aided genome shuffling to improve acetic acid tolerance in *Saccharomyces cerevisiae*. *J Ind Microbiol Biotechnol* 38: 415–422
- Ziman M, Preuss D, Mulholland J, O'Brien J, Botstein D & Johnson D (1994)** Subcellular localization of Cdc42p, a *Saccharomyces cerevisiae* GTP-binding protein involved in the control of cell polarity. *Mol Biol Cell* 4: 1307–16
- Zimmer S, Goody PR, Oelze M, Ghanem A, Mueller CF, Laufs U, Daiber A, Jansen F, Nickenig G & Wassmann S (2021)** Inhibition of Rac1 GTPase Decreases Vascular Oxidative Stress, Improves Endothelial Function, and Attenuates Atherosclerosis Development in Mice. *Front Cardiovasc Med* 8: 680775
- Zong H, Kaibuchi K & Quilliam LA (2001)** The insert region of RhoA is essential for Rho kinase activation and cellular transformation. *Mol Cell Biol* 21: 5287–5298
- Zong H, Raman N, Mickelson-Young LA, Atkinson SJ & Quilliam LA (1999)** Loop 6 of RhoA confers specificity for effector binding, stress fiber formation, and cellular transformation. *J Biol Chem* 274: 4551–4560
- Zonneveld BJM & Steensma H (2003)** Mating, Sporulation and Tetrad Analysis in *Kluyveromyces lactis*. In *Non-Conventional Yeasts in Genetics, Biochemistry and Biotechnology: Practical Protocols*, Wolf K Breunig KD & Bart G (eds) pp 151–154. Cham: Springer Science & Business Media

7. Acknowledgments

I would like to thank my supervisor Prof. Dr. Jürgen Heinisch for all the help and advice with this PhD. I would also like to thank Dr. Hans-Peter Schmitz for the support in technical matters and Christian Meyer and Prof Dr. Achim Paululat from the Zoology department for their support, as well as the whole genetics department of the University of Osnabrück for their support, the friendly atmosphere and for being great colleagues. Furthermore, I would like to thank my family and friends for their continuous support.

8. Statutory declaration

Erklärung über die Eigenständigkeit der erbrachten wissenschaftlichen Leistung

Ich erkläre hiermit, dass ich die vorliegende Arbeit ohne unzulässige Hilfe Dritter und ohne Benutzung anderer als der angegebenen Hilfsmittel angefertigt habe. Die aus anderen Quellen direkt oder indirekt übernommenen Daten und Konzepte sind unter Angabe der Quelle gekennzeichnet. Bei der Auswahl und Auswertung folgenden Materials haben mir die nachstehend aufgeführten Personen in der jeweils beschriebenen Weise entgeltlich / unentgeltlich geholfen

- Sämtliche Plasmide mit der Bezeichnung pMHO wurden von Miriam Hegemanns im Rahmen ihrer Bachelorarbeit angefertigt
- TEM-Mikroskopie wurde ab dem Inkubationsschritt mit 1 % (w/v) NaIO₃ von Christian Meyer aus der AG Zoologie der Universität Osnabrück durchgeführt.
- Sämtliche Plasmide und Stämme mit der Bezeichnung pJJH/KHO wurden von Jürgen Heinisch erstellt. Das Alignment in Abbildung 9 und die Tetradenplatten in Abbildung 22 wurden ebenfalls durch Jürgen Heinisch erstellt. Abbildung 15B entstand unter mithilfe von Jürgen Heinisch.

Weitere Personen waren an der inhaltlichen materiellen Erstellung der vorliegenden Arbeit nicht beteiligt. Insbesondere habe ich hierfür nicht die entgeltliche Hilfe von Vermittlungs- bzw. Beratungsdiensten (Promotionsberater oder andere Personen) in Anspruch genommen. Niemand hat von mir unmittelbar oder mittelbar geldwerte Leistungen für Arbeiten erhalten, die im Zusammenhang mit dem Inhalt der vorgelegten Dissertation stehen. Die Arbeit wurde bisher weder im In- noch im Ausland in gleicher oder ähnlicher Form einer anderen Prüfungsbehörde vorgelegt.

(Ort, Datum)

(Unterschrift)

9. Curriculum vitae

Name: Marius Musielak
Date of birth: 06.04.1991
Place of birth: Steinfurt
Nationality: German

Work practice:

Since 03.01.2022: Compliance Engineer
Ecospecs GmbH, Biberach an der Riß

University Education:

- 31.09.17-31.08.22: **Doctoral studies**
Department of genetics at the University of Osnabrück (Germany)
Supervisor: Prof. Dr. rer. nat. Jürgen J. Heinisch
Dissertation: „The role of the small GTPase Rho5 in *Kluyveromyces lactis*“
Presumed degree: Doctor rerum naturalium (Dr. rer. nat.)
- 01.10.15-04.08.17: **M. Sc. Biology** – Cell and molecular biology
Department of genetics at the University of Osnabrück (Germany)
Supervisor: Prof. Dr. rer. nat. Jürgen J. Heinisch
Master thesis: „Die Rolle des DLR-Komplexes in Hefen“
- 15.02.16-14.05.16: Research assistant
Department of genetics at the University of Osnabrück
- 01.10.12-01.09.15: **B. Sc Biowissenschaften**
Department of genetics at the University of Osnabrück (Germany)
Supervisor: Prof. Dr. rer. nat. Jürgen J. Heinisch
Bachelor thesis: „Die Rolle von Num1 und Mdm36 für die Lokalisierung des DLR-Komplexes in *Saccharomyces cerevisiae*“
- 01.10.11-30.09.12: B. Sc. Chemistry
University of Bielefeld (Germany)

School education:

2002-2010: Gymnasium Martinum in Emsdetten

Publications:

The small GTPase KIRho5 responds to oxidative stress and affects cytokinesis.

Musielak M, Sterk CC, Schubert F, Meyer C, Paululat A & Heinisch JJ (2021)
J Cell Sci 134: jcs258301, DOI: 10.1242/jcs.258301

Fungal homologues of human Rac1 as emerging players in signal transduction and morphogenesis.

Hühn J, Musielak M, Schmitz H-P & Heinisch JJ (2020)
Int Microbiol 23: 43–53, DOI: 10.1007/s10123-019-00077-1